EXAMINING PERMAFROST DETECTION AND VALIDATION TECHNIQUES IN THERMALLY COMPLEX MOUNTAINOUS TERRAIN: A CASE STUDY IN THE OGILVIE MOUNTAINS, YUKON, CANADA

RIA NICHOLSON
Bachelor of Science, University of Lethbridge, 2021

A thesis submitted

In partial fulfillment of the requirements for the degree of

MASTER OF SCIENCE

in

GEOGRAPHY

Department of Geography and Environment

University of Lethbridge

LETHBRIDGE, ALBERTA, CANADA

EXAMINING PERMAFROST DETECTION AND VALIDATION TECHNIQUES IN THERMALLY COMPLEX MOUNTAINOUS TERRAIN: A CASE STUDY IN THE OGILVIE MOUNTAINS, YUKON, CANADA

Ria Nicholson

Date of Defence: March 21, 2025

Dr. Philip Bonnaventure Thesis Supervisor	Associate Professor	Ph.D.
Dr. Laura Chasmer Thesis Examination Committee Member	Associate Professor	Ph.D.
Dr. René Barendregt Thesis Examination Committee Member	Professor Emeritus	Ph.D.
Dr. Kevin McGeough Chair, Thesis Examination	Professor	Ph.D.

DEDICATION

I was fortunate growing up to have many positive influences who fostered my desire to learn more about the world. Therefore, I would like to dedicate this thesis to the memory of the late Annie Vas-Balay, among my first and finest teachers --- and to the Little Red Hen, as she often suggested I should.

ABSTRACT

Climatic warming necessitates a more comprehensive understanding of permafrost distribution. However, permafrost cannot be directly observed due to its subsurface nature, leading to a reliance on predictive models. Models commonly lack comprehensive validation through independent field observation and are thus prone to uncertainty. The goal of this research is to explore the limitations of permafrost model validation in a heterogeneous periglacial environment. Permafrost evaluation through two independent models in the Ogilvie Mountains were sampled using 74 cryotic assessment sites. The sampling goal was to identify permafrost *in-situ*, examining the concept of "testability". Sampling was performed using the ground thermal profiling method. Interference from impenetrable substrates caused 51.4 % of tests to fail. This data informed a probability of testability model. Overall, the landscape exhibited polarized testability, with elevation as a predictor. This highlights a critical knowledge gap in permafrost research today regarding uncertainty and validation.

CONTRIBUTION OF AUTHORS

Chapter 1 is an introduction to the subject matter and objectives of this thesis. It introduces contextual information relevant to the topic and the project objectives associated with the research. This chapter was edited by Dr. Philip Bonnaventure.

Chapter 2 is a literature review which explores the environmental controls on permafrost distribution and the drivers of thermal heterogeneity in periglacial landscapes. It also includes a review of the methods currently and historically used to map the distribution of permafrost and detect its presence, with a focus on the northwestern Arctic and sub-Arctic. Dr. Laura Chasmer provided guidance on the writing process and Dr. Philip Bonnaventure edited the document.

Chapter 3 is a research article addressing the project objectives. It includes an introduction, a description of the study area, the key results of the methodology explored in this thesis, the results of a model developed as part of the thesis, and an extended discussion section. It was edited by Dr. Philip Bonnaventure and Nick Noad. Rabecca Thiessen assisted with the coding process, Dr. Will Kochtitzky provided the DEM, and Dr. Madeleine Garibaldi provided data assistance.

Chapter 4 concludes the thesis by summarising the key results of the research, discussing its limitations, and providing future recommendations related to the ongoing knowledge gaps.

ACKNOWLEDGEMENTS

I feel extraordinarily grateful that there are so many people who deserve to be in this acknowledgement section that I am overwhelmed to start writing it. You all know who you are.

Firstly, I would like to thank my supervisor, Dr. Philip Bonnaventure, for his guidance and expertise through both the highs and lows of this research project. I would also like to thank the members of my thesis committee, Dr. Laura Chasmer and Dr. René Barendregt, for their feedback and engagement throughout this process. Furthermore, thank you to the rest of my colleagues who assisted with this research in both the lab and the field, from project design to data collection to editing: Dr. Madeleine Garibaldi, Dr. Scott Lamoureux, Rabecca Thiessen, Nick Noad, Sophie MacLean, and Mitch Codd. I would like to thank the Tetlit Gwich'in and Na-Cho Nyäk Dun Indigenous peoples, who provided permission for us to conduct this research in their traditional territories. Also, thank you to my teachers and colleagues at the University Center in Svalbard, particularly Dr. Danni Pearce and Dr. Anna Pienkowski, for many engaging discussions. My time in the Yukon and Svalbard will forever impact the way I view the world.

My heartfelt thanks also goes to my friends and family, without whom this would never have been possible. Thank you to my parents, Mark and Trish, to my brother Zach and sister-in-law Denver, and to my "extra parents": Annie, Gene, Rose, and Harold, for their belief in me when I needed it most. Thank you to my best friend Kyle, for being my foundation (and design helper!), and to the rest of my incredible friends for only ever being a phone call away. It turns out that writing a thesis truly does take a village.

TABLE OF CONTENTS

LIST OF TABLES

LIST OF EQUATIONS

LIST OF FIGURES

LIST OF ABBREVIATIONS

ΔTg	Thermal Offset
ΔTs	Surface Offset
AMAT	Average Mean Air Temperature
BTS	Basal Temperature of Snow
CALM	Circumpolar Active Layer Monitoring
CARET	Classification and Regression Training
DEM	Digital Elevation Model
ECV	Essential Climate Variable
ERT	Electrical Resistance Tomography
GIPL	Geophysical Institute Permafrost Laboratory
GLM	Generalized Linear Model
GPR	Ground Penetrating Radar
GTN	Ground Temperature Node
GTN-P	Global Terrestrial Network for Permafrost
GTS	Ground Thermal State
InSAR	Interferometric Synthetic-Aperture Radar
LiDAR	Light Detection and Ranging
MAAT	Mean Annual Air Temperature
MAGST	Mean Annual Ground Surface Temperature
MAGT	Mean Annual Ground Temperature
NDVI	Normalized Difference Vegetation Index
NWT	Northwest Territories
PISR	Potential Incoming Solar Radiation
SBI	Surface-based Temperature Inversion
SLR	Surface Lapse Rate
TPI	Topographic Position Index
TTOP	Temperature at the Top of Permafrost
YT	Yukon Territory

CHAPTER 1: INTRODUCTION

1.0. Background

"Permafrost" is a term which was first coined by S.W. Muller (1947) to describe perennially frozen ground. However, the definition has since evolved. Researchers now define permafrost more specifically, referring to subsurface earth materials that remain cryotic (≤0°C) for at least two consecutive years (van Everdingen, 1998; French, 2007). The term "cryotic" is often preferred over "frozen" because freezing implies a phase transition, and not all permafrost contains water or ice (van Everdingen, 1976). This is called "dry" or "ice-poor" permafrost and can be present in numerous different substrates (*e.g.* mineral soils, organic horizons, bedrock, and colluvium) (Bonnaventure & Lamoureux, 2013). Permafrost may also be ice-rich, with massive or interstitial ground ice, ice wedges (French & Shur, 2010), or remnants of buried glacial ice (Harris & Murton, 2005). Ultimately, however, permafrost is not a physical material, but a temporal description of thermal state (Dobiński, 2011). This makes delineating the boundaries of permafrost difficult, because it is an attempt to map a condition, not a substance (Hegginbottom, 2002).

Permafrost environments also have an active layer, which is the uppermost portion of material above a permafrost body which freezes and thaws on a seasonal basis (French, 2007). However, progression of anthropogenic climate warming and subsequent Arctic Amplification is causing the active layer to thaw more than it refreezes in many regions (Åkerman & Johansson, 2008; Masson-Delmotte et al., 2013; Nyland et al., 2021; Strand et al., 2020). This process causes permafrost to warm and recede on varying spatiotemporal scales (Cheng & Wu, 2007; Schuur et al., 2013). Impacts of this include increased carbon emissions to the atmosphere

(Schuur et al., 2015), landform instability and infrastructure damage (Haeberli et al., 2017), and increased transport of pollutants and heavy metals (Revich et al., 2011).

Climate change has impacted all elements of the global cryosphere. However, unlike sea ice and glaciers, permafrost cannot be monitored or directly observed using the human eye or satellite remote sensing (Kääb 2008; Westermann et al. 2014; Obu et al., 2019, Bartsch et al., 2023). It also has not been listed as a "space-observable" Essential Climate Variable (ECV) by the Global Climate Observing System (GCOS, 2016). Although it is possible to observe and infer permafrost from diagnostic features (*e.g.* polygonal patterned ground and pingos), these are not consistently present. This is especially true in dry permafrost bodies (such as in mountains), where earth materials are perennially cryotic but lack the free water and ice essential to the formation of thermokarst topography and aggregational features (Harris, 1981; Bockheim & Tarnocai, 1998). Other methods of remote sensing for permafrost do exist but cannot penetrate deep soils (>10 cm) (Jiang et al., 2020) and produce limited spatial detail (Bartsch et al., 2023).

Limitations on satellite remote sensing are not the only issue. Collecting *in-situ* data about permafrost is a highly time- and labour-intensive endeavour because these environments are often remote, inaccessible, or hazardous. This is often the case in areas with steep slopes, rock glaciers, and in regions lacking critical infrastructure. Furthermore, permafrost distribution is not always uniform, and collecting discrete data points from a highly heterogeneous landscape is unlikely to produce results which are comprehensively representative. As a result, research on permafrost distribution is reliant on predictive models, but those models frequently go unvalidated.

Permafrost is largely a climatically governed phenomenon (Schuur et al., 2008; Harris et al., 2017) and is modelled accordingly (Heginbottom et al., 1995; French, 2007). Because of

these broad macro-scale controls, many models operate on circumpolar or regional scales (Gibson et al., 2021) (*e.g.* Guo & Wang, 2016; Obu et al., 2019; Saito et al., 2020). However, these large-scale models frequently struggle to capture the sub-grid variability of permafrost distribution caused by thermal heterogeneity in certain landscapes (Etzelmüller, 2013). In this context, thermal heterogeneity refers to variations in surface energy balance caused by topography, vegetation, and soil texture which create localized variations in permafrost distribution (Shur & Jorgensen, 2007; Gruber, 2012). This phenomenon is most prominent in the extensive-discontinuous zone (Shirley et al., 2022) and in mountainous regions (Etzelmüller, 2013), but can still occur in cold, high latitude environments which are typically assumed to be underlain by continuous permafrost (Garibaldi et al., 2021). These patterns of spatial and thermal heterogeneity are too fine to be captured by current Earth System Models (Shirley et al., 2022). One such example of this are the global climate models (GCMs) used by the IPCC to forecast global response to climate change (*e.g.* CMIP5 and CMIP6), which operate on scales of 100-300 km (Strandberg & Lind, 2021). This results in significant uncertainty regarding the actual distribution of permafrost.

At their core, models are mathematical and conceptual simplifications of reality (Inkpen, 2005) which are reliant on their constraining parameters for accuracy. These parameters often come in the form of field data, but *in-situ* observations of permafrost are notoriously spatiotemporally fragmented (Anisimov & Zimov, 2021). Although our ability to accurately characterize subsurface soil temperatures are fundamental to understanding permafrost evolution (Guglielmin, 2006; Jorgensen et al., 2010; Isaksen et al., 2011), our current knowledge of permafrost distribution is heavily dependent on modelling to evaluate and predict changes in a warming climate. Therefore, this thesis seeks to examine this issue in the context of an

environment where modelling issues are numerous due to the number of variables which influence permafrost distribution. This research will analyse possible avenues of validation for permafrost researchers when they are confronted with complex sites.

1.2. STUDY OBJECTIVES

The overarching goal of this research is to analyse the challenges of permafrost model validation. This is a challenging yet important endeavour as it aims to better understand the usefulness and robustness of models in specific environments. This can be especially crucial in environments which show greater thermal heterogeneity than the resolution that a model permits. To better understand this research gap, a field campaign was conducted in two proximal yet distinctive mountain valleys in the northcentral Yukon. Both valleys exhibit a strong degree of thermal heterogeneity, driven by variable surface characteristics and powerful surface-based temperature inversions (SBIs) (Noad & Bonnaventure, 2022). Large portions of the study area are also covered by blockfields, which are impenetrable to non-industrial instruments and make obtaining *in-situ* permafrost observations nearly impossible. The overarching goal of the research will be addressed by the following **Project Objectives (PO):**

PO1: Assess the feasibility of using frost probing, digging, and ground thermal profiling, with the goal of identifying permafrost presence or absence at several cryotic assessment sites (CAS) in the mountain valleys.

PO2: Identify the correlation between successful *in-situ* permafrost testability and environmental drivers of testability from DEM (Digital Elevation Model)-derived variables (land cover type, TPI, elevation, aspect, and slope).

PO3: Generate a probability surface illustrating the likelihood of a successful permafrost presence/absence validation test at a specific location within the study area. This product can then be overlaid in similar yet different nearby areas, potentially illuminating better sites for permafrost testing in the future.

PO4: Compare the results of different locally available permafrost models, focusing on areas of disagreement to examine *in-situ* testing feasibility.

CHAPTER TWO: LITERATURE REVIEW

2.0 Literature Review

2.1. Introduction

Permafrost is estimated to underlie 15-24 % of the Earth's terrestrial surface (Zhang et al., 2000; Obu et al., 2019) with the majority concentrated in the northern hemisphere due to the distribution of global landmasses (Brown et al., 1997). While it is most extensive in the circumpolar Arctic and Antarctic, it is also present at high elevations in mid-latitude regions, such as the Canadian Rocky Mountains, the European Alps, and the Qinghai-Tibet Plateau due to elevational cooling (Haeberli et al., 1993). On these macro scales, information about permafrost distribution is widely available and well-understood. However, permafrost distribution on local scales is far more variable and is likely to exceed the resolution of predictive models. This is problematic, because spatially detailed information on permafrost distribution is critical for land use planning, infrastructure development (Zhang et al., 2014), and carbon emissions (Miner et al., 2022). Furthermore, the ability to visualise permafrost spatial distribution is necessary for model input and validation (Gruber, 2012; Etzelmüller, 2013), and the lack thereof results in a high degree of uncertainty regarding the actual conditions of ground thermal state (GST).

To better understand this issue, this review will begin with a discussion of the significance of permafrost to the terrestrial environment and the climatic controls which determine its formation and maintenance. Special consideration will be given to mountainous environments. Permafrost presence or absence will be discussed through the lens of the surface energy balance conceptual model, with a focus on the drivers of thermal heterogeneity. I will then provide an overview of some of the major methods of permafrost detection techniques and permafrost model generation.

2.2. Impacts of permafrost thaw

It is well-documented that permafrost is warming and that its extent is decreasing due to climate change (Smith et al., 2009; Schuur et al., 2013; Streletskiy et al., 2015), with especially profound impacts in the circumpolar Arctic. This is due to Arctic Amplification, a phenomenon wherein the Arctic is more susceptible to shifts in temperature and precipitation than lower latitude regions due to differential radiative mechanisms (Masson-Delmotte et al., 2013). This has manifested in several ways, including stark reductions in the extent of sea ice (Onarheim et al., 2014; Kwok, 2018) and glaciers (Laenerts et al., 2013; Sommer et al., 2022). Permafrost has also been profoundly impacted, as average Arctic ground surface temperatures have increased two to three times faster than the global average since 1981 (>0.5°C per decade) (Comiso & Hall, 2014). Increasing wildfire intervals have also led to substantial and irreversible changes in permafrost landscapes, due to alterations in surface energy balance caused by charring (Holloway et al., 2020). As a result, permafrost and communities built on permafrost become vulnerable to several changes.

Permafrost is a significant moderator of the global climate due to its role as a terrestrial carbon reservoir (Schuur et al., 2008). When organisms die, microbial decomposition is prevented by the freezing process and halts the release of carbon dioxide (CO_2) and other greenhouse gases into the atmosphere (van Huissteden & Dolman, 2012). Current estimates suggest that the permafrost carbon reservoir contains approximately twice the amount of potential CO_2 than what is currently present in the atmosphere (1,700 petagrams) (Schuur et al., 2008; Hugelius et al., 2014). This issue drives concerns that ongoing warming will surpass a "climate tipping point" (Lenton et al., 2008) wherein the permafrost reservoir becomes a carbon source, fueling a positive feedback loop of global warming (French 2007, Schuur et al., 2015).

On a more local scale, thawing permafrost also presents risks to the stability of landforms and infrastructure due to losses of massive or interstitial ice (Hjort et al. 2018; Schneider et al., 2021). This creates a heightened risk of destructive slope processes, such as landslides and retrogressive thaw slumps (Lantz & Kokelj 2008; Haeberli et al., 2017) that have the potential to cause severe bodily harm and financial damages. There have been several documented occurrences of this already throughout the circumpolar Arctic. In 2022, the village of Newtok, Alaska began relocation efforts due to the river erosion and infrastructure damage associated with permafrost thaw (US Department of the Interior, 2022), and in 2023, the Yukon Territorial Government closed a section of the Alaska Highway due to the rapid progression of the Takhini River Thaw Slump in the Ibex Valley (Fig. 2.1). Permafrost thaw has also been problematic for the Dempster Highway, which has 90 % of it's 736.5 km length built on continuous permafrost (Burn et al., 2015).

These are some of the issues which necessitate a more local approach to understanding permafrost distribution (*i.e.*, Daly et al., 2022), as most spatial data products built to examine thaw operate at circumpolar scales (Gibson et al., 2021). The hazard assessment for Dawson City, Yukon, produced by Benkert et al., (2015), is another such example of community-based permafrost monitoring.

Fig. 2.1. A ground level view of the Takhini River Thaw Slump, located in the Ibex Valley (Yukon, Canada). Photo taken June 2024.

Permafrost thaw represents a multitude of other environmental concerns, all of which require their own specific monitoring techniques. These include transport of pollutants, heavy metals, exotoxins, and hazardous environmental agents (Revich et al., 2011; Potapowicz et al., 2019; Perryman et al., 2020), changes to the biogeochemical composition of Arctic watersheds (Frey & McClelland, 2009), changes to the hydrological character of drainage basins (Chasmer et al., 2011), increased rates of coastal erosion (Whalen et al., 2022), and impacts on the quality of food and drinking water in northern communities (Yang et al., 2016).

2.3. Environmental drivers of permafrost distribution and thermal heterogeneity

The extent and distribution of permafrost is governed by climate via the surface energy balance (Schuur et al., 2008; Harris et al., 2018). Surface energy balance is a conceptual model that describes energy fluxes as a budget equation (Mauder et al., 2020), considering contributions from convective, conductive, radiative, and latent heat fluxes (Painter et al., 2013). This makes it an especially effective way to conceptualise thermal heterogeneity, which is the phenomenon of

variations in surface energy balance altering the absorption and reflection of warmth on small scales (Shur & Jorgensen, 2007). This has an influence on both permafrost distribution and thermal state, which influences the magnitude of thaw required to degrade it beyond the 0°C isotherm.

Thermal heterogeneity is especially prominent in the extensive-discontinuous permafrost zone (Shirley et al., 2022) and in mountainous regions (Etzelmüller 2013). However, it has also been observed in high-latitude environments where permafrost coverage is typically assumed to be homogeneous (Garibaldi et al., 2021). Numerous micro- and meso-scale factors contribute to these patterns of thermal heterogeneity including geology, substrate, substrate moisture content (Riseborough et al., 2008), vegetation coverage and species (Shur & Jorgensen, 2007), elevational cooling, topographic shading (Etzelmüller, 2013), snowfall timing and depth (Kremer et al., 2011), solar insolation patterns, and proximity to glaciers or warm ocean currents (Bockheim & Hall, 2002). These natural variations, specifically in substrate, vegetation, and snow cover can also generate a difference between the mean annual air temperature (MAAT) and mean annual ground surface temperature (MAGST), which is referred to as the surface offset (ΔTs) (Oke, 2002; Beltrami & Kellman, 2003). Such surface offsets commonly occur in continental, mountainous regions such as the Yukon Territory (Burn & Smith, 1998) and represent a critical component of TTOP (Temperature at Top of Permafrost) modelling. The relationship is described by Henry & Smith (2001) (Fig. 2.2), where:

TTOP = MAAT + Surface Offset + Thermal Offset. *Equation 2.0.*

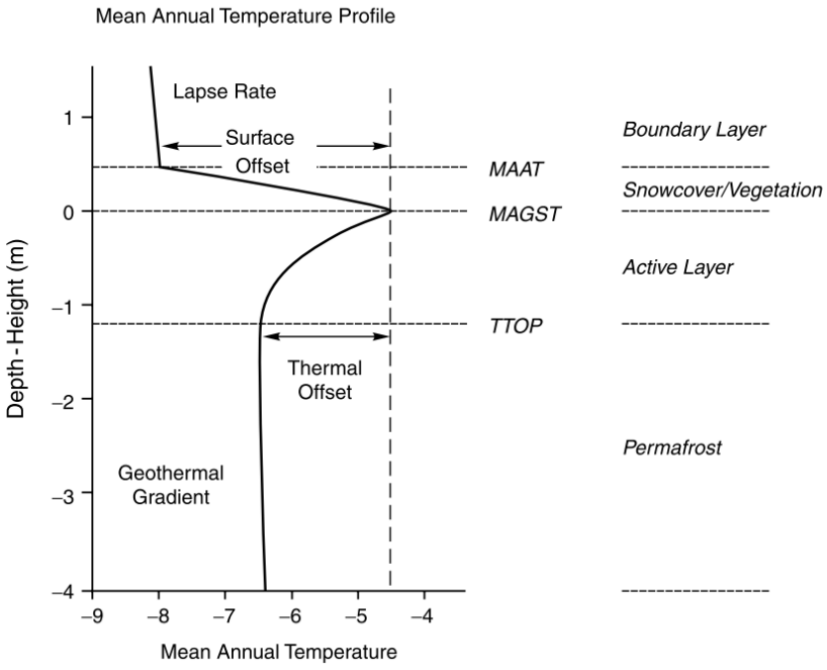

Fig. 2.2. A temperature profile describing the relationship between the lower atmosphere and the thermal state of the ground in permafrost terrain (Henry & Smith, 2001). Copyright © 2001 John Wiley & Sons, Ltd.

2.3.1. Substrate and moisture

Substrate type and composition is a major determinant of localised permafrost distribution because its conductivity determines how deeply the seasonal thawing and freezing fronts penetrate the ground (Shur & Jorgensen, 2007; Zhang et al., 2008). Substrate particle size also affects thaw and heat transfer because it influences porosity and moisture retention (van Vliet-Lanoë, 1985). Higher moisture content is associated with less thawing and longer zero curtain periods (Jiang et al., 2018) due to the latent heat of fusion, meaning that drier substrates facilitate much greater thaw depths during the melt season (Bonnaventure & Lamoureux, 2013).

Substrate is also associated with the *thermal offset* (ΔTg), which is generated by the difference in thermal conductivity between thawed versus frozen ground (Goodrich, 1982;

Romanovsky & Osterkamp, 1995). The thermal conductivity of ice is approximately four times greater than that of unfrozen water (Smith & Riseborough, 2002) and influences the timing of the zero curtain. The zero curtain is caused by latent heat maintaining temperatures near 0°C during freezing or thawing transitions, due to the energy required to initiate a phase change (Outcalt et al., 1990). Because of this, the magnitude of thaw is much greater in dry environments, such as bedrock and polar deserts (Bockheim & Tarnocai, 1998; Bonnaventure & Lamoureux, 2013).

2.3.2. Blockfields

Blockfields (also referred to as felsenmeer, periglacial facies, blockstreams, or *kurum)* are accumulations of clasts and rubble formed by frost-action weathering (French 2007) (Fig. 2.3). They were first defined by Walery Łoziński (1909) as a central feature of periglacial landscapes (Boelhouwers, 2004) and are common to cold, dry, continental regions (Harris & Pederson 1998). Blockfields formed by *in-situ* weathering processes are referred to as autochthonous (Boelhouwers, 2004), and if parent material is derived elsewhere (i.e. upslope), it is called allochthonous (Rea et al., 1996). Blockfields can also serve as an indicator of paleoclimate history, as they are unlikely to be removed or destroyed by anything other than glacial activity (Rea et al., 1996). Such coarse-grained rock debris on mountain slopes are generally well-drained (Haeberli et al., 2010) and are frequently associated with negative temperature anomalies, especially when compared to surrounding bedrock or fine-grained sediments (Harris & Pederson, 1998, Juliussen & Humlum, 2008). Therefore, they also tend to preserve buried ice or permafrost in otherwise unsuitable climatic conditions (Sawada et al., 2003). Four theories to explain this phenomenon have been proposed.

Balch ventilation (or the Balch effect) is a convective method of cooling in which dense cold air displaces warm air in the voids between the coarse materials of a blockfield (Balch,

1990; Barsch, 2012). This process prevents warm air at the surface from penetrating downwards, permitting heat transfer by conduction-only (Jones et al., 2019). However, this process would be limited by snow cover (Harris & Pederson, 1998). Wakonigg (1996) suggested an alternate theory called *"the chimney effect"*, wherein warm air within the voids is displaced by cold winter air entering through gaps in snow cover and pushes warm air to escape into the atmosphere through holes at the upper portion of the slope (Hanson and Hoelzle, 2004). Harris and Pedersen (1998) suggested a continuation of this idea ("continuous exchange of air exchanged with the atmosphere") relevant to areas lacking continuous snow cover, where any changes in air temperature result in nearly instantaneous temperature changes at depth due to the continuous exposure of the atmosphere to the bare surface of the blockfield. Finally, the fourth theory ("summertime evaporation/sublimation of water/ice in the blocky deposit") suggests that water and ice in the summer cools blocky debris as a result of latent heat loss (Juliussen & Humlum, 2008).

Fig. 2.3. A slope in the Ogilvie Mountains (northcentral Yukon) overlain by blockfield materials. Photo taken August 2022.

2.3.3. Vegetation

Vegetation coverage and species is another key control on permafrost distribution due to the multitude of ways it alters surface energy balance (Baughman et al., 2015). The shade provided by a treed canopy or by leaves significantly reduces the amount of shortwave radiation reaching the ground surface (Chasmer et al., 2011; Juszak et al., 2014), and evapotranspiration provides a natural cooling effect (Holloway et al., 2020). Presence of vegetation also changes snow accumulation (Holloway et al., 2020).

The impact of this on mountainous permafrost is especially profound in northwestern North America, especially when compared to similar regions featured in European studies (Kremer et al., 2011). In the Yukon, this is at least partially due to the strong continentality of the area, which results in subzero MAATs despite summer temperatures which are warm enough to allow for forest growth (Bonnaventure & Lewkowicz, 2012).

Various moss species (*e.g.* Fig. 2.4) also provide an insulative "thermal buffering" effect which allows the ground surface to expel more heat over winter than it absorbs in summer (Shur & Jorgensen, 2007). This "ecosystem-protected" permafrost (Shur & Jorgensen, 2007) is more resilient to climate change and can be sustained in an environment where the mean annual ground surface temperature (MAGST) is greater than 0°C (Smith & Riseborough, 2002; Bonnaventure & Lamoureux, 2013). This trait is common in *Sphagnum* spp. and feather mosses which exhibit variable thermal conductivities that dampen temperature fluctuations at the ground surface level (Fisher et al., 2016). This thermal conductivity is strongly influenced by moisture (Gornall et al., 2007; O'Donnell et al., 2009), with dry mosses in summer reducing downward heat conduction and wet mosses in shoulder seasons or frozen mosses in winter increasing upward heat conduction (Burn & Smith, 1998, Fisher et al., 2016). This is due to their high

porosity (O'Donnell et al., 2009). Vegetation can also trap windblown snow, further contributing to ground surface insulation (Zhang et al. 1997, Shur & Jorgensen, 2007).

Fig. 2.4. Dry *Hypnales spp.* (feather moss) at a permafrost site in the Ibex Valley, Yukon. Photo taken June 2024.

2.3.4. Snow cover

Snow cover impacts surface energy balance through its insulative properties, creating a disconnect between air and ground surface temperatures (Goodrich, 1982). This is called the *nival offset* (French, 2007), and it generally results in a net warming effect due to the insulation of the ground surface from cold winter air (Krinsley, 1962; Harris, 1981). When snow cover is heavy, less heat is lost through the winter, leading to warmer conditions in the active layer which require less energy to thaw in the spring season (Brenning et al., 2005). However, the magnitude of this warming depends on local conditions, including the timing of snowfall, thickness, and distribution (Zhang et al., 1997). This effect also drives heterogeneity in permafrost conditions when snow collects in topographic lows, in vegetation, or in areas sheltered from redistributing wind (Bonnaventure et al., 2017). As climate change drives increased precipitation in the Arctic

(McCrystall et al., 2021), snow cover may also increase near-surface permafrost loss via these insulative properties (IPCC, 2001; Johansson et al., 2013).

2.3.5. Topography, slope, and aspect

Topography, aspect, and slope are significant controls on permafrost distribution due to their effect on potential incoming solar radiation (PISR) (Riseborough et al., 2008). This effect becomes especially pronounced in High Arctic regions where vegetation contributes little to surface energy balance (Brown, 1972; Woo et al., 1986; Woo & Young, 1997) and in mountains, where they contribute strongly to the extreme thermal heterogeneity exhibited there (Etzelmüller, 2013). This is because topography and slope have a major influence on net diurnal heat flux, even when slope angles are as low as 5° (Harris et al., 2018). Slope angle also influences moisture distribution, which in turn affects latent heat transfer, which is a key factor in permafrost maintenance (Fan et al., 2022).

2.3.6. Elevation and surface-based temperature inversions (SBIs)

Elevational cooling is another driver of permafrost formation and maintenance (Kneisel et al., 2008), resulting in perennial cryotic temperatures in otherwise temperate or mid-latitude regions, such as the Rocky Mountains or the New Zealand Alps (Haeberli et al., 1993). In mountains, elevation and topographic aspect are the most important factors governing permafrost distribution (Etzelmüller & Frauenfelder, 2009). The standard rate of this cooling (called the standard elevational lapse rate or SLR) is typically considered to be -6.5 °C/km^{-1} (Oke, 2002). As a result, elevation is also frequently used as a proxy for MAAT (Gruber & Hoelzle, 2001). However, because many climate models make assumptions of a constant SLR, significant error is introduced (Minder et al., 2010). For example, the Ogilvie Mountains in north-central Yukon

do not generally adhere to this standard, due to surface-based temperature inversions (SBIs) caused by their high-latitude and continentality (Noad & Bonnaventure, 2022). In such mountains, low solar angles in winter do not reach the valley bottoms, which results in colder, denser air sinking to the bottom and not being remixed by warming (Malingowski et al., 2014). This complicates permafrost mapping and predication, because on a yearly scale, the coldest parts of these sites are located in the valley bottoms and mountain tops, while the warmest parts are located at middle elevations of the mountains (Bonnaventure & Lewkowicz, 2012; 2013) (Fig. 2.5).

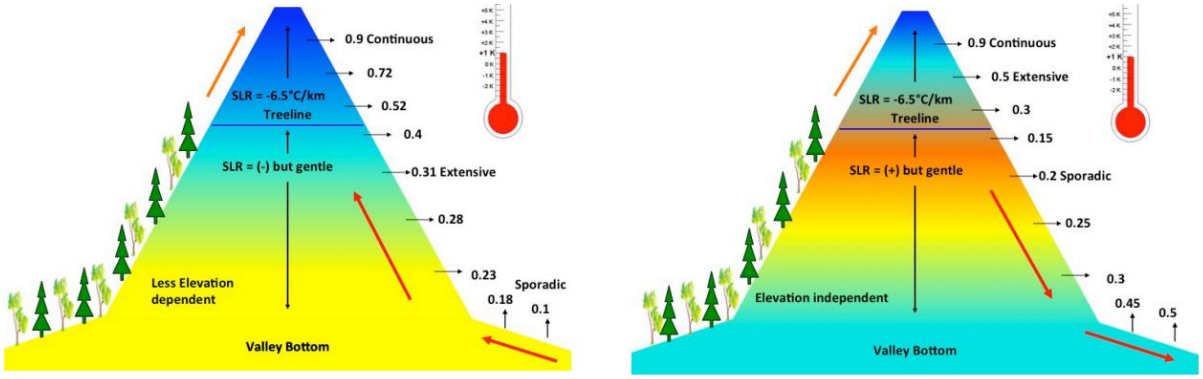

Fig. 2.5. Conceptual diagrams demonstrating the influence of inverted surface lapse rates on permafrost distribution in mountains following warming (Bonnaventure & Lewkowicz, 2013).

2.4. Techniques of permafrost mapping and modelling

Among the earliest attempts to map and model permafrost distribution was the spatial model developed by Wild (1882), which delineated a southern boundary of perennially frozen ground in Siberia using macro-scale patterns of air temperature (Shiklomanov, 2005; Riseborough et al., 2008). Wild suggested that the average annual ground temperature 1 metre depth below the surface should be 0.9°C warmer than the average air temperature, and that a negative mean annual ground temperature (MAGT) at the depth of zero annual amplitude is only

possible where MAAT is >-1.6°C (Wild, 1882; Shiklomanov, 2005). In the modern era, permafrost is usually mapped on circumpolar scales according to the assumption of average temperatures decreasing at higher latitudes (Burn & Nelson, 2006). It is thus mapped and categorised as continuous (90-100%), extensive discontinuous (50-90%), sporadic discontinuous (10-50%), or isolated (<10%) (Heginbottom, 1995) (Fig. 2.6). However, this is a generalised approach, as ground temperatures within a set geographic region tend to fluctuate due to variations in surface conditions (Burn & Nelson, 2006). The spatial resolution of permafrost models which operate on such large scales are limited by the availability of data categorising the thermal heterogeneity of the ground thermal regime (Riseborough et al., 2008), creating uncertainty.

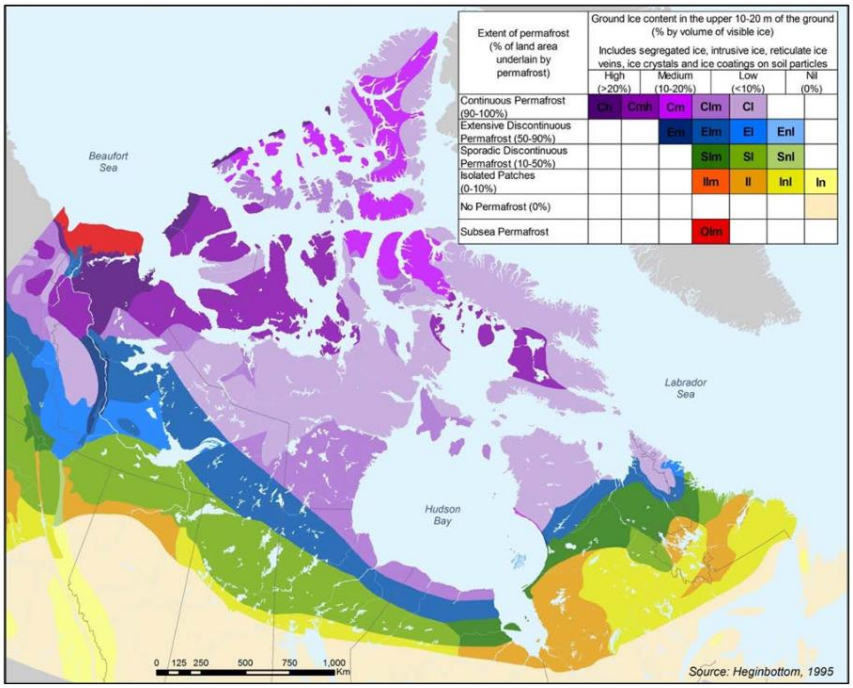

Fig. 2.6. Permafrost map of Canada with ground ice content (Heginbottom, 1995). From National Atlas of Canada, 5th edition, Plate 2.1 (MCR 4177), scale 1:7,500,000.

Permafrost models are constantly undergoing development, identifying new critical parameters and employing improved methodologies. Now, permafrost models combine both

stochastic and deterministic elements to map distribution (Hoelzle et al., 2001) and can be classified into three main categories: empirical, equilibrium, and numerical (Riseborough et al., 2008). However, few of these models are ever validated using field data, creating great uncertainty surrounding their accuracy - especially as climate change alters both permafrost thermal state and distribution every year. Furthermore, there is a lack of baseline information and established methods for effectively mapping permafrost on large scales at resolutions sufficient to detect changes (Walvoord et al., 2016). Although modelling is a critical tool utilised in understanding the spatial evolution of permafrost extent and thermal state, broad disagreements can exist between models (Sun et al., 2019).

2.4.1. Empirical models

Empirical permafrost models analyse the relationship between ground temperature, air temperature, and other available environmental parameters (Zhang et al., 2003). These parameters, both topographic and climatic, are then used as proxies to determine the energy exchange between the ground and the atmosphere (rather than explicitly calculating energy balance) (Hoelzle et al., 2001; Riseborough et al., 2008). This makes them both computationally efficient and easy to use, requiring fewer inputs than numerical models to function. These models are particularly well-suited for modelling in remote areas where data coverage is limited (Etzelmüller et al., 2006).

A similar type of model is the statistical-empirical model, which is frequently used in mountainous permafrost environments (*e.g.* Gruber & Hoelzle, 2001; Bonnaventure & Lewkowicz, 2012). These models are more complex and integrate a broader range of topo-climatic data inputs (*e.g.* elevation, slope, aspect, MAAT, and solar radiation) (Hoelzle et al., 2001; Riseborough et al., 2008) to conceptualise interactions between the ground surface and the

upper portion of the active layer (Bonnaventure & Lamoureux, 2013). These models are useful when an empirical model may be too simple to capture the complexities of the target environment (Riseborough et al., 2008). Cost of input on statistical-empirical models is low, but they still require local calibration to be effective (Hoelzle et al., 2001).

2.4.1.1. Basal Temperature of Snow (BTS)

Basal temperature of snow (BTS) is a method of empirical-statistical modelling which was developed by Haeberli (1973) to assess permafrost distribution in mountainous environments. Although it was originally developed to characterise permafrost in the Swiss Alps and has seen frequent use there (*e.g.* Imhof et al., 2000; Gruber & Hoelzle 2001), it has also seen use in northern Canada (Lewkowicz & Ednie, 2004; Bonnaventure & Lewkowicz, 2012). It is based on the principle that sufficiently heavy snow cover (>80 cm) decouples ground surface temperatures from the atmosphere (Goodrich, 1982) by insulating it from diurnal variations in surface energy balance (Lewkowicz & Ednie, 2004). BTS functions by considering the statistical relationship between MAAT, potential incoming solar radiation (PISR) derived from slope, elevation, and topography, and the obtained BTS measurements to determine the likelihood of permafrost presence of absence (Lewkowicz & Ednie, 2004; Riseborough et al., 2008). Generally, when BTS is ≤-3°C, permafrost is considered present, and when BTS is ≥-2°C, it is considered absent (Mühll et al., 2002).

BTS measurements are obtained by measuring the temperature at the base of midwinter snow cover (Brenning et al., 2005). This method is relatively cost-effective, requiring only thermistors to operate, but must be performed when snowfall cover is thick, thus increasing cold-related hazards to researchers and reducing accessibility to remote areas. Consideration must also

be given to the year's snowfall history when BTS is performed, as it has a strong influence on the results and may not represent the average (Mühll et al., 2002).

2.4.2. Numerical models

Numerical (or process-oriented) models focus on describing the relationship between permafrost and the atmosphere through energy fluxes (Hoelzle et al., 2001). They operate by creating a surface energy balance equation wherein ground temperature is an outcome of heat transfer between the ground and the atmosphere (Zhang et al., 2003; Riseborough et al., 2008). Numerical models are especially valuable when addressing an issue where transient phase change is important (Jafarov et al., 2012). However, the requirement for extensive climatological inputs make utilising a numerical model computationally intensive, particularly in complex or remote environments (Bonnaventure & Lamoureux, 2013). Additionally, accurately defining the different types of heat transfer (convective, conductive, and radiative) requires a significant amount of different data which must be monitored in the field, making numerical models difficult to constrain (Riseborough et al., 2008). Smith & Riseborough (2002) also note that models based on surface energy exchange are impractical above the site scale due to limits on data about microclimatic variables.

A transient numerical model illustrates how permafrost changes over time under simulated present or future conditions (Riseborough et al., 2008) and is commonly used to forecast permafrost response to climate change. One such example is the Geophysical Institute Permafrost Laboratory (GIPL) 2.0 model developed by Marchenko et al., (2008), which operates by simulating soil temperature dynamics and the depth of seasonal freeze-thaw using numerical solutions of heat transfer. This equation considers air temperature, precipitation, snow cover, vegetation, ground temperatures, and lithologic data. The model was informed using empirical

observations of soil characteristics in the study region (Alaska) and was validated against discrete borehole measurements.

2.4.3. Equilibrium models

Equilibrium models are considered to be the "middle ground" between numerical and empirical models and are suitable when data is sparse. These simplified models assume "steady state" conditions with stationary temperature and snow cover (Riseborough, 2007). They employ transfer functions between the air and ground temperatures to define the active layer depth (Jafarov et al., 2012), and by relating permafrost presence or absence to climatic and topographic factors, such as moisture, vegetation, and soil (Wang et al., 2020). This simplicity makes them simpler to use, with fewer inputs and less demand on computational power, but they are therefore only suitable for problems where transient effects can be overlooked or are of little importance (Jafarov et al., 2012).

2.4.3.1. Temperature at Top of Permafrost (TTOP)

TTOP is an equilibrium model developed by Smith & Riseborough (1996) which analyses the connectivity of climate and permafrost by using seasonal n-factors as an empirical alternative to surface energy balance (Lunardini, 1981; Wright et al., 2003). N-factors are used in permafrost regions to summarise the relationship between air and ground surface temperatures (Klene et al., 2001; Lin et al., 2019); they are transfer functions between MAGST and MAAT (Karunaratne & Burn, 2003). Obu et al. (2019) is a contemporary example of a TTOP model (Fig. 2.7) and a major recent contribution to knowledge of permafrost distribution in the northern hemisphere. Despite its circumpolar scale, it operates at a resolution of 1 km^2. Although this is still too coarse to delineate variations in highly heterogeneous permafrost, it is extremely high

resolution for its scale. The model was derived from remotely sensed land surface temperature data, land cover data, and climate reanalysis data provided by the European Centre for Medium-Range Weather Forecasts. The model forecasted permafrost coverage in the northern hemisphere to be approximately 14.6 %, which is slightly below the average of other estimates (Obu et al., 2019). This model was validated and informed largely by data provided by the GTN-P, with the accuracy of modelled mean annual ground temperature (MAGT) at TTOP being compared primarily to borehole data. However, the authors note that the model's accuracy decreases when modelled MAGT approaches 0 °C, potentially because it does not include transient response of the ground's surface to changes in temperature. This model has also been criticized by Dobiński (2020) for its exclusion of some azonal and mountainous permafrost, subsea permafrost, and potential transition zones between permafrost and previously glaciated areas. This criticism highlights the numerous challenges associated with circumpolar models, including those which are validated with *in-situ* measurements.

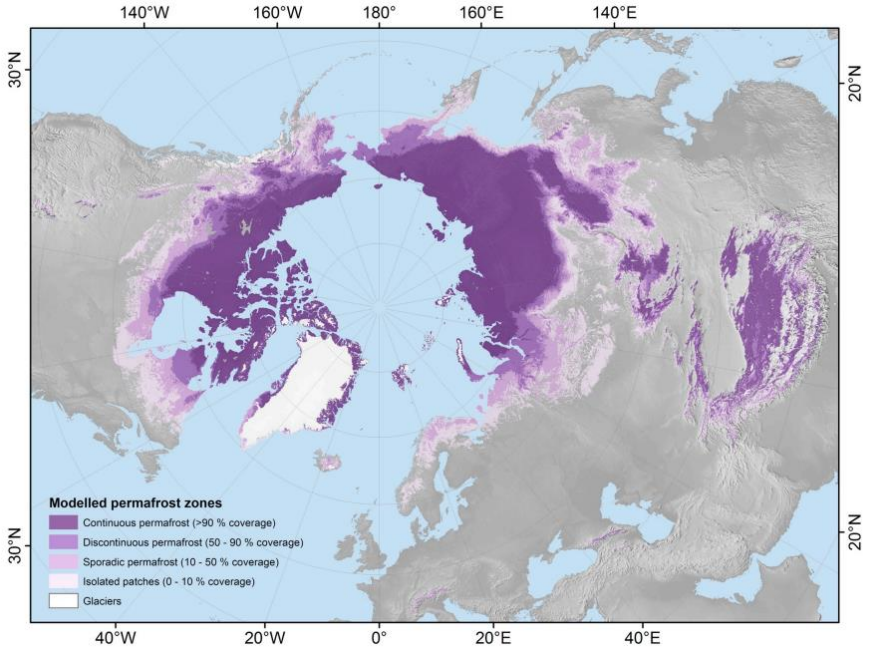

Fig. 2.7. A TTOP model product generated by Obu et al. (2019), displaying probabilities of permafrost distribution as zones in the northern hemisphere.

2.5. Permafrost detection techniques

Systematic quantification of ground surface temperatures is an important part of understanding near-surface permafrost (Etzelmüller, 2013). However, it is challenging to obtain meaningful amounts of point data in heterogeneous permafrost over vast landscapes. Potential methods of detection can be separated into direct methods and indirect methods, and either can be used for ground-truthing. The term "ground-truthing" is generally taken to mean validation of remotely collected data but can also be used to describe efforts to validate permafrost predictions. However, it is worth noting that the word "truth" in this context refers to interpretation, not that the data is perfect (Hargrave, 2006). Several methods of ground truthing exist, each with their own advantages and disadvantages. Cost, substrate, site accessibility, and other logistical difficulties associated with the remote nature of mountainous terrain and Arctic environments make many methods challenging, impractical, or impossible.

2.5.1. Direct methods

Direct methods of permafrost detection involve taking physical measurements of subsurface thermal state, rather than relying on proxies of permafrost presence. Although direct methods produce more reliable results, they are also more time and labour intensive. Furthermore, data produced is discrete and are not necessarily comprehensive for vast landscapes.

2.5.1.1. Digging and frost probing

The simplest methods of permafrost detection involve direct attempts to reach cryotic temperatures at a single given point in the landscape, usually either by digging with a shovel or attempting to locate the top of permafrost using a frost probe. The cost of employing these methods is low, but they are time and labour intensive. Digging is simply performed by using a

shovel to attempt to reach cryotic materials or massive ground ice at a site. One such example of the digging method of verification was employed by Lewkowicz & Ednie (2004) in their study of permafrost distribution in Wolf Creek, Yukon, Canada. In this study, the results of their Basal Temperature of Snow (BTS) model were physically verified by digging 201 pits over the course of two months.

A frost probe (Fig. 2.8) is a steel or titanium rod which can be used to penetrate the ground during the season of maximum thaw to determine the depth of the frost table, based on encountered resistance (Bonnaventure & Lamoureux, 2013). However, this method varies in effectiveness based on the physical strength of individual researchers and coarseness of the soil matrix. Frost probe tests are often impossible or effectively useless in sites with thin or nonexistent soil profiles or highly coarse substrates, such as those found in polar deserts, periglacial facies, mountain sides, and rock glaciers. Additionally, testing with a frost probe is insufficient to make observations over a widespread area because each individual test covers such a small area. It is also important to note that for monitoring the effects of climate change, it is more accurate to determine the maximum depth of the 0°C isotherm, rather than the physical depth of frozen ground, due to the potential for unfrozen cryotic materials because of salinity or pressure (Guglielmin, 2006). This procedure should be performed during late summer to allow for the maximum amount of thawing degree days, and therefore the greatest depth of active layer thickness (Bonnaventure & Lamoureux, 2013).

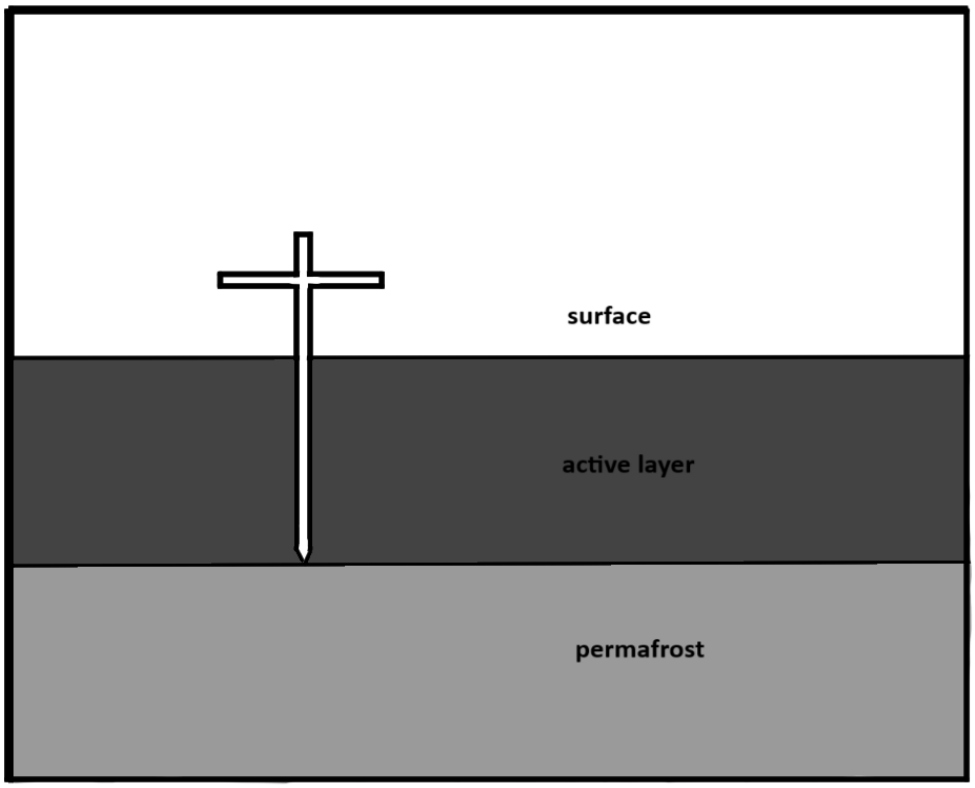

Fig. 2.8. A schematic diagram of a frost probe. The frost probe penetrates to the base of the active layer, but may be hindered by tree roots, gravel, or large clasts.

2.5.1.2. Thaw tubes

Thaw tubes, also known as frost tubes, are a direct method of permafrost observation. The instrument consists of two tubes, where the outer tube (usually PVC piping) is anchored within the permafrost body, and the clear inner tube is filled with liquid to determine the limits of seasonal thaw depth (Nixon et al., 1995; Iwata et al. 2012). This method has been in use as early as the 1970's (*e.g.* Mackay, 1973). The maximum thaw depth each year is determined by the position of a marble, which sits on the frozen surface and then descends to the point of maximum thaw (Nixon & Taylor, 1994). This method can also be used to measure changes in ground surface elevation because of the thaw and formation of ground ice, using the same thaw tube instrument to provide a reference height (O'Neill et al., 2023) (Fig. 2.9).

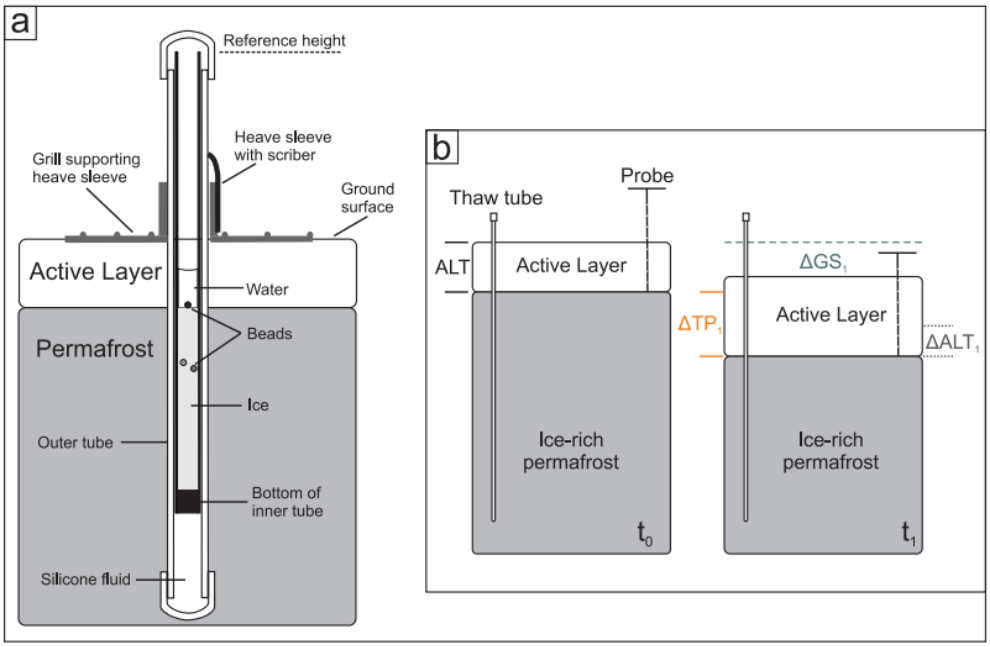

Fig. 2.9. A figure by O'Neill et al. 2023, where a) is a schematic representation of a thaw tube instrument and b) is a conceptual diagram of the influence of ice-rich permafrost thaw on active layer thickness and ground surface height.

The benefit of this method is that it doesn't require daily monitoring by personnel. However, the thaw tubes do need to be visited on an annual basis, as the record of freeze-thaw is destroyed the subsequent year (Smith et al., 2009). The method has been used with success particularly in northwestern Canada. Long term measurements (1991–2016) were taken by O'Neill et al. (2019) in the Mackenzie Delta area of the Northwest Territories, revealing significant permafrost degradation and ground surface subsidence. Similar research using thaw tubes in the same area was conducted by Nixon et al. (1995) and Smith et al. (2009).

2.5.1.3. Ground thermal profiling

Ground thermal profiling is another method of direct permafrost testing. The instrument may be made of different materials, but the main principle is that several sensors are placed at fixed intervals along or inside of a probe, then inserted into the ground (Fig. 2.10). This allows researchers to extrapolate the probability of permafrost at depth using linear regression if cryotic

temperatures cannot be reached directly (*e.g.* Holloway & Lewkowicz 2019, Daly et al. 2022), giving it great value in environments where the likelihood of reaching the frost table is hindered by roots or clasts. However, thermal profiling is a discrete method and is still limited by the number of data points which can be collected in a vast landscape. Furthermore, accuracy of the linear regression may be limited by the number of *in-situ* temperature measurements collected, which may be low if substrate is difficult to penetrate. Other methods of regression, such as exponential, were considered. However, linear regression was chosen to maintain consistency with existing literature.

Fig. 2.10. A ground thermal profiling probe (right) made of an aluminium avalanche probe. Four thermistor wires are strung through the interior, with sensors placed at fixed intervals to record ground temperatures. Photo taken August 2023.

2.5.1.4. CALM Program

The Circumpolar Active Layer Monitoring (CALM) Program was developed through the 1990s by numerous international researchers seeking to collect geocryological data in a remote,

standardised fashion, such that it could be shared freely amongst them (Brown et al., 2000). Data from CALM grids is then stored by the Global Terrestrial Network for Permafrost (GTN-P), with the goal of establishing both an 'early warning' system for consequences of climate change in permafrost regions and to provide standardised data for model input use (Biskaborn et al., 2015).

CALM is a direct method which utilises frost probing. A grid of varying size (often 100x100m or 1000x1000m) is set over the test area, and 100 grid boxes are delineated within (Bonnaventure & Lamoureux 2013). Using a combination of linear and random sampling within the grid, researchers collect thaw depth data using a frost probe, after which the results can be plotted in a GIS program (Bonnaventure & Lamoureux 2013). Optionally but optimally, researchers may also include air and ground temperature monitors or other secondary permafrost verification techniques (*e.g.* thaw tubes) to strengthen their dataset (Bonnaventure & Lamoureux 2013). CALM Grids can be found in both the Arctic (*e.g.* Tarnocai et al., 2004) and Antarctic (*e.g.* Ramos et al., 2007), but because it relies on ground penetration, it is challenging to deploy in mountains and other hard or clast-rich substrates (Sudakova et al., 2021).

2.5.1.5. Boreholes

Boreholes (Fig 2.11) are the most commonly employed method for monitoring permafrost thermal state and response to climate change because they provide high-quality, long-term sequence data (Noetzli et al., 2021). However, although the data they provide is detailed, it is still discrete point data about a singular spot in a vast landscape (Mühll et al., 2002). Though they are effective in even mountain permafrost, deploying them is difficult due to remoteness, operational difficulties, and cost (Mühll et al., 2002). Furthermore, there is currently no accepted standardised method for deploying boreholes in mountains (Noetzli et al., 2021).

Fig. 2.11. An example of a permafrost borehole, located in Red Creek, Yukon. The borehole has been stabilised with metal piping. Photo taken August 2022.

2.5.2. Indirect methods

Indirect methods of permafrost detection rely on identifying signals of subsurface cryotic temperatures, rather than the permafrost itself. Negative mean annual ground surface temperature (MAGST) has historically been used as a proxy for permafrost presence, though the effectiveness of this has been debated (Way & Lewkowicz, 2018). Geophysical methods are also used effectively because they can continuously characterise the subsurface over a large area at relatively low cost (Kneisel et al., 2008), although they are not without limitations.

2.5.2.1. Electrical resistance tomography (ERT)

Electrical resistance tomography (ERT) is an indirect geophysical technique used to detect permafrost by measuring the electrical resistivity of the subsurface (Buckel et al., 2021). The results can then be displayed as a profile of different resistivities, with higher resistivities representing zones of frozen ground (*e.g.* Holloway & Lewkowicz, 2019) (Fig. 2.12). Resistivity is the opposite of conductivity. ERT functions because resistivity increases significantly when materials freeze, due to the phase change from electrically conductive water to less conductive ice (Kneisel et al., 2008). During ERT surveys, multiple electrode configurations are used to collect resistivity data, forming a two-dimensional representation of subsurface conditions along a profile (Kneisel et al., 2008) (Fig. 2.13). The process involves injecting electrical currents into the ground via two electrodes, generating a resistivity distribution that varies according to the conductivity of the materials below the surface (Buckel et al., 2021). ERT has been used to characterise numerous different periglacial landforms, such as talus slopes (Kenner et al., 2017), protalus ramparts (Scapozza, 2015), and rock glaciers (Onaca et al., 2015; Buckel et al., 2023). However, the standard equipment for deploying an ERT survey involves the control unit, cables, several steel spikes, salt, hammers, canisters, and potentially large amounts of water, making it challenging to transport all necessary equipment up large and remote slopes (Buckel et al., 2023).

Fig. 2.12. An example of an ERT control unit in operation at the Takhini River Thaw Slump, YT. Photo taken June 2024.

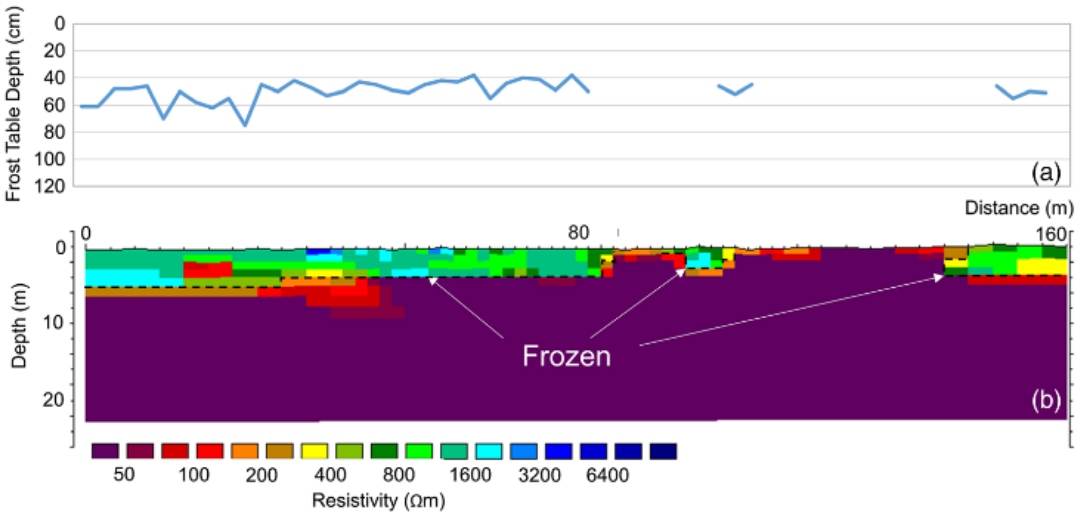

Fig. 2.13. An example of an ERT profile generated by Holloway & Lewkowicz (2019). It depicts a 160-metre-long permafrost survey, where resistivity values >350 MΩm are interpreted as frozen ground. © 2019 John Wiley & Sons, Ltd.

2.5.2.2. Ground-penetrating radar (GPR)

Unlike ERT, GPR functions by detecting differences in dielectric permittivity rather than electrical resistivity (Kniesel et al., 2008). It operates by generating high-frequency

electromagnetic pulses into the shallow subsurface (~<50 m) and recording the reflection and reception of that energy (Neal, 2004). For the purposes of permafrost research, GPR identifies the boundary of frozen and unfrozen materials at the top of the frost table, thereby allowing it to detect the thickness of the active layer (Gusmeroli et al., 2018). It can also identify ice wedges and ice lenses (Hinkel et al., 2001) and map bedrock depth, stratigraphy, water depth, and ice thickness (Davis & Annan, 1989; Campbell et al., 2018) (Fig. 2.14). The lack of need to penetrate the ground makes GPR a more ideal candidate for permafrost investigations in mountains, but it can be difficult to deploy in those locations due to remoteness and physical labour requirements. It has commonly been used to improve data collection at CALM grids (*e.g.* Hinkel et al., 2001; Sadurtdinov et al., 2019).

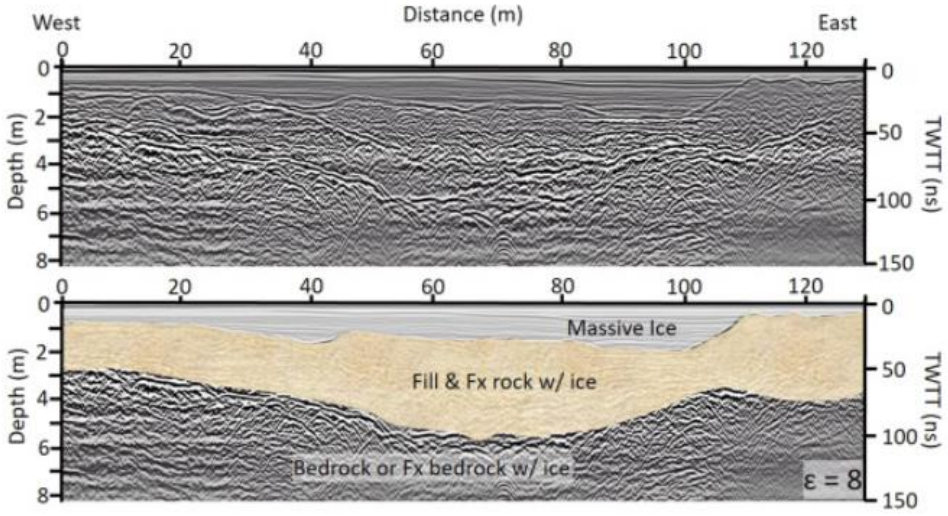

Fig. 2.14. An example of a GPR output with interpretation by Campbell et al. (2018), identifying a stratified ice-rich matrix and bedrock at McMurdo Station, Antarctica.

2.5.2.3. Satellite remote sensing

Several methods of satellite remote sensing can be applied to indirect permafrost detection, and numerous applications can be used to obtain high resolution data of difficult-to-access periglacial environments (Rouyet et al., 2019). Among many others, these techniques include time series image acquisition (Nitze et al., 2018), SPOT panchromatic imagery (Lewkowicz & Duguay, 1999), passive microwave sensing (Jiang et al., 2020), light detection and ranging (LiDAR) (Chasmer & Hopkinson, 2017), and airborne electromagnetic survey (Rey et al., 2019). Useful products include snow cover extent and depth, surface albedo and wetness, soil moisture, land cover type, and Normalised Difference Vegetation Index (NDVI) (Zhang et al., 2011). However, the use of satellite data for monitoring permafrost proxies has primarily been demonstrated on local to regional scales, with limited application at larger scales due to a lack of consistency in data acquisition and demands of resolution (Bartsch et al., 2023). Limitations on resolution are especially problematic in mountainous regions and in the discontinuous zone due to thermal heterogeneity (Westermann et al., 2014).

One method of satellite remote sensing frequently used to monitor permafrost is differential interferometric synthetic aperture radar (InSAR), a technique which detects surface displacements by analysing the difference in phase information from repeat radar acquisitions (Gabriel et al., 1989; Zwieback et al., 2024). InSAR is especially useful in lowland permafrost areas due to the frequency of large accumulations of ground ice (Strozzi et al., 2018) because it can be used to detect thermokarst disturbances such as frost heave and subsidence (Rouyet et al., 2019). It has seen frequent use in areas rich in ground ice, such as in the United States (Alaska) (Liu et al., 2015), Canada (Yukon) (Chen et al., 2016), Svalbard (Rouyet et al., 2019), China (Wang et al., 2019), and many others. However, inSAR cannot be used in dry permafrost bodies, such as in mountains or polar deserts, because these environments lack water and ice.

2.6. Gaps and areas for future work

There are a multitude of potential methods available for detecting permafrost and validating permafrost models, each with their own advantages and disadvantages. However, there is currently no recognised standard approach for doing so. The issue also becomes increasingly complex in regions of high thermal heterogeneity, such as in mountains or in the discontinuous permafrost zone. As a result, when permafrost model validation does take place, the method of validation is usually chosen based on the limitations of the site. This lack of standardisation poses a challenge for circumpolar models, as it is impossible to account for all variables, and many models also suffer from a lack of *in-situ* validation measurements.

CHAPTER 3: RESEARCH ARTICLE

EVALUATING VALIDATION POTENTIAL OF PERMAFROST MODELS THROUGH PHYSICAL AND THERMAL TESTING IN COMPLEX MOUNTAIN TERRAIN, YUKON, CANADA

Authorship: Ria Nicholson[1], Philip P. Bonnaventure[1], Nick C. Noad[1], Rabecca Thiessen[1] & Will Kochtitzky[2,3,4]

Manuscript planned for submission to: *Permafrost and Periglacial Processes*

[1] Department of Geography and Environment, University of Lethbridge, Lethbridge, Alberta, Canada, T1K 3M4.

[2]Climate Change Institute, University of Maine, Orono, ME, USA

[3]Department of Geography, Environment and Geomatics, University of Ottawa, Ottawa, ON, Canada

[4]School of Marine and Environmental Programs, University of New England, Biddeford, ME, USA

Key words: permafrost, thermal heterogeneity, permafrost model validation, ground truthing, ground thermal profiling, Yukon, Dempster Highway

ABSTRACT

The impacts of permafrost thaw on infrastructure, land stability, and carbon emissions are well-documented. However, accurately delineating permafrost distribution is challenging due to its subsurface nature. Unlike sea ice and glaciers, permafrost cannot be directly observed with the naked eye or optical remote sensing, resulting in a reliance on predictive models. These models are constrained by limited baseline data on permafrost thermal state, particularly in mountainous regions where high thermal heterogeneity exceeds the resolution of large-scale models. As a result, many permafrost models have limited validation or lack this all together. To address this, we conducted ground-truthing tests in two thermally complex valleys in a subrange of the Ogilvie Mountains. The explicit goal was to address the feasibility and ease of testability in these complex environments. A ground thermal profiling probe was used at 74 cryotic assessment sites (CAS). Although the area is within the zone of continuous permafrost, only nine of the CAS tests produced cryotic temperatures *in-situ* due to active layer thickness exceeding the probe's maximum inserted length. A simple linear regression analysis estimated the likelihood of cryotic temperatures at depth. Overall, the CAS results were in good agreement with two locally calibrated models. Tests were deemed unsuccessful if the probe failed to penetrate beyond 45 cm. Metrics of test success/failure informed a generalized linear model predicting the probability of conducting a successful permafrost test (P(TEST)) elsewhere in the subrange. The landscape exhibited polarized testability. Low P(TEST) values were concentrated at high-elevations and ridgetops and high P(TEST) values concentrated in valley bottoms, highlighting the uncertainty still associated with mountainous permafrost environments.

3.0 INTRODUCTION

It is widely accepted that permafrost thaw is being driven by anthropogenic climate change (Schuur et al., 2008; Streletskiy et al., 2015), with increased warming occurring in the circumpolar Arctic (Masson-Delmotte et al., 2013) and in mountainous regions (Haeberli et al., 1993; Kohler et al., 2010). The resultant permafrost degradation has made significant contributions to greenhouse gas emissions (Schuur et al., 2015), decreased the stability of critical infrastructure (Burn et al., 2015; Hjort et al., 2022), increased the transport of pollutants and heavy metals (Schaefer et al., 2020), and jeopardized the security of food and drinking water in northern communities (Yang et al., 2016). In mountainous permafrost environments, there is also an increased risk of destructive slope processes, such as landslides and retrogressive thaw slumps (Lantz & Kokelj, 2008; Haeberli et al., 2017). However, monitoring these issues is challenging due to uncertainties surrounding permafrost distribution and ground thermal state on local and regional scales.

Permafrost is a subsurface, temporal, thermally defined phenomenon (Dobiński, 2011), which makes it challenging to observe directly and consistently. Although permafrost is estimated to underlie approximately 15-24 % of the Earth's terrestrial surface (Zhang et al., 2000; Obu et al., 2019), delineating the specific "boundaries" of permafrost is difficult because it is an attempt to map a condition, not a substance (Hegginbottom, 2002). Furthermore, unlike the other two major portions of the cryosphere (sea ice and glaciers), permafrost cannot be monitored with optical remote sensing (Duguay, 2005; Kääb, 2008; Westermann et al., 2014; Obu et al., 2019; Bartsch et al., 2023) and is not considered to be a "space-observable" Essential Climate Variable (ECV) by the Global Climate Observing System (GCOS, 2016). Although it is possible to use optical remote sensing to detect diagnostic features of permafrost (*e.g.* polygonal patterned

ground), these are not always present. This is especially true in dry or "ice-poor" permafrost bodies, where earth materials are perennially cryotic but lack the free water and ice essential to the formation of aggradational features or thermokarst expressions (Harris, 1981; Bockheim & Tarnocai, 1998). Even in mountains where ice-rich permafrost is present, estimating its coverage is challenging (Cable et al., 2018).

Numerous models have been developed to address this issue, but comparatively few undergo any kind of field validation. This is problematic for several reasons. Firstly, natural systems such as permafrost and surface energy balance are inherently variable and have a near infinite number of inputs. Comparatively, models are idealised representations of reality that describe the elements of the system in conceptual or mathematical terms (Inkpen, 2005). Essentially, models can only be as accurate as the parameters constraining them, but *in-situ* observations of permafrost are notoriously spatiotemporally fragmented (Anisimov & Zimov, 2021). This lack of data that would otherwise inform permafrost models increases uncertainty regarding both extent and ground thermal state (Woo et al., 2008; Koven et al., 2013), which in turn increases uncertainty about the future impacts of climate change. Secondly, physically based models are often validated with environmental variables which vary strongly within grid cells, resulting in potential bias (Gubler et al., 2011).

Obtaining *in-situ* permafrost measurements is labour intensive, regardless of the chosen method. This is especially true in highly remote areas, where site access is limited by both distance and environmental hazards. There is also the issue of substrate, which may be too hard or clast-rich to allow enough penetration to take meaningful thermal measurements. Boreholes can solve this problem and provide extremely valuable long-term sequence data, but deploying them is difficult due to remoteness, operational difficulties, and cost (Mühll et al., 2002).

Furthermore, discrete data points are limited in their capability to describe a vast landscape comprehensively, especially in thermally heterogeneous terrain where discrete points are unlikely to capture the degree of variations present.

Thermal heterogeneity in the landscape is caused by numerous micro- and meso-scale factors, including geology, substrate, substrate moisture content (Nelson et al., 1997; Riseborough et al., 2008), vegetation coverage and species (Shur & Jorgensen, 2007), elevational cooling, aspect and topographic shading (Etzelmüller, 2013), and snow cover (Kremer et al., 2011). This can cause permafrost to vary significantly over short horizontal distances (Bonnaventure et al., 2017), even in High Arctic environments which are usually considered to have homogeneous permafrost coverage (Garibaldi et al., 2021). Thermal states can also be heterogeneous, with some near-surface permafrost as cold as -15.0 °C or as warm as 0 °C (Smith et al., 2010). These variable states will alter the response time to climate change and require monitoring.

Although the ability to envision and validate permafrost spatial distribution is necessary for model input (Gruber, 2012; Etzelmüller, 2013), there is still a lack of established methods for effective direct mapping of permafrost on large scales at resolutions sufficient to detect changes (Walvoord et al., 2016). Additionally, there are no standardised global data sets of permafrost observations for model validation (Biskaborn et al., 2019). This has resulted in a high degree of uncertainty regarding the actual conditions of ground thermal state. This issue is especially problematic in mountains (Etzelmüller, 2013) and in the discontinuous zone where patterns of spatial heterogeneity are too fine to be captured by Earth System Models (Shirley et al., 2022). Furthermore, this presents problems when information about permafrost is required for planning and adaptation strategy management at the community level (Daly et al., 2022).

Therefore, the objective of this research is to examine permafrost testability at the local level in the context of model validation through ground truthing. In this context, “ground truthing” refers to the practice of attempting to collect direct temperature measurements to validate predictions made by permafrost models. However, it is worth noting that the word "truth" in this context refers to interpretation, not that the data is perfect (Hargrave, 2006). This study also aims to identify the difficulties associated with permafrost model validation over variable terrain, highlighting the areas most and least susceptible to these issues. To do this, several types of ground truthing (frost probing, digging, and ground thermal profiling) were applied to a vegetatively heterogenous high-latitude mountain study area. Testing was applied to blockfields, organic soils, and forested zones at a variety of elevations throughout the two heterogeneous mountain valleys. Furthermore, this study aims to assess the value of validation in these variable terrain types to expose existing knowledge gaps.

2.0 STUDY AREA

Research for this study was conducted in a subrange of the Ogilvie Mountains, located in the north-central Yukon along the Dempster Highway (Fig. 3.1). This area is classified as sub-Arctic, with short, cool summers and long, cold winters (Dfc) according to the Köppen-Geiger climate index (Peel et al., 2007). The region is dominated by alpine-tundra vegetation (Frappier et al., 2023). The nearest Environment Canada climate station is located approximately 160 km southwest in Dawson City. Climate normals (1991-2020) from this station report seasonal average temperatures ranging from -26.0 °C to 15.7 °C and approximately 360 mm of annual precipitation (with 42.6 % falling as snow) (Environment Canada, 2023). The nearest Global Terrestrial Network for Permafrost (GTN-P) active layer monitoring station is also located in

Dawson City (*see* Streletskiy et al., 2017) and the nearest permafrost borehole is in Red Creek valley (Lacelle et al., 2009; Throop et al., 2012).

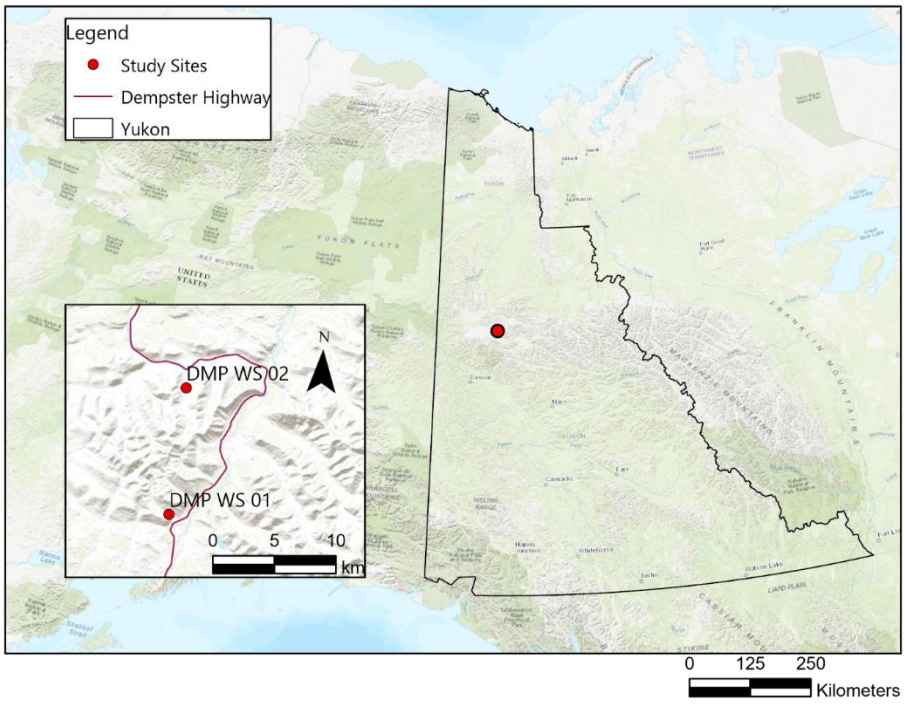

Fig. 3.1. A map of the study area, displayed on the local scale of the Ogilvie Subrange (right) and in the larger Yukon Territory (left). Basemap imagery provided by ESRI (2025).

The Dempster Highway is of special concern for permafrost monitoring because it is the only all-season artery of transportation in the Canadian northwestern Arctic and links the Arctic Ocean coast to the rest of Canada. However, 90 % of its 737.5 km length is built over continuous permafrost, making it vulnerable to damage and deformation (Burn et al., 2015). Despite its significance to surrounding communities, however, a limited number of studies have been conducted assessing the conditions of the local state of permafrost (*e.g.* Idrees et al., 2015; O'Neill et al., 2015).

The subrange of interest in the Ogilvie Mountains is characterised by narrow colluvium walls and experiences intense cold-air drainage (Burn et al., 2015). This region has not been glaciated since the Mid-Pleistocene (2.6 Ma to >200 Ka), leaving it uninsulated from the cold air of the Last Glacial Maximum (Duk-Rodkin, 1996; Duk-Rodkin, 1999). Resultant *in-situ* bedrock weathering of the mountainous landscape has caused a prominent portion of the study area being overlain by periglacial facies, also known as felsenmeer (French, 2007). The southernmost portion of the study area is located approximately 13 km north of Chapman Lake. Chapman Lake is the largest of several kettle lakes within the terminal moraine complex in the Blackstone River Valley (Beierle, 2002) and a remnant of the most recent glaciation period.

Focus was placed on two mountain valleys within the subrange which lie adjacent to the Dempster Highway. The study was conducted at these locations due to the presence of an existing comprehensive network of air and ground temperature sensors. Additionally, these valleys have also been the site of recent air, ground surface, and permafrost distribution modelling using the Temperature at the Top of Permafrost (TTOP) model (Garibaldi et al., 2024a; 2024b). The network includes ground temperature nodes (GTNs), and air temperature sensors laid in elevational transects, deployed to monitor surface-based temperature inversions (SBIs) and the impact to permafrost distribution (see Noad & Bonnaventure, 2022; 2024; Garibaldi et al., 2024a; 2024b). Heginbottom et al., (1995) classified the area as having extensive-continuous permafrost (50-90 % permafrost coverage) with medium to low ground ice content (<10 %-20 %). O'Neill et al., (2019) also mapped the area to have negligible ground ice. Brown et al. (2000) modelled the area to have extensive-continuous permafrost albeit at a course scale, showing little topographic variability. Probability modelling on the study area was also done by Bonnaventure et al. (2012), which saw permafrost probabilities decreasing at middle

elevations, particularly on south-facing slopes, and increasing at high elevations and in valley bottoms as a response to the presence of SBIs (Bonnaventure and Lewkowicz, 2013). Most recent attempts are still in good agreement (Garibaldi et al., 2024a) with SBI patterns influencing permafrost distribution but at a much finer and localized level of detail.

For the purposes of this study, the southern valley is called Weather Station Valley 01 (WS01) (unofficial name) (64°57'N, -138°16'W) and the northern valley is called Weather Station Valley 02 (WS02) (unofficial name) (65°02'N, -138°16'W) (Fig. 3.1). They are located approximately 10 km apart, with dissimilarities of orientation, vegetation type and coverage, fetch length, and geometry (Noad & Bonnaventure, 2022). Forest cover is largely coniferous and dominated by black spruce *(Picea mariana).* Other vegetation species observed include Labrador tea *(Rhododendron groenlandicum),* field horsetail *(Equisetum arvense),* dwarf birch shrubs *(Betula nana),* net-leaved willow shrubs *(Salix reticulata),* alpine bearberry *(Arctostaphylos spp.),* bog bilberry shrubs *(Vaccinium uliginosum),* and black crow berry *(Empetrum nigrum).*

WS01 (Fig. 3.2) is a V-shaped, eastern-facing mountain valley bisected by a creek with a fetch length of 5.3 km. Average annual mean air temperature (AMAT) for the WS01 valley is modelled to be –6.4 °C (2019–2021) (Garibaldi et al., 2024b). The south-facing slope is forested, with vegetation prominently featuring black spruce and thick *Sphagnum spp.* mosses growing over felsenmeer. The north-facing slope is untreed felsenmeer, sparsely vegetated with some soil development in eroded drainage channels on the slope. Per a supervised land cover classification, WS01 is overlain by 59.1 % felsenmeer, 25.7 % herbaceous, and 15.2 % forest.

WS02 (Fig 3.3) is a U-shaped valley with a north-facing orientation and a 4.7 km fetch length. Despite its proximity to WS01, it differs considerably in terms of vegetation. A small number of trees are present near the road and cluster around the creek which bisects the fetch at

the mouth of the valley but are otherwise absent. Instead, the valley floor is thickly vegetated by *Sphagnum spp.* mosses and grassy hummocks. Average AMAT for the WS02 valley was modelled to be –5.1 °C (2019–2021) (Garibaldi et al., 2024b). The land cover classification indicates WS02 is covered by 68.8 % felsenmeer, 28.2 % herbaceous, and 3.0 % forest.

Although permafrost is estimated to be continuous in this region (Heginbottom et al., 1995; Brown et al., 2000), recent localised studies (Garibaldi et al., 2024a) have modelled more variable permafrost distribution within the valleys, especially in WS01. This is due to the strong thermal heterogeneity inherent to mountainous environments (Haeberli et al., 1993), which is generated by topographic shading (Etzelmüller, 2013), SBI frequency (Bonnaventure & Lewkowicz, 2012), and differential land and vegetation cover (Shur & Jorgensen, 2007). These factors create greater uncertainties regarding permafrost distribution which may not be captured by even high-resolution models.

Fig. 3.2. Aerial imagery of WS01 produced by a drone in the study area in August 2023, facing eastwards down the valley fetch. Image by Dr. Philip Bonnaventure.

Fig. 3.3. Aerial imagery of WS02 produced by a drone in the study area in August 2023, facing southwards down the valley fetch. Images by Dr. Philip Bonnaventure.

3.2 METHODS

3.2.1. Temperature network

Since 2017, WS01 and WS02 have been equipped with an annually expanding network of air and ground temperature sensors. The network includes several elevational transects of over 100 GTNs, more than 50 air temperature stations, and two main weather stations (HOBO USB Micro Station Data Loggers, accurate within +/- 0.25 °C). The weather stations record wind speed and direction, atmospheric and relative humidity, incoming solar radiation, air temperature, and ground surface temperature (GST) (Fig. 3.4). Most sites are GTN-only, but each air temperature sensor is also associated with a GTN. Each GTN is buried approximately 2-5 cm below the surface (Bonnaventure et al., 2017) and sensors log every two hours. Data

retrieval occurs annually in August. All mean annual air temperature (MAAT) and mean annual ground surface temperature (MAGST) data used in this research was obtained from these sensors.

Fig. 3.4. The weather station in WS02 (right) and an air temperature sensor/GTN site (left).

3.2.2. Cryotic assessment site selection

Prior to the field season, several cryotic assessment sites (CAS) were selected from the larger suite of sites belonging to the temperature networks in WS01 and WS02. Selected sites represent all three prominent land cover types. The CAS were selected to align with the pre-existing climatological network, such that long-term annual time series data of temperature averages and fluctuations would be readily available to compare with the results of *in-situ* testing.

To select appropriate CAS, a database of all temperature network sites in the valleys was compiled. The database includes site photographs, elevation, notes on vegetation and topography, and all available MAGST and MAAT data. Numerous sites in the valleys have what we consider to be highly certain indicators of permafrost, such as subzero MAGST and MAAT in addition to their environmental conditions (*e.g.* felsenmeer or highly insulating mosses). MAGST ≤0 °C was used as a proxy to indicate suspected permafrost presence (Luo et al., 2018), with some exceptions. At sites where MAGST was slightly greater than 0 °C (*e.g.* 0.1-0.9 °C) and conditions were favourable for environmentally protected permafrost (Shur & Jorgensen, 2007), we considered these sites "permafrost marginal". Therefore, additional testing focus was set on permafrost marginal sites, with the goal of discerning which locations could be potentially problematic in the future if testability is low. Additional focus was placed on permafrost marginal sites because they represent the greatest possible point of uncertainty in the landscape.

The distribution of CAS was limited by access, due to time constraints and difficulty associated with traversing the terrain. In the field, an additional 15 CAS were selected impromptu to improve resolution. These sites were more accessible but lack an associated logger, meaning that they do not have MAGST data associated with them. Two of the sites (referred to as GT8 and GT12) were chosen because they represent areas of visible thaw disruption in the landscape.

The herbaceous land cover type (Fig. 3.5) is defined by thick mats of vegetative materials, primarily *Sphagnum spp.* mosses, tundra grasses, foliose lichens, and earth hummocks. Earth hummocks are sub-meter circular mounds which develop in fine-grained frost-susceptible sediments (Mackay, 1980) and can be indicative of cryoturbation (Verret et al., 2019). Sparse tree cover may be present, but individuals are few (i.e., less than three within one meter of the

site) and do not dominate the landscape. These sites tend to be low-lying and poorly-drained, with large offsets between the MAGST and MAAT. Such offsets are well-documented in the Yukon Territory (Burn & Smith, 1998; Lewkowicz et al., 2011) and occur due to a disconnect between the atmosphere and the ground surface. The disconnect is generated by the thermal buffering effect of insulative mosses (*e.g. Sphagnum*). The high porosity of such mosses (O'Donnell et al., 2009) causes their thermal conductivities to vary with moisture or state (Gornall et al., 2007). Dry mosses in summer reduce downward heat conduction whereas wet mosses in shoulder or freezing seasons increase upward heat conduction (Burn & Smith, 1998, Fisher et al., 2016). This dampens temperature fluctuations at the ground surface level (Fisher et al., 2016) and may result in "ecosystem-protected" permafrost (Shur & Jorgensen, 2007) with slow response times to change (Bonnaventure & Lamoureux, 2013). Such ecosystem-protected permafrost can be sustained in an environment where the MAGST is greater than 0 °C (Smith & Riseborough, 2002), and this was a key consideration during site selection.

Fig. 3.5. An example of the herbaceous land cover class and the hummocks which form due to cryoturbation in this landscape.

Forest (Fig. 3.6) is the least common land cover type across both valleys, accounting for a total of 18.17 %. Most of this land cover type is located on the south-facing slope of WS01, with minor clustering around a widened portion of the ephemeral stream in WS02. Ground surface conditions vary in this zone between rocky mineral soils and thick vegetative cover, such as that which is seen in the herbaceous zone. However, the distinction was made between them due to the potential for alterations in permafrost presence due to shading and snow accumulation.

Fig. 3.6. A portion of the forested zone of WS01, approximately 10 meters from the WS01 Weather Station at an elevation of 980 meters. The felsenmeer land cover type can be seen in the distance.

Felsenmeer (Fig. 3.7) as a category is predominantly restricted to the slopes and ridgetops which are present in both valleys and was defined by the presence of large, irregularly sorted frost-shattered clasts. Surficial geologies in WS01 and WS02 include a bedrock of black shales and laminated siltstones, while the valley walls are weathered dolostone and limestone (Yukon Geological Survey, 2022; Noad & Bonnaventure., 2022). Felsenmeer may also be partially

vegetated by thin grasses, mosses, or lichens, or have a shallow soil profile (Fig. 3.8). Felsenmeer land cover is frequently associated with negative temperature anomalies relative to surrounding bedrock or fine-grained sediments (Harris & Pederson, 1998, Juliussen & Humlum, 2008). Therefore, they also tend to preserve buried ice or permafrost in otherwise unsuitable climatic conditions (Sawada et al., 2003). However, it is largely impenetrable to human-powered physical instruments.

Fig. 3.7. Unvegetated felsenmeer on the north-facing slope of WS01 and black spruce forest on the south-facing slope.

Fig. 3.8. Partially vegetated felsenmeer, with tundra grasses and a shallow soil profile.

3.2.3. Ground thermal profiling and data collection

Data collection was performed over the course of two weeks in August 2023, close to the annual period of maximum active layer thickness (ALT). This decreased the likelihood that any encountered cryotic temperatures were the remnants of seasonal freezing and not true permafrost. Data retrieval was done on foot, using the Dempster Highway as an access point.

The primary method of ground truthing at the CAS for this study is ground thermal profiling, previously used by Bonnaventure & Lewkowicz (2008), Léger et al. (2019), Holloway & Lewkowicz (2020), and Daly et al. (2022). Ground thermal profiling can serve as both a direct and indirect method of permafrost detection. While direct methods of permafrost detection obtain a temperature measurement, indirect methods extrapolate permafrost presence based on other indicators.

As a direct method, ground thermal profiling can be used to identify cryotic temperatures at depth using a probe, within which sensors are placed at fixed intervals. Indirectly, this allows researchers to extrapolate the likelihood of cryotic temperatures at depth using linear regression if they cannot be detected directly due to ALT or interference in the substrate. Therefore, this method has great value in environments such as this one where the likelihood of reaching the frost table is reduced by roots or clasts. However, ground thermal profiling is a discrete method and is still limited by the number of data points which can be collected in a vast landscape.

The probe used for this study was constructed from an aluminium avalanche probe. Three thermistors were secured at 25 cm fixed intervals within the probe, with the lowest being at the bottom (Fig. 3.9). Holes were drilled into the probe where the thermistors were fixed to reduce interference by insulation. Ice-point calibration testing determined the sensors to be accurate

within +/- 0.3 °C. In the field, the thermistors were connected to an ONSET 4-Channel Analog MX1105 logger (±0.3% accuracy).

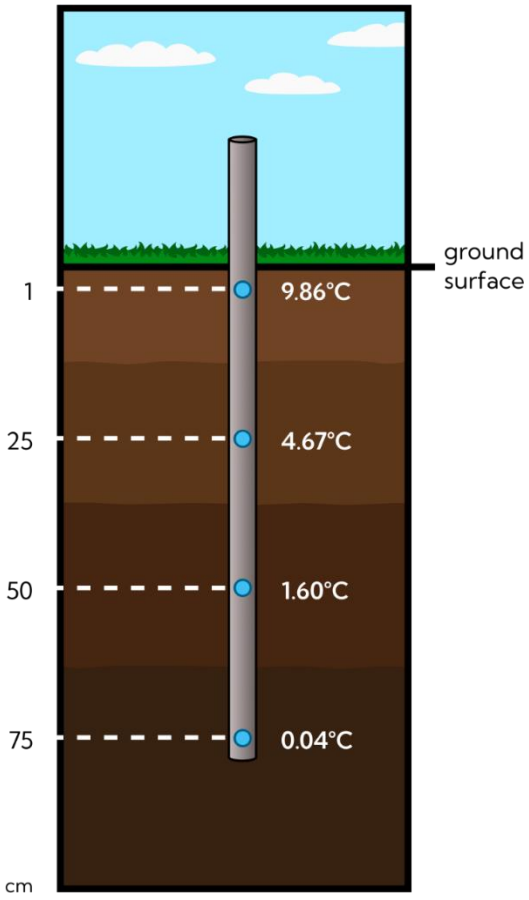

Fig. 3.9. A schematic of the ground thermal profiling instruments with example temperatures to demonstrate the procedure.

Site observations included aspect, substrate type, and vegetation. Geographic location was recorded using waypoint averaging using a Garmin eTrex 10 Worldwide Handheld GPS Navigator (accuracy 1-4 m). Upon arrival at each site, a steel frost probe and hammer were used to make a pilot hole for the ground thermal profiling probe. All pilot holes were made within 1 metre of the local GTN, on the same surface type (*e.g.* moss, felsenmeer, mineral soil). The pilot hole was driven to the maximum possible depth, determined either by the presence of clasts, tree roots, or the frost table. A depth measurement was then taken, excluding any overlying

vegetative materials such as moss. A fourth thermistor was placed 1 cm below the ground cover to take the surface temperature without the influence of direct solar radiation. The four thermistors remained in the ground until all channels reached equilibrium (<0.1°C change per minute, to a maximum of fifteen minutes (Holloway & Lewkowicz, 2020)). The 0.5 °C isotherm was used as a permafrost-positive indicator, due to the impenetrability of the frost table / 0 °C materials, as per Lewkowicz & Ednie (2004).

3.2.4. Field data processing

At the majority of CAS, cryotic temperatures were unable to be reached directly due to presence of impeding materials (clasts, tree roots) and potentially the thickness of the active layer. In these cases, permafrost temperature at depth was extrapolated using field measurements and a simple linear regression equation (Equation 3.0) in R Studio (v.4.4.1.).

$$\textbf{Depth} = 0 - \beta_0 / \beta_1 \qquad \textit{Equation 3.0.}$$

Where β_0 is the intercept (temperature at depth = 0) and β_1 is the slope, or rate of temperature change with depth.

This process extrapolates the possibility of reaching the 0 °C isotherm within the first three metres of earth materials. If the equation did not predict the cryotic isotherm within the first three metres, the site was considered not to contain permafrost. Rocky environments such as felsenmeer can have very thick active layer depths (up to five meters deep) (Isaksen et al., 2000; Bonnaventure & Lamoureux, 2013), but three meters was chosen because the instrument's capability is limited in extrapolating deeper due to the low number of sensors to inform the gradient.

Where available, MAGST was also considered when deciding about permafrost presence or absence at sites where cryotic temperatures were not reached *in-situ* (Fig. 3.10). We considered sites with an MAGST ≤0 °C as being highly likely to have permafrost present, as this area has not experienced wildfire or other environmental disturbances.

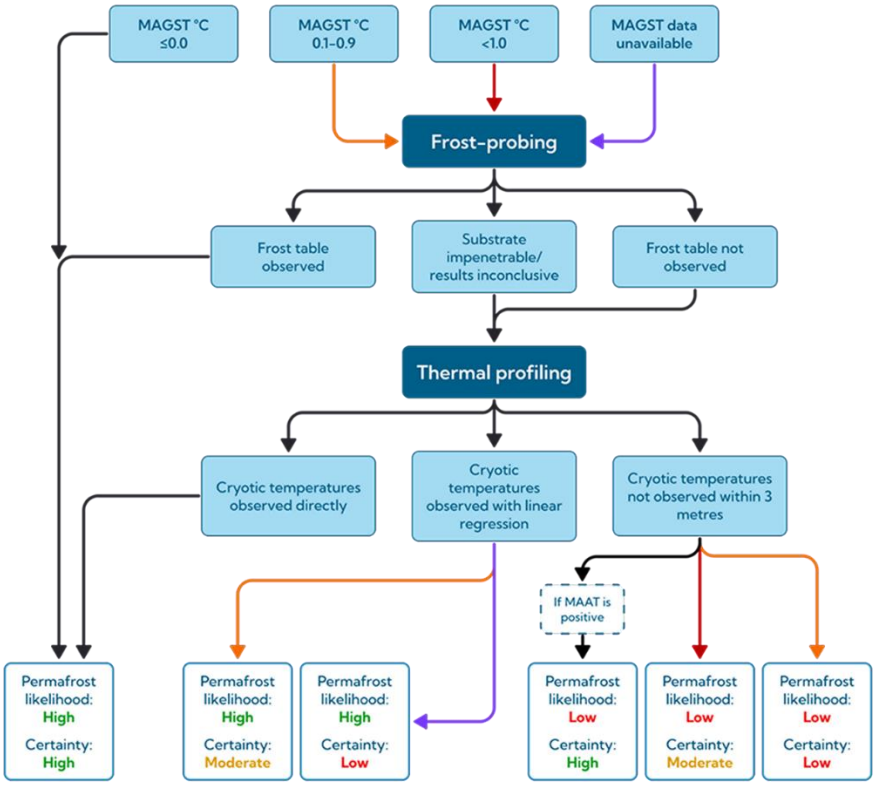

Fig. 3.10. A flowchart demonstrating the decision-making process regarding permafrost presence or absence at CAS.

3.2.5. Probability surface generation

The next objective was to generate a probability surface of permafrost testability P(TEST) which can be applied to the larger subrange of the Ogilvie Mountains. At this stage, permafrost presence or absence was not considered. The main metric of consideration was whether each test at sampled CAS was successful or not. We defined a successful permafrost test as reaching a minimum of 45 cm below depth (B.D.), because this was the shallowest depth at which cryotic temperatures were recorded. Each CAS was assigned a binary number indicating test success (where 1 = successful test and 0 = failed test). Because a large portion of field testing focused on zones where MAGST was considered permafrost marginal, the data set was imbalanced towards herbaceous class sites. To remedy this, we selected an additional 25 sites from the preexisting network of loggers already known to be untestable. Untestable sites were selected where the soil profile was either absent or extremely shallow with a high density of clasts. The sites were chosen from a range of elevations from both WS01 and WS02.

To create the model, a Digital Elevation Model (DEM) of the study area at 2-meter resolution was used. The DEM was derived from GeoEye optical imagery (Imagery © [2017] DigitalGlobe, Inc.). The Polar Geospatial Center at the University of Minnesota produced the surface model through surface extraction with the TIN-based search and space minimization (SETSM) algorithm (Noh & Howat, 2017). Potentially relevant variables were extracted from the DEM using ArcPro v. 3.3.0. In this version, current to the time of the study, there was no native tool to extract TPI values. Therefore, the Topographic Position Index extension tool (v. 1.3a; Jenness Enterprises, 2006) was used instead.

The DEM-derived variables were tested using a Pearson's correlation statistical test in RStudio (v. 4.4.1.) and determined not to be correlated with one another. The model was then coded using

the "caret" (Classification and REgression Training) package, developed by Kuhn (2008). The package was used to determine which of the variables were significant predictors of a successful test. Field data was then split into a training set for the model (comprising 70 % of the data) and a testing set (comprising 30 %). Probabilities were then produced, ranging from 0.0-1.0, using Equation 3.1., where -y represents elevation variables.

$$\mathbf{P_{TEST} = 1 / (1 + (-y))} \qquad \textit{Equation 3.1.}$$

We then used the Raster Calculator function in ArcPro (v. 3.4.) to generate the probability surface, using the information derived from this equation. The data was then migrated into ArcPro (v. 3.3.0), where the probabilities were used in the Raster Calculator tool to generate a probability distribution surface. The probability distribution surface describes the likelihood of conducting a successful permafrost test as a variable between 0.0 and 1.0. This was then used to compare results with high-resolution local models of permafrost distribution, specifically Bonnaventure et al. (2012) and Garibaldi et al. (2024a).

The Bonnaventure et al. (2012) model is a high-resolution (30 x 30 m) permafrost probability model which covers large portions of northern British Columbia and the Yukon Territory, including the study area. This subrange of the Ogilvie Mountains is located near the northernmost limit of the model extent. It was created with a combination of several other statistical-empirical models and was validated broadly using a combination of discrete ground truthing points and long-term borehole sequence data specific testing areas (8). The closest of these to this study area is in Dawson City, YT. This model categorizes permafrost probability which can then be expressed as continuity classes including sporadic, extensive-discontinuous, or continuous. To compare this model with the results of the P(TEST) model, we considered extensive-discontinuous permafrost to represent the “permafrost marginal” class. No portions of

the study area were predicted to have sporadic permafrost by the Bonnaventure et al. (2012) model.

The TTOP model is considered to generate reasonably accurate spatial distribution maps of permafrost in mountainous regions, including in the Yukon Territory and in northern British Columbia (Bevington & Lewkowicz, 2015). The Garibaldi et al. (2024a) model is a process-based TTOP model derived from *in-situ* climatological data collected from the network over several years. This model categorizes zones of the study area into predicted subsurface temperatures. To compare the Garibaldi et al. (2024a) model with the P(TEST) model, TTOP temperatures were reclassified into temperature intervals of permafrost present (MAGST ≤ 0°C), permafrost marginal (MAGST 0.1-0.9 °C), and permafrost absent (MAGST ≥ 1.0 °C).

3.3. Results

3.3.1. Field Results

The ground-truthing portion of the field research had two main objectives. The first objective was to determine permafrost presence or absence at each CAS. Specific focus was placed on sites deemed "permafrost marginal", where MAGST = 0.1-0.9 °C, to emphasize the importance of identifying zones of low testability and high permafrost uncertainty. The second objective was to test the likelihood of performing a successful ground-truthing test within the study area.

74 CAS were sampled throughout the field season, with 40 tests in WS01 (Fig. 3.11) and 34 tests in WS02 (Fig. 3.12). 36 total tests (48.6 %) were considered successful. Of the successful tests, nine (12.1 %) of the produced cryotic temperatures *in-situ*, and the remaining 27 (36.4 %) were analyzed using a simple linear regression equation to determine the likelihood of

cryotic temperatures being present at depth. The highest elevation that a successful test was conducted was 1212 m, but on average successful tests were clustered towards lower elevations (average 1066 m).

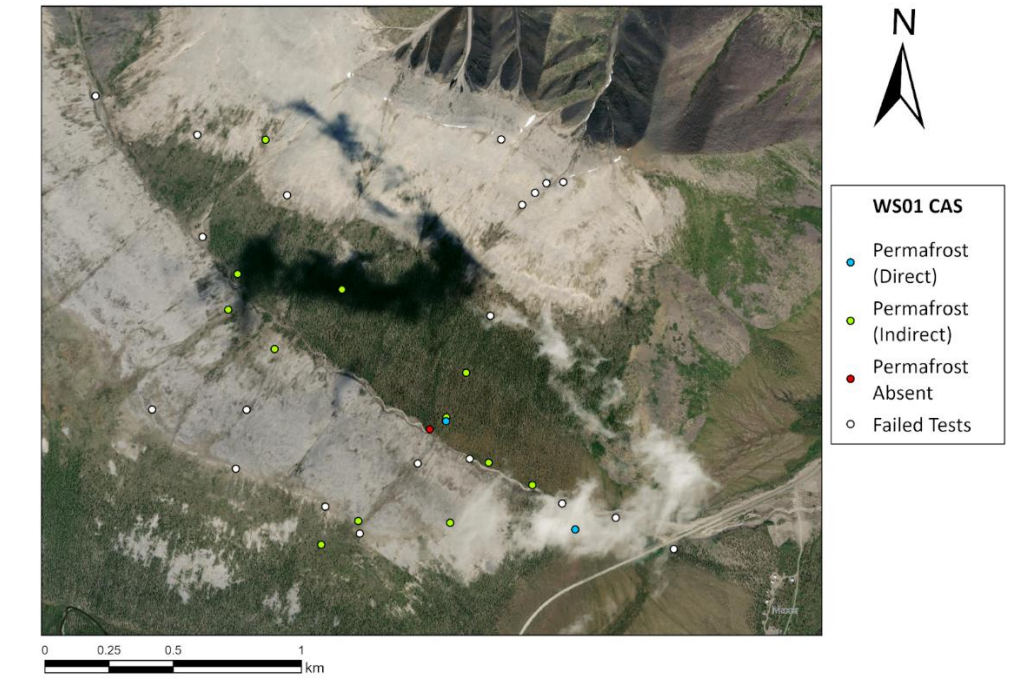

Fig. 3.11. Distribution and results of CAS in WS01. *Basemap Imagery: © Maxar Technologies, Esri, Earthstar Geographics.*

Fig 3.12. Distribution and results of CAS in WS02. *Basemap Imagery: © Maxar Technologies, Esri, Earthstar Geographics.*

3.3.1.1. Permafrost detected directly

The nine CAS which produced cryotic temperatures *in-situ* were all the herbaceous land cover type. The average depth of cryotic materials was 88.7 cm B.D., at a minimum of 45 cm and a maximum of 184 cm (Table 3.0). All the sites except one had a positive MAGST, which ranged from 0.12-0.97 °C. Overall, the sites were constrained to the lower elevations of the valleys, ranging from 531-1132 m elevation at an average of 967.7 m.

Three of the sites (GT 8, GT 12, and GT 14) (Fig. 3.13) were sampled impromptu in the field and are not a part of the pre-existing temperature network in the valleys. Although monitoring thaw-related disturbances was not originally part of the research objectives, they were recorded because they provided key insight into the variable active layer depths present in

the field that could not otherwise be recorded. Therefore, MAGST data is not available for these sites.

Table 3.0. CAS where a successful ground truthing test was performed and near-cryotic or cryotic temperatures were detected at depth.

Site	MAGST (°C)	Min. Temp. at Depth (°C)	Active Layer Depth (cm B.D.)	Elevation (m)
WS01 G16	0.97	0.12	63	959
WS02 G11	0.66	0.04	59	1070
WS02 G25	-1.50	0.23	61	1064
DMP WS02	0.12	-0.04	80	1102
DMP 02	0.98	0.04	74	668
DMP 56	1.05	0.1	45	1069
GT 8	N/A	0.08	165	1132
GT 12	N/A	0.4	68	1087
GT 14	N/A	0.1	184	1080

Fig. 3.13. Site GT8, located in WS02, is an example of the thaw-related permafrost disturbances recorded during the August 2023 field season. Cryotic temperatures below the base of the fissure. No ground ice was visibly present. Gleysol materials with large clasts were found beneath the lifting vegetation.

3.3.1.2. Permafrost detected via linear regression

Of the successful CAS tests, 23 (57.5%) did not reach cryotic temperatures *in-situ* but are predicted to have cryotic materials within three meters of the surface (Table 3.1). The site with the coldest cryotic temperatures *in-situ,* and therefore the most certainty regarding the results of linear regression, was DMP WS01 (Fig. 3.14). This is the weather station site in the southern valley and is located within the herbaceous land cover class.

At felsenmeer land cover sites in this group of tests, minimum ALT ranged from 49-77 cm. At herbaceous land cover sites in this group of tests, minimum ALT ranged from 55-98 cm and projected ALT ranged from 608.8-250.9 cm (average 146 cm). However, predicted ALT (via linear regression) ranged from 134.7-259.6 cm, with an average ALT of 206.2 cm. This is in good agreement with other studies on ALT in similar land cover types (*e.g.* Isaksen et al., 2000; Bonnaventure & Lamoureux, 2013).

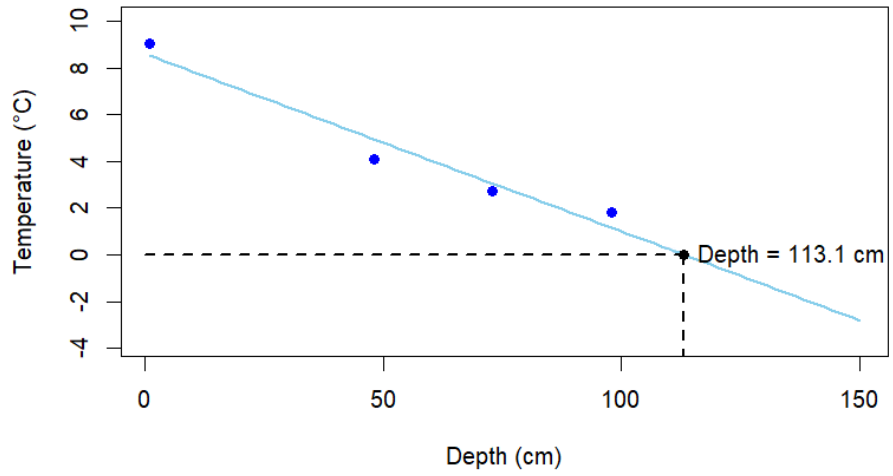

Fig. 3.14. A graph displaying the linear regression analysis performed on site DMP WS01, where the deepest *in-situ* point taken was at 98 cm. The 0 °C is predicted at approximately 113 cm B.D.

Table 3.1. Sites where cryotic temperatures are estimated within 3 metres of the surface, via linear regression.

SITE	MAGST (°C)	Landcover	Min. Temp. at Depth (°C)	Maximum Test Depth (cm)	Predicted Depth of 0°C Isotherm (cm)	Elev (m)
DMP WS01	0.1	Herbaceous	1.8	98	113.1	980
WS01 G04	2.0	Forest	9.7	49	184.2	1211
WS01 G08	-0.3	Felsenmeer	7.8	61	222.3	1046
WS01 G13	0.7	Herbaceous	8.1	69	250.9	1039
WS01 G14	0.4	Forest	5.8	58	132.5	1078
WS01 G21	0.5	Forest	9.6	52	201.1	1189
WS01 G24	-1.6	Felsenmeer	9.9	50	134.7	1103
WS01 G46	0.0	Herbaceous	0.6	83	97.9	978
WS02 G03	-0.2	Felsenmeer	10.2	77	259.6	1071
WS02 G04	0.7	Herbaceous	4.3	70	118.1	1142
WS02 G23	-1.5	Felsenmeer	10.5	55	214.7	1173
WS02 G24	-1.9	Herbaceous	5.3	93	188.2	1064
DMP 09	-1.4	Felsenmeer	7.7	70	235.6	1195
DMP 11	-6.5	Felsenmeer	9.5	55	170.6	1212
DMP 12	-6.8	Forest	4.03	69	87.0	1020
DMP 20	2.33	Forest	9.4	51	235.6	1024
DMP 26	-2.19	Herbaceous	5.4	90	191.7	1141
GT2	N/A	Herbaceous	4.0	74	226.1	976
GT3	N/A	Herbaceous	8.8	71	193.1	970
GT6	N/A	Herbaceous	3.7	55	68.8	1010

GT7	N/A	Herbaceous	1.7	79	94.5	1096
GT11	N/A	Herbaceous	3.5	61	83.3	1101

3.3.1.3. No permafrost detected

Sites were declared as “permafrost absent” when the linear regression equation did not predict crossing the 0 °C isotherm within the first three meters of the surface (Table 3.2). Four of the CAS samples determined to be successful tests produced results that suggest permafrost is not present below the subsurface. The site with the shallowest anticipated cryotic isotherm was DMP 14 (Fig. 3.15).

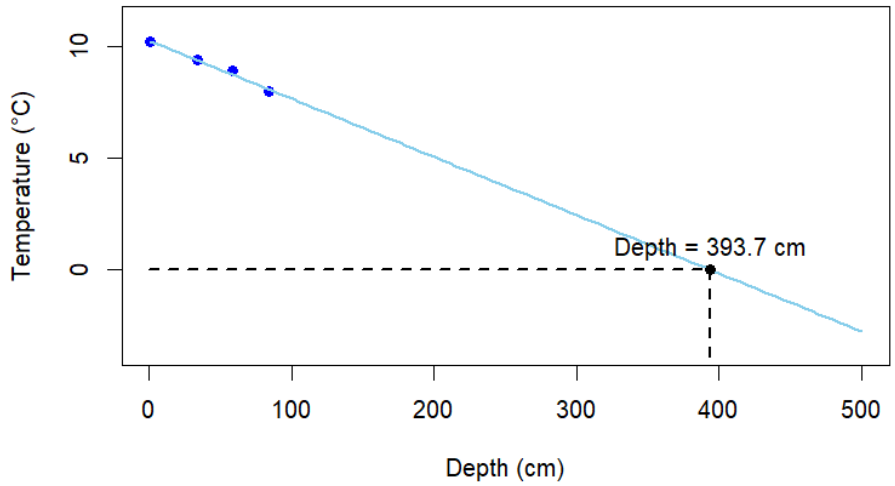

Fig. 3.15. A graph displaying the linear regression analysis performed on site DMP 14, where the deepest *in-situ* point taken was at 84 cm. The 0 °C isotherm is predicted at approximately 393 cm B.D., so the site was declared to be "permafrost absent".

Table 3.2. Permafrost tests determined to be negative via linear regression.

Site	MAGST (°C)	Landcover	Lowest Temp. Recorded (°C)	Max. Test Depth (cm)	Predicted Depth of 0°C Isotherm (cm)	Elev (m)
DMP 14	-1.6	Herbaceous	8.01	84	393.7	1149
DMP 15	-4.1	Felsenmeer	10.42	83	1751.4	1123
DMP 32	-4.9	Herbaceous	8.5	75	699.5	1042
DMP 57	N/A	Herbaceous	10.97	67	727.2	985

3.3.1.4. Failed tests

Of the 74 total CAS sampled, 39 tests were considered to have failed due to not reaching the 45 cm B.D. benchmark (Table 3.3). The average depth achieved at failed sites was 13.1 cm. Sites ranged in elevation from 945-1480 m, with an average elevation of 1202 m. Of all the failed tests, 87.1 % occurred in the felsenmeer landcover type. The majority of failed tests (89.7 %) were at an elevation of greater than 1000 m. Test failures occurred due to the presence of impenetrable substrates, clasts in the subsurface, or tree roots.

Table 3.3. Sites where permafrost testing failed.

Site	MAGST (°C)	Landcover	Max. Test Depth (cm)	Elevation (m)
WS01 G09	-0.68	Felsenmeer	2	1174
WS01 G10	-0.60	Felsenmeer	1	1157
WS01 G17	-1.9	Felsenmeer	26	1274
WS01 G19	0.52	Felsenmeer	1	1155

WS01 G22	0.3	Felsenmeer	32	1270
WS01 G25	-0.95	Felsenmeer	1	1214
WS01 G27	3.2	Felsenmeer	1	1033
WS01 G32	-1.2	Felsenmeer	5	1391
WS01 G35	1.8	Felsenmeer	0	1053
WS01 G38	-2.7	Felsenmeer	0	1432
WS01 G39	-3.2	Felsenmeer	1	1435
WS02 G01	-2.2	Felsenmeer	4	1097
WS02 G08	-2.5	Felsenmeer	24	1097
WS02 G09	-2.3	Felsenmeer	2	1244
WS02 G10	-3.8	Felsenmeer	1	1229
WS02 G13	1.1	Forest	35	1077
WS02 G16	-2.4	Felsenmeer	10	1235
WS02 G17	-3.0	Felsenmeer	1	1227
WS02 G19	-2.8	Felsenmer	2	1154
WS02 G22	-0.9	Felsenmeer	32	1115
WS02 G27	-1.1	Felsenmeer	2	1237
WS02 G28	-0.98	Felsenmeer	6	1358
WS02 G36	-1.2	Felsenmeer	1	1413
WS02 G38	0.68	Felsenmeer	2	1480
DMP 04	1.76	Felsenmeer	26	1132
DMP 06	-2.3	Felsenmeer	1	1195

DMP 10	-1.28	Felsenmeer	15	1352
DMP 13	-0.9	Felsenmeer	31	1046
DMP 16	-2.3	Felsenmeer	32	1477
DMP 19	N/A	Felsenmeer	0	1427
DMP 23	-2.6	Felsenmeer	0	1400
DMP 31	3.54	Herbaceous	19	952
GT 1	N/A	Felsenmeer	15	975
GT 4	N/A	Felsenmeer	39	962
GT 5	N/A	Herbaceous	28	945
GT 9	N/A	Felsenmeer	25	1080
GT 10	N/A	Felsenmeer	37	1092
GT 13	N/A	Herbaceous	18	1081
GT 15	N/A	Felsenmeer	35	1247

3.3.2. Statistical results

3.3.2.1. Analysis of predictor variables

Potentially relevant predictor variables of test success (TPI, aspect, slope, and elevation) were extracted from the DEM. These variables were then tested using a Pearson's correlation statistical test in RStudio (v. 4.4.1.) and determined not to be correlated with one another. Using the caret package (Kuhn, 2008), we employed logistic regression (a type of generalized linear model) to assess the influence of selected predictor variables on the likelihood of test success. Among the variables considered, only elevation was found to be a significant predictor (Table

3.4). Therefore, elevation was the only predictor variable considered going forward in model creation.

Table 3.4. The coefficients table associated with the general linear model produced by the caret package in R Studio.

	Estimate	**Standard Error**	**z value**	**Pr(>|z|)**
Intercept	23.5441905	9.3274613	2.524	0.0116
Land Cover	-0.1031750	0.5790599	-0.178	0.8586
Aspect	-0.0001016	0.0042850	-0.024	0.9811
Slope	-0.0054994	0.0387279	-0.142	0.8871
TPI	1.2661861	1.1235530	1.127	0.2598
Elevation	-0.0201476	0.0078750	-2.558	**0.0105**

3.3.2.2. Testability Model

The probability model of testability was overlaid across the entire subrange and reclassified into probability zones, ranging from 0-100% likelihood of a successful P(TEST) (Fig. 3.16). 44.5% of the subrange falls within the 0-25 % likelihood category, with 33.2 % being in the 0-10 % category. 30.0% falls within the 75-100 % likelihood category. The probability of P(TEST) success increases towards areas of lower elevation.

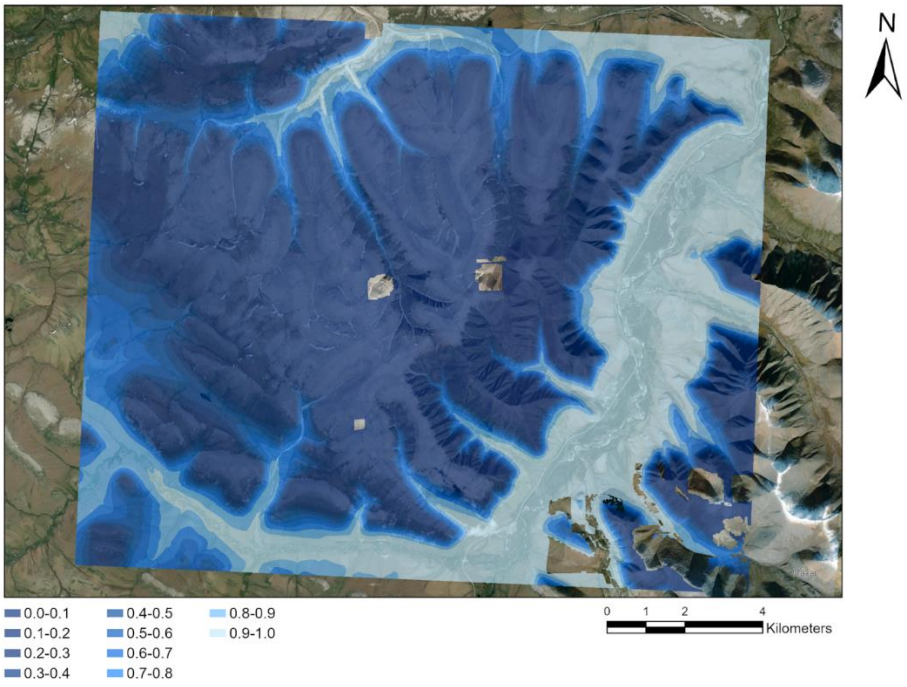

Fig. 3.16. Depicts the probabilities of conducting a successful permafrost test in an expanded zone beyond the original study areas. Areas with no modeled results represent gaps in the DEM. The P(TEST) model layer is set at 50 % transparency for clarity. *Basemap Imagery: © Maxar Technologies, Esri, Earthstar Geographics.*

In both WS01 and WS02, most of the landscape falls either into the extremely low or extremely high P(TEST) probabilities. The majority of WS01 (51.3 %) falls within the range of low testability (0-25 % likelihood), and 26.6 % falls within the range of high testability (75-100 %) (Fig 3.17). The majority of WS02 (68.7 %) falls within the realm of low testability, and only 6.4 % falls within zones of high testability (Fig. 3.18).

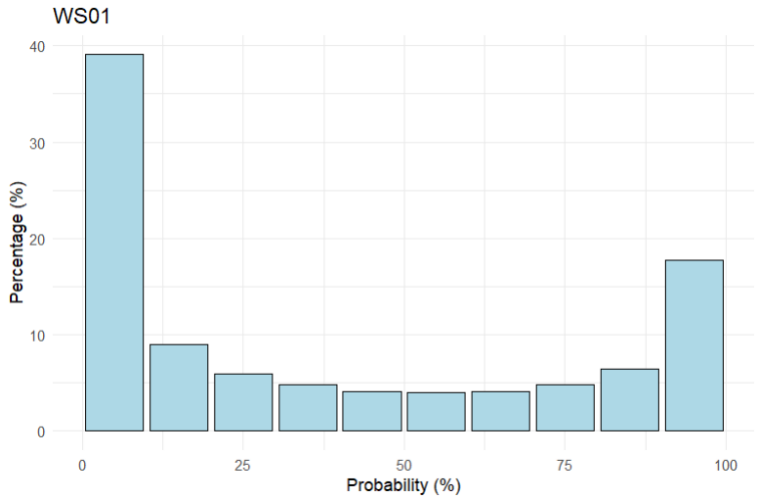

Fig. 3.17. Histogram representing the distribution of probabilities for a successful permafrost test in WS01 against percentage of landscape cover.

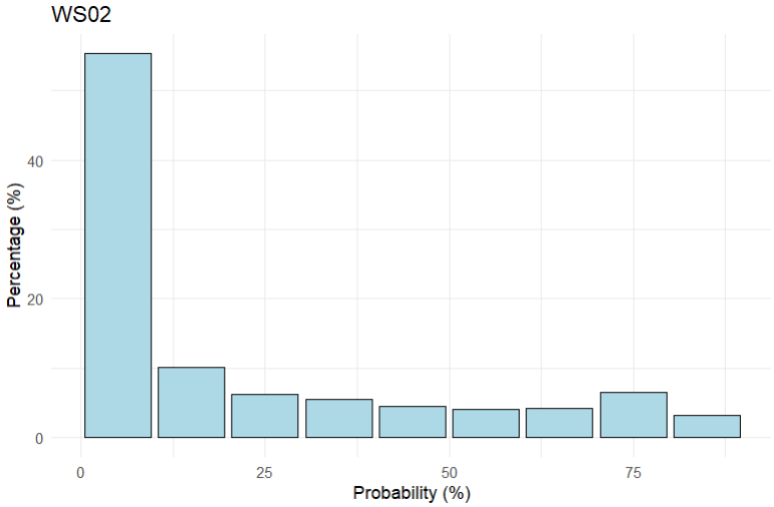

Fig. 3.18. Histogram representing the distribution of probabilities for a successful permafrost test in WS02 against percentage of landscape cover.

3.3.3. Model Comparisons

3.3.3.1. Comparison with Bonnaventure et al. (2012)

The Bonnaventure et al. (2012) model predicts permafrost throughout the study area as a probability value. The lowest probability of permafrost in the overall subrange is 40.0 %. For comparison purposes, we chose 40-70 % probability to represent extensive-discontinuous or "marginal" permafrost. This category covers 75.4 % of the subrange, and the remaining 24.6 % is estimated to be underlain by continuous permafrost (80 - 100% probability).

In WS01, the Bonnaventure et al. (2012) model predicts the lowest permafrost values (40-50 % probability) to be concentrated in the forest on the south-facing slope. Both tests in that probability zone were inconclusive, due to a failure to penetrate deeply enough into the substrate (Fig. 3.19). The singular permafrost-absent CAS point in WS01 intersects with a zone of relatively high permafrost likelihood (80-90 %) in the valley bottom.

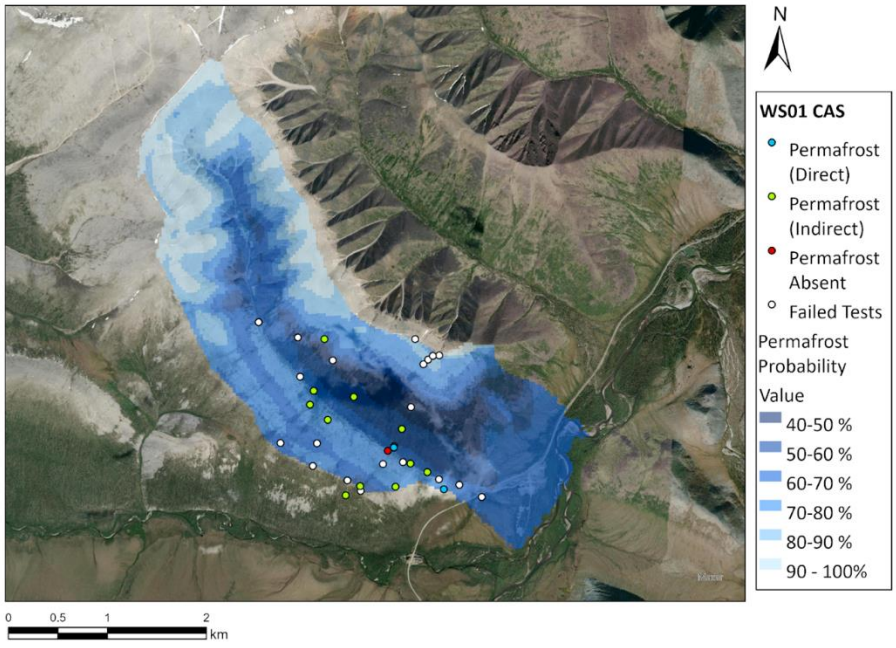

Fig. 3.19. Results of CAS testing against the Bonnaventure et al. (2012) probability model in WS01, set to 50 % transparency for clarity. *Basemap Imagery: © Maxar Technologies, Esri, Earthstar Geographics.*

When compared with the P(TEST) model (Table 3.5), zones of low testability (0-25 % likelihood) strongly intersect with zones of high permafrost probabilities in WS01. The average permafrost probability in the 0-25 % P(TEST) category is 80.0 % in this valley. Permafrost probability is lowest (69. 2%) in the high P(TEST) likelihood category (75-100 %).

Table 3.5. A comparison of permafrost probability values modelled by Bonnaventure et al. (2012) and P(TEST) values in WS01.

P(TEST)	Permafrost Probability (Min.) (%)	Permafrost Probability (Max.) (%)	Permafrost Probability (Mean) (%)
Low: 0-25%	46.1	98.4	80.0
Low-Moderate: 25-50%	40.7	73.0	57.7
High-Moderate: 50-75%	42.8	74.7	60.0
High: 75-100%	46.6	78.7	62.9

In WS02, the Bonnaventure et al. (2012) model predicts the lowest permafrost probability values (50-60 %) to be in the valley bottom (Fig. 3.20). One CAS sample in this low probability class was determined to be permafrost-absent using linear regression analysis. However, cryotic temperatures were detected *in-situ* in the same probability zone only 378 m away. Of the three permafrost-absent CAS in WS02 determined to be permafrost-absent, two were in the 60-70 % probability zone and one was in the 40-50 % probability zone.

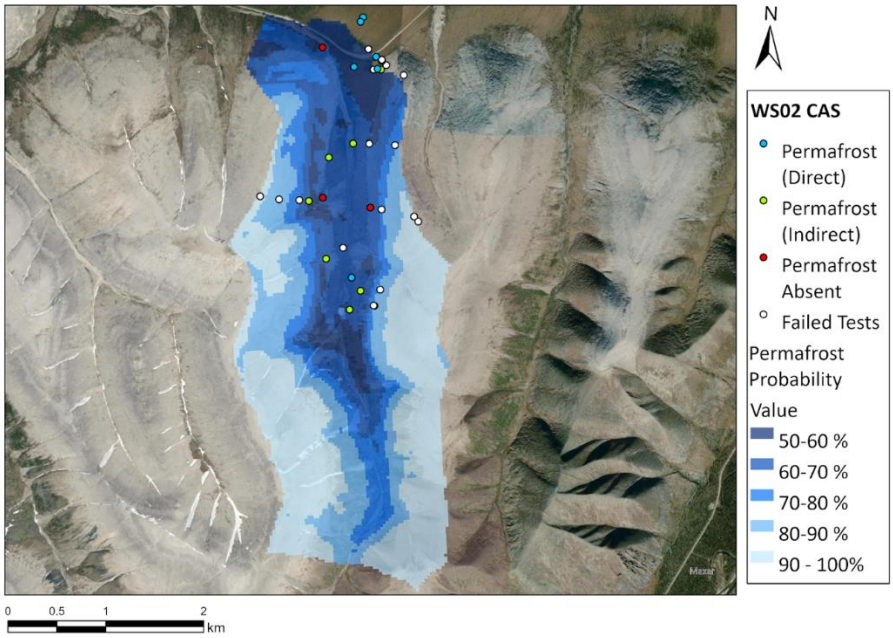

Fig. 3.20. Results of CAS testing against the Bonnaventure et al. (2012) probability model in WS02, set to 50 % transparency for clarity. *Basemap Imagery: © Maxar Technologies, Esri, Earthstar Geographics.*

Similarly to WS01, mean permafrost probability is highest in the low testability class and lowest in the high testability class (Table 3.6). The average permafrost probability in the 0-25 % P(TEST) category in WS02 is 88.1 %, and the average permafrost probability in the 75-100 % P(TEST) category is 59.6 %.

Table 3.6. A comparison of permafrost probability values modelled by Bonnaventure et al. (2012) and P(TEST) values in WS02.

P(TEST)	Permafrost Probability (Min.) (%)	Permafrost Probability (Max.) (%)	Permafrost Probability (Mean) (%)
Low: 0-25%	58.8	98.5	88.1
Low-Moderate: 25-50%	50.8	75.4	62.3
High-Moderate: 50-75%	50.9	74.1	62.2
High: 75-100%	51.4	72.3	59.6

3.3.3.2. Comparison with Garibaldi et al. (2024a)

The TTOP model produced by Garibaldi et al. (2024a) has not been expanded to the overall subrange of the Ogilvie Mountains and is restricted to WS01 and WS02. In WS01, the model predicts 82.5 % of the valley to be underlain by permafrost (TTOP = ≤0 °C), with an additional 8.6 % to be underlain by marginal permafrost (where TTOP = 0.1-0.9 °C) (Fig. 3.21). The remaining 8.7 % is modelled to be permafrost-absent (TTOP = ≥1 °C).

The results of CAS sampling are in good agreement with these results in this valley, except for one point. One CAS (WS01 G04), which was deemed permafrost-present (indirect) via linear regression analysis, intersects with a pixel of permafrost-absence on the model surface. Several other points of indirect permafrost presence are closely adjacent to pixels of either marginal or absent permafrost. However, CAS where permafrost was detected *in-situ* were in agreement with the model, as was the only sampled point of permafrost-absence in this valley.

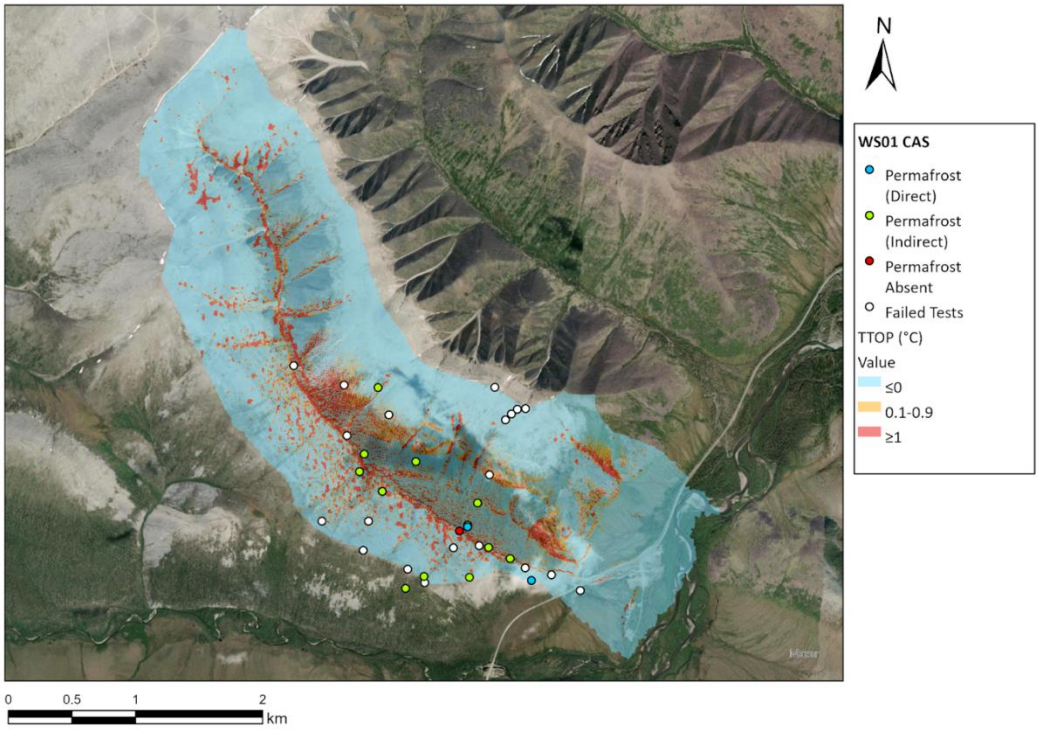

Fig. 3.21. The TTOP model by Garibaldi et al. (2024a) compared against the results of CAS testing in WS01. The model is set to 50 % transparency for clarity purposes. *Basemap Imagery: © Maxar Technologies, Esri, Earthstar Geographics.*

When compared with the P(TEST) model, colder TTOP temperatures intersect with the zones of low (0-25 %) and high (75-100 %) testability, and relatively warm TTOP temperatures (averaging -0.1 °C) intersect with zones of moderate P(TEST) probabilities (25-75 %) (Table 3.7). Average modelled TTOP temperature in the low P(TEST) category was -2.3 °C and -1.3 °C in the high P(TEST) category.

Table 3.7. A comparison of TTOP (°C) values modelled by Garibaldi et al. (2024a) with categories of P(TEST) in WS01.

P(TEST)	TTOP MIN. (°C)	TTOP MAX. (°C)	TTOP MEAN (°C)
Low: 0-25%	-5.3	3.7	-2.3
Low-Moderate: 25-50%	-5.8	3.3	-0.1
High-Moderate: 50-75%	-5.7	3.3	-0.1
High: 75-100%	-9.4	3.1	-1.3

In WS02, 99.2 % of the valley is predicted to have permafrost, with 0.71 % underlain by marginal permafrost and 0.09 % underlain by no permafrost (Fig. 3.22).

There are more points of disagreement between the model's prediction and the results of the CAS in WS02 than in WS01. Three CAS were permafrost-absent in this valley, but intersect with zones modelled by the Garibaldi et al. (2024a) model to have TTOP temperatures ≤0 °C. However, the north most of these CAS is adjacent to pixels of marginal permafrost.

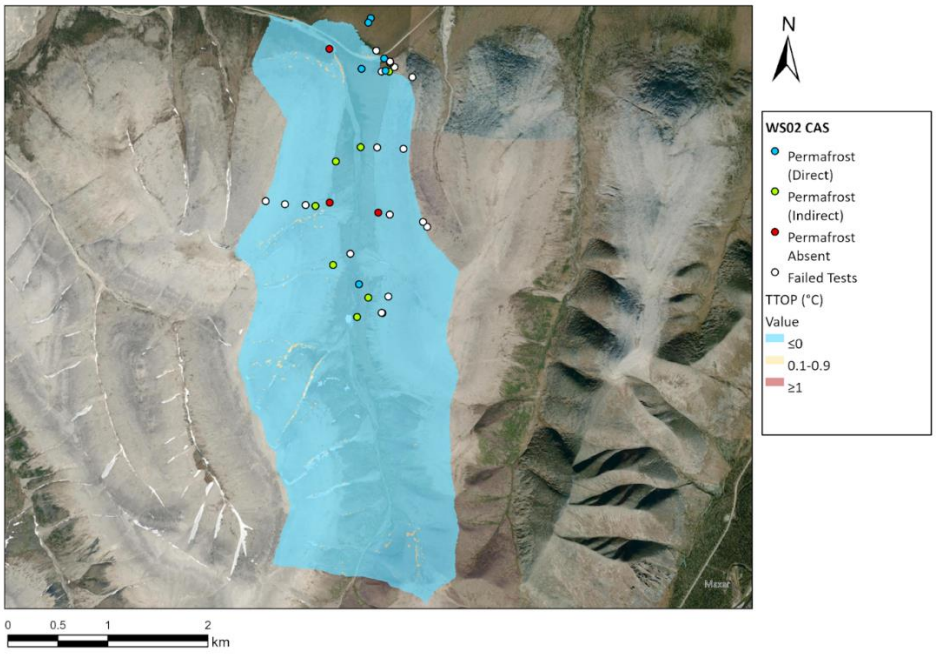

Fig. 3.22. The TTOP model by Garibaldi et al. (2024a) compared against the results of CAS testing in WS02. The model is set to 50 % transparency for clarity purposes. *Basemap Imagery: © Maxar Technologies, Esri, Earthstar Geographics.*

Comparison results between the Garibaldi et al. (2024a) and P(TEST) models are dissimilar between WS01 and WS02, with much colder average TTOP temperatures across all testability categories (Table 3.8). The warmest TTOP temperatures, by a slight margin, are located within the 75-100 % testability class and average at -1.8 °C. The coldest average TTOP temperatures are found within a more moderate testability class (50-75 %).

Table 3.8. A comparison of TTOP (°C) values modelled by Garibaldi et al. (2024a) with categories of P(TEST) in WS02.

P (TEST)	TTOP MIN. (°C)	TTOP MAX. (°C)	TTOP MEAN (°C)
Low: 0-25 %	-5.5	0.52	-2.1
Low-Moderate: 25-50 %	-4.8	0.58	-1.9
High-Moderate: 50-75 %	-5.9	0.75	-2.2
High: 75-100 %	-4.9	1.0	-1.8

3.4. Discussion

Despite the challenges associated with ground-truthing in the study area overall, the results of the CAS align well with the comprehensive near-surface permafrost distribution predicted in both WS01 and WS02 by regional (Obu et al., 2019) and localized (Bonnaventure et al., 2012; Garibaldi et al., 2024a) models. However, the high number of failed tests (51.4 % of all tests) still indicate that the Ogilvies are emblematic of a significant knowledge gap in our understanding of permafrost distribution and in our ability to test and calibrate permafrost models. These tests were considered to have failed because they did not reach a meaningful depth, and therefore did not produce reliable results, demonstrating a greater problem with testability which is illustrated by the P(TEST) model. In this context, the following section will

discuss the potential for false positives or negatives, influences on the field results of the ground-truthing tests, impacts on the results of the model, usefulness of MAGST as a permafrost indicator in this case study, errors and uncertainties in the study, and suggestions for future work.

3.4.1. Potential for false negatives and false positives in CAS testing

It is unlikely that any of the cryotic temperatures encountered *in-situ* in the field were false positives (i.e., the remnants of seasonal freezing) due to the timing of the fieldwork and the observed ALT across all sampled CAS. False positives may have occurred at the sites where cryotic temperatures at depth were only predicted using the linear regression equation, but this also seems unlikely due to the widely sub-zero MAGSTs encountered in the study area. Observations of thaw disturbances in the field suggest that it is more likely that ALT exceeded the maximum length of the probe in the majority of cases, and that cryotic temperatures are feasible at depth across most of the study area.

False negatives are more feasible. Of the 36 successful tests performed, only 4 were determined not to have permafrost present via linear regression. Although these areas may represent zones of near-surface permafrost loss, the limitations of the instrument and lacking baseline data on ground thermal state make it difficult to comment on that with any confidence. Sites determined not to have permafrost in this context were given this designation because linear regression did not predict cryotic temperatures within the first three meters of the surface, but it is possible for ALT to have exceeded that depth in some cases (i.e., Isaksen et al., 2000). Thaw-related disturbances were observed in the field and are becoming more visible along the Dempster Highway (*e.g.* Stockton et al., 2019; Schetselaar & Burn, 2024), but it is unclear if these will refreeze or develop as taliks.

3.4.2. Influences on CAS field results

3.4.2.1. Felsenmeer

The majority of logistical challenges associated with ground-truthing in WS01 and WS02 are associated with the felsenmeer land cover type, which covers the majority of the subrange. The valley walls are extremely steep (up to 69°) and made of unstable individual boulders, which made traversing them both time-consuming and potentially hazardous for researchers. Where the valley walls aren't steep (such as on the ridgetops and in proximity to the valley bottoms), the terrain is still potentially unstable due to the unfixed clasts. However, these sites likely do have comprehensive permafrost coverage. Felsenmeer sites made up the majority of untestable CAS due to their shallow or nonexistent soil profiles. Where soil was present, the probe was generally incapable of reaching meaningful depths due to dense concentrations of clasts. Although it was sometimes possible to maneuver the probe between the clasts, this rarely yielded meaningful results. The maximum depth achieved at a felsenmeer land cover class site was 83 cm B.D., but the average depth achieved was 41 cm. This is lower than the threshold for a successful test. At sites where no soil profile was present, probing between the clasts would have only yielded an air temperature measurement at no meaningful depth.

Felsenmeer sites in both WS01 and WS02 are very cold on average, with MAGSTs at sampled CAS averaging -1.3 °C. However, we were unable to reach cryotic temperatures *in-situ* at any of them. This may have been due to active layer thickness. The felsenmeer land cover type (and similar rocky, low-moisture environments) is well understood to have a fast response time to ambient air temperatures due to a lack of ground ice, meaning that large amounts of thaw can occur in a relatively short period of time (Bonnaventure & Lamoureux, 2013).

In these environments, permafrost is categorized as dry due to the lack of ground or pore ice, and cryotic materials are largely restricted to the clasts. The result is that permafrost thaw is unlikely to be visibly dramatic and will not produce surface features like retrogressive thaw slumps and active layer detachments like it would in other environments. This lack of ice and organic carbon means that thaw in dry permafrost environments is less likely to result in environmental disturbances (Gruber & Haeberli, 2007). Therefore, although uncertainty associated with distribution and thermal state in dry permafrost environments isn't ideal, it is less detrimental than uncertainty associated with ice-rich permafrost environments.

There are no rock glaciers present within the study area. However, the felsenmeer sites represent a close analog to what attempting to ground-truth a rock glacier would be like, due to the similar composition of the substrate. There is very little in the literature to suggest that any kind of comprehensive investigation into physically probing rock glaciers has been done. This is due to the impossibility of the task, and analysis of rock glaciers on a site-specific level is typically done though indirect geophysical imaging techniques such as electrical resistance tomography (*e.g.* Merz et al., 2016) and ground penetrating radar (*e.g.* Monnier et al., 2008; Merz et al., 2015). However, these are still indirect methods of assessing the interior structure of the rock glacier (Monnier et al., 2009) and present similar issues to the uncertainty regarding permafrost detection which were previously discussed.

3.4.2.2. Forest

The forested CAS land cover class was the least tested land cover class because it is the least present in the landscape overall (representing just 18.2 % of the land cover in both valleys).

Although many of the forested CAS featured the thick organic layer which we generally associated with successful ground-truthing tests, tree roots made it challenging to achieve the

depth necessary to reach cryotic materials. This is partially due to the shallow lateral spread of black spruce roots (Lieffers & Rothwell, 1987) in saturated or cryotic soils.

The forested sites also presented logistical challenges in terms of accessibility, as most of the sites were located on steep slopes. Although the forested slopes did not present the same instability as the felsenmeer class, significant deadfall and deep moss made it challenging to traverse the terrain.

3.4.2.3. Herbaceous

All tests where cryotic temperatures were reached *in-situ* occurred in the herbaceous class, although this does not necessarily indicate that the sites in other land cover classes lack near-surface permafrost. It is more likely that the insulative effect of overlying vegetation reduced ALT, making it more likely for the probe to reach the frost table without being hindered by clasts or hard substrate.

Our ability to penetrate the substrate was reduced in proximity to the valley walls. High clast concentrations hidden underneath the thick overlying vegetative cover caused some of the herbaceous CAS tests to fail.

In terms of accessibility, the herbaceous class was the least problematic. However, although the valley bottoms are relatively flat, they are often saturated or flooded.

3.4.3. Impacts on model results

Five DEM-derived variables were considered as potential drivers for the likelihood of P(TEST) success: land cover, TPI, aspect, slope, and elevation. However, only elevation was identified as a significant predictor by the logistic regression analysis, showing a small but

statistically significant negative impact on the dependent variable P(TEST). This is likely due to the relationship between elevation and soil development in the study area.

Felsenmeer slopes are generally well-drained (Haeberli et al., 2010), and this is also the case in the study area. Most soil development is concentrated at low elevations, where pooling water and organic matter collect to form soft soil profiles which are conducive to successful ground truthing tests. As elevation increases, soil development in the felsenmeer land cover class decreases. Although there is some soil at mid-elevation felsenmeer sites which allowed for deeper penetration, the majority of the substrate was still clast-based. This mid-elevation soil is often present in fan-shapes, indicating that finer sediments are being deposited by water at this elevation. At even higher elevation sites, soil development ceases entirely, resulting in large voids between clasts such that any cryotic materials would be restricted to the clasts themselves. Testing failed unanimously at sites with these conditions because there was simply no soil to probe, and the thermistors were functionally measuring air temperature. Tests at the ridgetops also failed unanimously. Although there is more soil development at the ridgetops due to their low relief, the profiles are thin and wind-scoured.

Aspect was initially considered a potential driver of testability due to its influence on surface energy balance, which affects vegetation species and coverage, moisture content, permafrost distribution, frequency of freeze-thaw cycles, and soil texture (Fan et al., 2023). However, the logistic regression analysis revealed it to be the most statistically insignificant variable, with a Pr(>|z|) value of 0.98. In WS01, the influence of aspect manifests visibly as a forest-covered south-facing slope and a felsenmeer-covered north-facing slope. The next nearest valley, north of WS01, lacks this extremely stark difference and strong visible treeline. In WS02, aspect seems to have a weaker visible influence. Neither side of that valley is treed and soil

distribution on the slopes is uniformly lacking on both sides. Ultimately, it is likely that aspect was statistically insignificant because 1) aspect did not have a strong influence on soil development in WS02 and 2) the majority of failed tests (97.4 %) occurred due to impenetrable substrate and clast presence, not tree roots.

Following aspect, slope is the next most statistically insignificant variable ($Pr(>|z|) = 0.88$). It was initially considered a potential predictor due to its strong influence on drainage and association with the felsenmeer land cover type. The maximum slope angle tested was 69.3°, the minimum was -0.54°, and the average was 16.9°. CAS were slightly biased toward sites with less extreme slope angles due to the hazardousness of traversing steep terrain and the instability of some upper portions of felsenmeer, where clasts were loose and lacked a securing soil profile. This bias may explain the variable's insignificance.

Land cover is only marginally less significant than slope ($Pr(>|z|) = 0.85$), which was surprising given it was initially hypothesized to be the determining factor for P(TEST) success. From aerial or site-level observations, it seemed intuitive that rocky areas would be less testable than herbaceous areas. Felsenmeer seemed to be totally lacking in testability, while the herbaceous class was anticipated to be uniformly successful. However, this does not appear to be the case for several reasons. The study area ultimately represents not only an extreme example of thermal heterogeneity but also a high degree of heterogeneity in testability. While this was generally true, the deepest successful CAS test at a felsenmeer-class CAS reached 83 cm B.D. With persistence, it was occasionally possible to penetrate significantly deeper into the substrate at felsenmeer sites by forcing the frost probe between clasts. Conversely, some herbaceous sites proximal to the valley walls concealed felsenmeer beneath vegetation, resulting in limited test success.

TPI is the final remaining variable in the analysis, and it also did not approach statistical significance ($Pr(>|z|) = 0.25$). Although it is marginally more significant than land cover, slope, and aspect, this is likely due to random chance rather than actual influence. TPI was originally selected because it seemed likely that concave sites such as ridgetops would have significantly lower testability than convex places, where water pooling would be more likely to occur, but this was not the case.

Overall, it is unlikely that elevation is the sole predictor of test success, but the resolution of the sampled sites may be too low to capture the full complexity of the actual variables. Ultimately, all variables other than elevation were excluded from the probability model, as they added noise rather than contributing meaningful information. However, there are drawbacks. Because WS01 is situated approximately 100 meters lower than WS02, the model predicts a broader range of testability probabilities in WS01 compared to WS02. In WS01, probabilities range from 0-100%, whereas in WS02, probabilities range from 0-90%. This occurs despite WS02 having more coverage of the herbaceous land cover class, which is the most successful land cover class for P(TEST).

3.4.4. Surficial temperature measurements as permafrost indicators

Many assessments of permafrost conditions assess GST or land surface temperatures as potential indicators of permafrost presence (*e.g.* Westermann et al., 2011; Hachem et al., 2012; Langer et al., 2013). GST is considered to be a reliable indicator of permafrost presence (Luo et al., 2018) and a good indicator of overall climate, as it integrates the influence of atmospheric conditions with ground conditions (*e.g.* snow cover, vegetation, microrelief) (Guglielmin, 2006). This is the general principle behind some remote sensing-based permafrost evaluations (*e.g.* Westermann et al., 2015; Batbaatar et al., 2020). Collecting data from remote sensing

instruments is a much faster and cost-effective way to obtain spatially dense temperature data across vast landscapes (Batbaatar et al., 2020). However, the effectiveness of using surficial measurements to indicate conditions deeper in the soil profile have been challenged (Ødegård, et al., 2008; Way & Lewkowicz, 2018). Using surficial measurements to indicate permafrost presence is especially problematic in areas like the north-central Yukon, where there is frequently a large disconnect between the air and ground surface temperature (thermal offset) (Burn & Smith, 1998). Furthermore, this method does not necessarily describe the thermal state of the subsurface sediment column.

This research considered MAGST as a permafrost proxy, where MAGST = ≤0 °C was considered to be an indicator of permafrost presence. However, special considerations had to be made to ensure that this functioned, primarily at sites that were overlain by *Sphagnum* and other insulative mosses. All but one of the CAS with insulative vegetation which produced cryotic temperatures *in-situ* had a marginally positive MAGST (0.1-1.0 °C). Furthermore, six of the 22 sites with permafrost predicted by linear regression also had positive MAGSTs, with one as warm as 2.0 °C.

Although MAGST is not a perfect permafrost proxy in this environment, having those values was key in determining permafrost presence at sites where cryotic temperatures could not be reached *in-situ.* In numerous cases, the probe was incapable of reaching the frost table, potentially due to ALT. This would be consistent with findings at other CAS, where thaw depths reached an observed maximum of 184 cm in the herbaceous land cover class. This depth was only achieved because of a thaw disturbance and exceeded the maximum limit of the probe length otherwise. The deepest depth reached by the probe naturally was 98 cm, and this was in the forested land cover class.

3.4.5. Errors and uncertainties

3.4.5.1. Field

The use of ground thermal profiling was key in determining permafrost presence or absence at the majority of CAS, as most did not reach cryotic temperatures *in-situ.* However, the method was not without its challenges.

We elected to use a method of ground thermal profiling where the individual thermistors were held at fixed intervals within the probe's casing, such that the clasts in the ground wouldn't dislodge or damage them. However, only a limited number of thermistors could fit inside. Placing the thermistors inside of the casing was still seen as preferable to attaching them to the outside of the probe to reduce the potential for damaging the sensors or dislodging them. It would theoretically be possible to increase the diameter of the probe, but that would be to the detriment of its ability to navigate between clasts effectively. Regardless, the instrument would be improved by increasing the number of thermistors in the probe, or by reducing the space between them (i.e., Léger et al., 2019). For this project, 25 cm intervals were chosen because it was anticipated that the herbaceous land cover class would be more easily probed, and that ALT would not be as thick. However, in most cases, the full length of the probe did not enter the ground, resulting in more limited measurements for some sites.

Using ground thermal profiling allowed us to extrapolate for potential cryotic temperatures at depth, but it is unlikely that this method was sufficient to fully capture the variability of temperature change due to the lag effect of heat moving through the soil column. This may have reduced the accuracy of the linear regression predictions. Although it did not occur frequently, in a few cases, there was a minor increase in temperature at the second

thermistor in the probe which represented this. The same simple regression equation was applied to all substrate types, but each would conduct the heat in a different manner.

3.4.5.2. Model

This model is subject to the same limiting factors as all other models, in that any number of discrete training sites in a heterogeneous landscape cannot be comprehensive of the characteristics of the overall landscape. This is especially problematic in the Ogilvies, where the testability of the landscape proved to be just as heterogeneous as the ground thermal state. It was initially anticipated that tests would reach no significant depth in the felsenmeer class and unanimously succeed in the herbaceous class, but the results were more mixed. Although the herbaceous class was the only class to produce *in-situ* cryotic temperatures, more depth was achieved in the felsenmeer class than was originally anticipated due to an unexpected variety of soil profile depths.

There is also some bias in the training set towards accessibility, as is frequently an issue in permafrost testing (Léger et al., 2019). Large portions of the study area were too steep and unstable to be accessed by researchers, and time constraints skewed data collection towards the front of the valleys, rather than deeper down the fetch.

Finally, it is likely that elevation is not truly the only indicator of testability. The model predicts general low testability on rocky portions of the mountains and high testability in soft substrate, low elevation sites, which is consistent with the field results. However, predictions about the testability of individual micro-sites on the scale of the entire subrange are limited. Testability is a complex metric to measure and is diverse at the microsite level, and the lack of significance for the other considered predictors (TPI, slope, land cover, and aspect) may simply be the result of a resolution issue. The heterogeneity of the landscape is likely to be much

higher than what was captured by the limited number of sampled CAS. If more CAS were sampled in additional valleys with higher frequency and at more diverse sites, it is likely that one of the other predictors would become more prominent.

3.4.6. Model Comparison Results

3.4.6.1. Comparison of CAS sampling and P(TEST) model with Bonnaventure et al. (2012)

It is more challenging to compare the results of CAS sampling to the Bonnaventure et al. (2012) model because it is mapping probability of permafrost presence, rather than actual temperature values. As a result, it is difficult to say that any individual CAS points disagree with the model, only that they are more or less reflective of the predicted probability.

However, overall, this model may be less accurate than the Garibaldi et al. (2024a) model because it was calibrated using a less localized data set, sourced from Dawson City (YT). Finally, this model was also 12 years old at the time of CAS sampling and may be less representative of ground thermal state due to ongoing climatic disequilibrium.

In both WS01 and WS02, zones of low testability (0-25 % likelihood) strongly intersect with zones of high permafrost probability (averaging 80.0 % and 88.1 %, respectively). Inversely, the model predicts permafrost probabilities to be relatively low (average 62.9 % and 59.6 % respectively) in the zone of high testability (75-100 %). Several tests in the valley bottoms, which is where high testability is concentrated, produced cryotic temperatures *in-situ.* This lower modelled permafrost probability may be the result of the less localized data set used to build the model, as it accounts less for the influence of cold air drainage and SBIs.

Problematically, zones of moderate permafrost probability also largely intersect with zones of moderate testability (25-75 %). In the 25-50 % testability category, average permafrost

probability is 57.7 % in WS01 and 62.3 % in WS02. This highlights a considerable degree of uncertainty.

3.4.6.2. Comparison of CAS sampling and P(TEST) model with Garibaldi et al. (2024a)

The Garibaldi et al. (2024a) model is a TTOP model which was calibrated using the localized temperature networks in WS01 and WS02. It also considers the influence of cold air drainage and SBIs, which are well-understood to impact permafrost distribution in the study area (Noad & Bonnaventure, 2022). It is also more recent to the time of CAS sampling. Although it predicts much more heterogeneous permafrost distribution in WS01 than in WS02, it is still largely in agreement with the results of sampling.

Similarly to the Bonnaventure et al. (2012) model, areas more certain to be underlain by permafrost by the Garibaldi et al. (2024a) model intersect with test failures in both valleys. These zones both largely cover high elevation felsenmeer slopes and ridgetops. This relationship may be due to the negative temperature anomalies associated with felsenmeer, wherein voids between clasts facilitate strong convective heat losses (Juliussen & Humlum, 2008). Although it is unideal when testability is low, it is less problematic in areas where certainty about permafrost presence is higher.

More problematically, and similarly to the Bonnaventure et al. (2012) model, areas of moderate testability (25-75 %) strongly intersect with relatively warm TTOP temperatures (averaging -0.1 °C). This is largely emblematic of the problem this research seeks to address, because these warm permafrost temperatures are both at more immediate risk of thawing and are difficult to detect.

3.4.7. Recommendations for future work

3.4.7.1. Local scale

This study has illustrated several challenges in our ability to test for permafrost in this environment, primarily centered around substrate penetrability and site accessibility. The following section outlines suggestions for future research in this environment or other challenging periglacial terrain. Overall, future work should focus on 1) building a baseline understanding of ground thermal state in the valleys, 2) clarifying the drivers of testability, and 3) identifying areas of marginal permafrost vulnerable to future thaw.

The high thermal heterogeneity present in both WS01 and WS02 makes it challenging to discern which areas are most vulnerable to thaw. It is well-established that permafrost temperatures vary considerably on a global scale, with some bodies of near surface permafrost being as cold as -15.0 °C or as warm as 0 °C (Smith et al., 2010). However, despite observations of variable ALT temperatures throughout the study area and observations of *in-situ* permafrost, there is no baseline of information about ground thermal state in the Ogilvie Mountains. Future predictions of permafrost thaw are therefore more uncertain because it is unclear what degree of warming will be sufficient to warm local permafrost bodies above the critical 0 °C isotherm. Although obtaining this data *in-situ* would require a significant network of boreholes, future work may supplement borehole data with additional ground-truthing tests. A focus on the distribution and variations of ALT could be used to interpolate more responsive areas which are more immediately vulnerable.

This research considered several potential drivers of testability in the landscape, but the results of the statistical analysis demonstrated that only elevation was a significant predictor of testability. However, even that significance was marginal. Future studies should consider attempting to delineate a stronger predictor, such that it can be applied at a broader scale. This

could be achieved with a higher resolution network of CAS samples, specifically in the zones where the P(TEST) model identified what we consider to be "moderate" probability (25-75%). The P(TEST) model identified the bulk of the subrange to fall either within the extremely low (0-25%) or extremely high (75-100%) likelihood of permafrost testability. Zones of moderate probability are clustered around mid-slope elevations, which is also where fewer CAS tests occurred. Additional points in these zones, focusing on test success, could be used to improve this model, clarify environmental drivers of testability, and better highlight problematic areas. However, it is ultimately likely that testability is not driven by a single factor, but instead by a complex series of environmental drivers interacting with one another.

Installing temperature monitoring networks (such as those in WS01 and WS02) on a broader scale could also improve overall resolution. Although these networks are expensive and labour-intensive to maintain, the data they generated significantly contributed to the accuracy of the Garibaldi et al. (2024a) model. It also improved the confidence of many of the results presented in this paper, where cryotic temperatures could not be reached *in-situ.* Having MAGST and MAAT values for the various microsites in the study area proved to be critical in understanding permafrost distribution with any accuracy. These values can not only be used to identify zones of climatic resilience (i.e., areas where insulative vegetation is reducing permafrost thaw (Shur & Jorgensen, 2007), but also to pinpoint areas where change is occurring more rapidly.

3.4.7.2. Circumpolar Arctic scale

Permafrost thermal state on a circumpolar scale is still largely surreptitious due to landscape heterogeneity and the spatiotemporal fragmentation of *in-situ* measurements. Going

forward, researchers should consider the thermal state of permafrost as a network, in which the state of our understanding needs to be maintained with consistent monitoring.

Some such efforts already exist to do this, such as the Global Terrestrial Network for Permafrost (GTN-P) (Biskaborn et al., 2015). Although this network is not yet comprehensive, it is a critical tool which can be used to both improve resolution on our understanding of GTS and to identify data gaps and zones of priority for more intensive testing. Performing frequent *in-situ* testing by hand is time and labour-intensive, but a more diverse and comprehensive network of boreholes (especially in mountainous regions) could be used to supplement this. In particular, northwestern Arctic and sub-Arctic permafrost studies would benefit immensely from initiatives like the PACE (Permafrost and Climate in Europe) project, which maintains a north-south transect of seven deep boreholes from the Sierra Nevada Mountain range in Spain to Svalbard (Etzelmüller et al., 2020).

Additional support should also be considered for pre-existing initiatives, such as the Yukon Permafrost Database compiled by Lipovsky et al. (2022). The Yukon Permafrost Database includes several hundred contributions from numerous stakeholders and sources (i.e., Yukon University, the territorial Department of Highways and Public Works, and the Alaska Highway Borehole Database). However, the vast majority of data is concentrated around infrastructure corridors and communities. Although this is valuable for supporting projects concerned with immediate changes to the environment which will affect people, it leaves massive gaps in our understanding of GTS across the rest of the territory.

Funding, maintaining, and improving projects such as GTN-P, PACE, and the Yukon Permafrost Database is key, but cannot be the only side of the work. New permafrost models should both 1) integrate the information generated by these long-term databases and 2) be

designed with validation and testing in mind. However, to do this, we also require a better understanding of testability.

The limited number of studies on permafrost ground-truthing are focused around obtaining thermal information, and this research is the first of its kind in determining testability as a variable. Future studies in this vein of research (testability) should place special emphasis on areas which are the most immediately vulnerable to future change, particularly heterogeneous mountain environments like the Ogilvies, Tombstone Territorial Park, Alaska (Yi et al., 2018; Shirley et al., 2022), and the Qinghai-Tibet Plateau (Cao et al., 2019). As climate change progresses, more typically High Arctic environments should also be considered as potential points of permafrost heterogeneity, such as in the Canadian Arctic Archipelago, Svalbard, and Russia.

New assessments of testability should also be applied to a number of different terrains. We understand that mountainous zones represent an area of low testability due to hard or clast-rich substrates, inaccessibility, instability, and steepness, but there have been no studies of this type on any other terrain.

French (2007) identifies 6 types of periglacial environments: High Arctic, continental, alpine, montane, low temperature range, and Antarctic. We additionally suggest boreal/peatlands and low/sub-Arctic, to accommodate for the range of permafrost environments which are more commonly seen in both the northwestern Arctic and central Canada (*e.g.* northern Alberta). Performing additional testability studies will both improve our understanding of overall permafrost distribution and focus modelling and mapping efforts onto areas of high uncertainty.

3.5. Conclusions

This study was focused on two central goals. The first was to explore the distribution of permafrost in two mountain valleys in the Ogilvie Mountains, and the second was to examine permafrost testability as a concept in the context of model validation. Although the issue of model validation has been discussed in previous literature, no other studies have attempted to quantify permafrost testability as a variable. This is also the first systematic attempt to ground-truth the study area for permafrost. Both the ground thermal profiling and P(TEST) methodologies used for these goals are transferable to other studies.

74 CAS were sampled during the field campaign between the two mountain valleys of interest. Of these, 36 were considered to be successful tests because the probe was able to reach a minimum of 45 cm B.D. This benchmark was chosen because it was the shallowest depth at which *in-situ* cryotic temperatures were detected in the study area. Nine of the successful tests produced cryotic temperatures *in-situ,* and all these tests were in the herbaceous land cover class. This is likely due to the influence of thermally insulative vegetation reducing over ALT depth, which is suspected to have exceeded the maximum length of the probe at several other sites. 27 of the successful tests were predicted to have cryotic temperatures at depth, via an analysis of ground thermal profiling using linear regression. The remaining 4 successful tests were predicted not to have permafrost using the same method.

The study used these results to attempt to retroactively validate two localized permafrost models. A common issue in permafrost modelling, particularly for heterogeneous permafrost environments, is that the subgrid variability of permafrost is likely to exceed the resolution of large-scale models (Etzelmüller, 2013). This is the case in the study area, where results of the CAS ground-truthing tests indicates that permafrost heterogeneity is variable above the

resolution of some contemporary models (i.e., Obu et al. (2019), which has a resolution of 1km²). The models chosen for validation were the probability model by Bonnaventure et al. (2012) and the TTOP model by Garibaldi et al. (2024a), and the CAS results were in good agreement with both. This provides a positive outlook for the knowledge gap being addressed here. Both models were calibrated using a more localized data set and performed well against validation tests.

The pre-existing temperature network was key in both the success of the Garibaldi et al. (2024a) model in providing accurate predictions about permafrost distribution in the valleys and in providing supplemental data which strengthened the results of the ground-truthing tests. Although this network is expensive and labour-intensive to maintain, having consistent access to MAAT and MAGST values, the associated offsets, and the distribution of temperature in a highly heterogeneous landscape is a very effective tool.

The majority (51.4 %) of attempted ground-truthing tests failed, due to not reaching the 45 cm benchmark we designated for the study area. This benchmark is not universally applicable and was chosen for this study because it was the minimum depth at which cryotic temperatures were found. These test failures were largely due to the presence of impenetrable substrate and hard clasts, due to the study area's mountainous terrain. This high degree of test failure illustrates that there are still large portions of the landscape which are "invisible" to permafrost researchers. Although it is widely understood that permafrost is thawing due to climatic change, large portions of certain vulnerable landscapes (such as mountains) remain a mystery due to issues of impenetrability and accessibility.

A model predicting the likelihood of conducting a successful permafrost test (P(TEST)) in the terrain was generated using the data collected at the CAS. Elevation was determined to be the only significant predictor of test success via a logistic regression analysis. According to the

model, most of the landscape falls within two polarized categories: extremely low likelihood (0-25 %) or extremely high (75-100 %). However, mid-slope elevations fall within a more moderate category (25-75 %) and warrant further testing.

The results of this research illustrate that understanding permafrost distribution in thermally complex environments, such as in mountains and in the discontinuous zone, is challenging. These environments are the most immediately vulnerable to climate change and represent the highest degree of uncertainty surrounding distribution, which is likely to continue impacting infrastructure under predicted warming scenarios. As climate change progresses, permafrost uncertainty will only increase. Therefore, it is critical that future studies continue to examine testability and to apply validation to distribution models.

CHAPTER FOUR: CONCLUSION

4.0. Conclusion

The main objective of this thesis was to explore the methodological issue of model validation in permafrost research, using a complex and unique periglacial environment as a case study. Thermal heterogeneity and the uncertainty that it causes is a recognized issue in the field (*e.g.* Gruber, 2012; Etzelmüller, 2013; Yi et al., 2018) but has seldom been explored with dedicated research. This research is the first of its kind in attempting to quantify ground temperature distributions in the study area, in validating the Bonnaventure et al. (2012) and Garibaldi et al. (2024a) models, and in the creation of the P(TEST) variable.

4.1. Summary of results

Ground thermal profiling was performed at a total of 74 CAS distributed between the two valleys across three land cover types: forest, herbaceous, and felsenmeer. The tests were performed to fulfill two main goals.

The first goal was to identify cryotic temperatures at depth, with specific focus placed on sites considered to be "permafrost marginal", where vegetative conditions were conducive to environmentally-protected permafrost (Shur & Jorgensen, 2007) and MAGST = 0.1-0.9 °C. This was done to better identify zones of uncertainty in the landscape and where permafrost is most sensitive to immediate future thaw. Thaw disturbances were recorded in the field, but it is challenging to assess if those disturbances represent imminent near-surface permafrost loss due to a lack of baseline thermal data.

The second goal was to determine the overall testability of the subrange by performing discrete tests in different land cover types. Permafrost tests at each individual CAS were considered to be successful if a minimum depth of 45 cm B.D. was achieved. Of the 74 tests

performed, 48.6 % were considered successful by this metric. Cryotic temperatures were only reached *in-situ* in the herbaceous land cover class, and the majority of failed tests (89.7 %) were at an elevation greater than 1000 m. As hypothesized, this suggests a relationship between soil development and successful permafrost tests, further highlighting the challenges associated with mountainous periglacial environments.

The collected field data was used to train a generalized linear model in RStudio. Several DEM-derived variables were considered as potential predictors of testability, but only elevation was found to be statistically significant via a logistic regression analysis. The result was a probability surface overlaid across a larger portion of the subrange which identified areas of high and low potential testability. As originally hypothesized, large portions of the study area (44.5 %) fall within the range of low testability (0-25% likelihood). This number essentially represents the portions of the study area covered by felsenmeer and mountains. Areas of high potential testability (75-100% likelihood) are restricted to areas of low elevation dominated by spongy vegetation and cover 30.0 % of the study area. The distribution of other probabilities is low overall, with most of the subrange being polarized to high or low testability likelihoods.

Results of the field testing were compared with two models: a regional-scale permafrost probability model by Bonnaventure et al. (2012) and a localized TTOP model by Garibaldi et al. (2024a). In contrast with other, larger scale models which struggle to capture the subgrid variability of temperature distributions present at the site, these models were in generally good agreement with the results of the CAS sampling. This is due to their original calibration with local data. In the case of Bonnaventure et al. (2012), which is a larger, more regional-scale model, validation data came from long-term borehole sequence data in Dawson City, YT. It was

still largely in agreement with the results of field testing but captured the influence of SBIs less accurately. Garibaldi et al. (2024a) was calibrated using the local temperature network and provided accurate predictions as well. When compared to coarser, larger scale models (*i.e.* Obu et al., 2019) which do not capture the actual variability of ground thermal state, the importance of that locally derived baseline data becomes clear.

4.2. Closing Remarks

The Ogilvie Mountains are emblematic of a significant knowledge gap in our understanding of permafrost distribution and in our ability to validate permafrost models. However, they are not the only environment where this issue is present. In the future, it is key for permafrost researchers to assess our reliance on predictive models and work towards better solutions. It should become increasingly common practice to identify places where we can and cannot test our models, and when we identify places we cannot test, we should focus on finding new alternatives. Furthermore, permafrost models should be built with this goal in mind. It is significantly more challenging and far less useful to retroactively attempt to validate a permafrost model than it is to calibrate with locally sourced data to begin with. This is especially key where model products will be used for land use planning and environmental assessments.

Applying studies such as this one to different periglacial environments is the first step towards this goal. We already understand that permafrost testing will be largely successful in environments where substrate is soft, such as in the boreal wetlands of Whatì, NT (Daly et al., 2022) or where permafrost creates visible aggradational features, such as the pingos around Tuktoyaktuk (Wolfe et al., 2023). However, our understanding is still lacking in more extreme environments, such as the Mackenzie Mountains, the Canadian Rockies, the Torngats, and the Arctic Cordillera.

Permafrost is a critical aspect of the cryosphere and provides invaluable ecosystem services to both the circumpolar Arctic and the rest of the globe. It is the only portion of the cryosphere which humans live on year-round and has a profound impact on global climate, landform stability, infrastructure, and hydrology. The full effects of climate change on this important environmental resource are yet to be fully realized, and as warming progresses, permafrost distribution will only become more uncertain. Therefore, it is critical to garner as much baseline thermal data as possible before the information is permanently lost.

REFERENCES

Åkerman, H. J., & Johansson, M. (2008). Thawing permafrost and thicker active layers in sub-arctic Sweden. *Permafrost and Periglacial Processes*, *19*(3), 279–292. https://doi.org/10.1002/ppp.626

Anisimov, O., & Zimov, S. (2020). Thawing permafrost and methane emission in Siberia: Synthesis of observations, reanalysis, and predictive modeling. *Ambio*. https://doi.org/10.1007/s13280-020-01392-y

Balch, E. S. (1990). *Glaciers or freezing caverns*. Philadelphia, PA: Allen, Lane, Scott.

Barsch, D. (2012). *Rockglaciers: Indicators for the present and former geoecology in high mountain environments* (Vol. 16). Springer Science & Business Media.

Bartsch, A., Strozzi, T., & Nitze, I. (2023). Permafrost Monitoring from Space. *Surveys in Geophysics*, *44*(5), 1579–1613. https://doi.org/10.1007/s10712-023-09770-3

Batbaatar, J., Gillespie, A. R., Sletten, R. S., Mushkin, A., Amit, R., Trombotto Liaudat, D., Liu, L., & Petrie, G. (2020). Toward the Detection of Permafrost Using Land-Surface Temperature Mapping. *Remote Sensing*, *12*(4), 695. https://doi.org/10.3390/rs12040695

Beierle, B. D. (2002). Late Quaternary glaciation in the Northern Ogilvie Mountains: revised correlations and implications for the stratigraphic record. *Canadian Journal of Earth Sciences*, *39*(11), 1709–1717. https://doi.org/10.1139/e02-062

Beltrami, H., & Kellman, L. (2003). An examination of short- and long-term air–ground temperature coupling. *Global and Planetary Change*, *38*(3-4), 291–303. https://doi.org/10.1016/s0921-8181(03)00112-7

Benkert, B., Kennedy, K., Fortier, D., Lewkowicz, A. G., Roy, L. P., Grandmont, K., ... & Moote, K. (2015). Dawson City landscape hazards: Geoscience mapping for climate change adaptation planning.

Bevington, A., & Lewkowicz, A. G. (2015). Assessment of a land cover driven TTOP model for mountain and lowland permafrost using field data, southern Yukon and northern British Columbia, Canada. In *Proceedings of GéoQuebec: 68th Canadian Geotechnical Conference and 7th Canadian Permafrost Conference. Quebec City, Canada (p. 9).*

Biden-Harris administration makes $135 million commitment to support relocation of tribal communities affected by climate change. (2022, November 30). www.doi.gov. https://www.doi.gov/pressreleases/biden-harris-administration-makes-135-million-commitment-support-relocation-tribal

Biskaborn, B. K., Lanckman, J.-P., Lantuit, H., Elger, K., Streletskiy, D. A., Cable, W. L., & Romanovsky, V. E. (2015). The new database of the Global Terrestrial Network for Permafrost (GTN-P). *Earth System Science Data*, *7*(2), 245–259. https://doi.org/10.5194/essd-7-245-2015

Biskaborn, B. K., Smith, S. L., Noetzli, J., Matthes, H., Vieira, G., Streletskiy, D. A., Schoeneich, P., Romanovsky, V. E., Lewkowicz, A. G., Abramov, A., Allard, M., Boike, J., Cable, W. L., Christiansen, H. H., Delaloye, R., Diekmann, B., Drozdov, D., Etzelmüller, B., Grosse, G., & Guglielmin, M. (2019). Permafrost is warming at a global scale. *Nature Communications*, *10*(1). https://doi.org/10.1038/s41467-018-08240-4

Bockheim, J. G., & Hall, K. J. (2002). Permafrost, active-layer dynamics and periglacial environments of continental Antarctica: Periglacial and permafrost research in the Southern Hemisphere. *South African Journal of Science, 98*(1), 82-90.

Bockheim, J. G., & Tarnocai, C. (1998). Nature, occurrence and origin of dry permafrost. In *Proceedings of the Seventh International Conference on Permafrost* (Vol. 55, pp. 57-63).

Boelhouwers, J. (2004). New Perspectives on Autochthonous Blockfield Development. *Polar Geography*, *28*(2), 133–146. https://doi.org/10.1080/789610122

Bonnaventure, P. P., & Lewkowicz, A. G. (2012). Permafrost probability modeling above and below treeline, Yukon, Canada. *Cold Regions Science and Technology*, *79*, 92-106.

Bonnaventure, P. P., & Lamoureux, S. F. (2013). The active layer: A conceptual review of monitoring, modelling techniques and changes in a warming climate. *Permafrost and Periglacial Processes*, *37*(3), 352–376. https://doi.org/10.1177/0309133313478314

Bonnaventure, P. P., Lamoureux, S. F., & Favaro, E. A. (2016). Over-Winter Channel Bed Temperature Regimes Generated by Contrasting Snow Accumulation in a High Arctic River. *Permafrost and Periglacial Processes*, *28*(1), 339–346. https://doi.org/10.1002/ppp.1902

Bonnaventure, P. P., & Lewkowicz, A. G. (2012). Permafrost probability modeling above and below treeline, Yukon, Canada. *Cold Regions Science and Technology*, *79-80*, 92–106. https://doi.org/10.1016/j.coldregions.2012.03.004

Bonnaventure, P. P., Lewkowicz, A. G., Kremer, M., & Sawada, M. C. (2012). A Permafrost Probability Model for the Southern Yukon and Northern British Columbia, Canada. *Permafrost and Periglacial Processes*, *23*(1), 52–68. https://doi.org/10.1002/ppp.1733

Brenning, A., Gruber, S., & Hoelzle, M. (2005). Sampling and statistical analyses of BTS measurements. *Permafrost and Periglacial Processes*, *16*(4), 383–393. https://doi.org/10.1002/ppp.541

Brown, J., Ferrians, O., Jr., Heginbottom, J., & Melnikov, E. (1997). Circum-Arctic map of permafrost and ground-ice conditions. *US Geological Survey Circum-Pacific Map*.

Brown, J., Hinkel, K. M., & Nelson, F. E. (2000). The circumpolar active layer monitoring (calm) program: Research designs and initial results. *Polar Geography*, *24*(3), 166–258. https://doi.org/10.1080/10889370009377698

Buckel, J., Mudler, J., Gardeweg, R., Hauck, C., Hilbich, C., Frauenfelder, R., Kneisel, C., Buchelt, S., Blöthe, J. H., Hördt, A., & Bücker, M. (2023). Identifying mountain permafrost degradation by repeating historical electrical resistivity tomography (ERT) measurements. *The Cryosphere*, *17*(7), 2919–2940. https://doi.org/10.5194/tc-17-2919-2023

Buckel, J., Reinosch, E., Hördt, A., Zhang, F., Riedel, B., Gerke, M., Schwalb, A., & Mäusbacher, R. (2021). Insights into a remote cryosphere: a multi-method approach to assess permafrost occurrence at the Qugaqie basin, western Nyainqêntanglha Range, Tibetan Plateau. *The Cryosphere*, *15*(1), 149–168. https://doi.org/10.5194/tc-15-149-2021

Burn, C. R., & Moore, J. O., O'Neill, B., Hayley, D., Trimble, J., Calmels, F., Orban, S. N., & Idrees, M. M. (2015). Permafrost characterization of the Dempster Highway, Yukon and Northwest Territories.

Burn, C. R., & Nelson, F. E. (2006). Comment on "A projection of severe near-surface permafrost degradation during the 21st century" by David M. Lawrence and Andrew G. Slater. *Geophysical Research Letters, 33,* L21503. https://doi.org/10.1029/2006GL027077

Burn, C. R., & Smith, C. A. S. (1988). Observations of the "thermal offset" in near-surface mean annual ground temperatures at several sites near Mayo, Yukon Territory, Canada. *Arctic, 41*(2), 99–104. http://www.jstor.org/stable/40510685

Cable, S., Elberling, B., & Kroon, A. (2018). Holocene permafrost history and cryostratigraphy in the High-Arctic Adventdalen Valley, central Svalbard. *Boreas*, *47*(2), 423-442.

Campbell, S., Affleck, R. T., & Sinclair, S. (2018). Ground-penetrating radar studies of permafrost, periglacial, and near-surface geology at McMurdo Station, Antarctica. *Cold Regions Science and Technology*, *148*, 38-49.

Cao, B., Zhang, T., Wu, Q., Sheng, Y., Zhao, L., & Zou, D. (2019). Permafrost zonation index map and statistics over the Qinghai–Tibet plateau based on field evidence. *Permafrost and Periglacial Processes*, 30(3), 178-194. https://doi.org/10.1002/ppp.2006

Carpino, O., Haynes, K., Connon, R., Craig, J., Devoie, É., & Quinton, W. (2021). The trajectory of landcover change in peatland complexes with discontinuous permafrost, northwestern Canada. *Hydrology and Earth System Sciences Discussions*, *25*, 3301-3317.

Chasmer, L., & Hopkinson, C. (2017). Threshold loss of discontinuous permafrost and landscape evolution. *Global Change Biology*, *23*(7), 2672–2686. https://doi.org/10.1111/gcb.13537

Chasmer, L., Quinton, W., Hopkinson, C., Petrone, R., & Whittington, P. (2011). Vegetation Canopy and Radiation Controls on Permafrost Plateau Evolution within the Discontinuous Permafrost Zone, Northwest Territories, Canada. *Permafrost and Periglacial Processes*, n/a-n/a. https://doi.org/10.1002/ppp.724

Chen, Z., English, J., & Adlakha, P. (2016). InSAR Monitoring of Alaska Highway Instability in Permafrost Regions Near Beaver Creek, Yukon. *All Days*. https://doi.org/10.4043/27454-ms

Cheng, G., & Wu, T. (2007). Responses of permafrost to climate change and their environmental significance, Qinghai-Tibet Plateau. *Journal of Geophysical Research*, *112*(F2). https://doi.org/10.1029/2006jf000631

Comiso, J. C., & Hall, D. K. (2014). Climate trends in the Arctic as observed from space. *Wiley Interdisciplinary Reviews: Climate Change*, *5*(3), 389–409. https://doi.org/10.1002/wcc.277

Daly, S. V., Bonnaventure, P. P., & Kochtitzky, W. (2022). Influence of ecosystem and disturbance on near-surface permafrost distribution, Whatì, Northwest Territories, Canada. *Permafrost and Periglacial Processes*. https://doi.org/10.1002/ppp.2160

Davis, J. L., & Annan, A. P. (1989). Ground-penetrating radar for high-resolution mapping of soil and rocky stratigraphy. *Geophysical Prospecting*, *37*(5), 531–551. https://doi.org/10.1111/j.1365-2478.1989.tb02221.x

Dobinski, W. (2011). Permafrost. *Earth-Science Reviews*, *108*(3-4), 158–169. https://doi.org/10.1016/j.earscirev.2011.06.007

Dobiński, W. (2019). Northern Hemisphere permafrost extent: Drylands, glaciers and sea floor. Comment to the paper: Obu, J., et al. 2019. Northern Hemisphere permafrost map based on TTOP modeling for 2000–2016 at 1 km2 scale, Earth Science Reviews, 193, 299–316. *Earth-Science Reviews*, 103037. https://doi.org/10.1016/j.earscirev.2019.103037

Duguay, C. R., & Alain Pietroniro. (2005). Remote Sensing in Northern Hydrology: Measuring Environmental Change. In *Geophysical monograph*. American Geophysical Union. https://doi.org/10.1029/gm163

Duk-Rodkin, A. (1996). *Surficial geology, Dawson, Yukon Territory, 1:250,000.*

Duk-Rodkin, A. (1999). Glacial limits map of Yukon. *Indian & Northern Affairs Canada/Department of Indian & Northern Development: Exploration & Geological Services Division, Geoscience Map 1999-2.*

Etzelmüller, B., Guglielmin, M., Hauck, C., Hilbich, C., Hoelzle, M., Isaksen, K., ... & Ramos, M. (2020). Twenty years of European mountain permafrost dynamics—the PACE legacy. *Environmental Research Letters*, 15(10), 104070.

Etzelmüller, B. (2013). Recent Advances in Mountain Permafrost Research. *Permafrost and Periglacial Processes*, *24*(2), 99–107. https://doi.org/10.1002/ppp.1772

Etzelmüller, B., & Frauenfelder, R. (2009). Factors Controlling the Distribution of Mountain Permafrost in The Northern Hemisphere and Their Influence on Sediment Transfer. *Arctic, Antarctic, and Alpine Research*, *41*(1), 48–58. https://doi.org/10.1657/1523-0430-41.1.48

Etzelmüller, B., Heggem, E. S. F., Sharkhuu, N., Frauenfelder, R., Kääb, A., & Goulden, C. (2006). Mountain permafrost distribution modelling using a multi-criteria approach in the Hövsgöl area,

northern Mongolia. *Permafrost and Periglacial Processes*, *17*(2), 91–104. https://doi.org/10.1002/ppp.554

Everdingen, van. R. O. (1976). Geocryological terminology. *Canadian Journal of Earth Sciences*, *13*(6), 862–867. https://doi.org/10.1139/e76-089

Everdingen, van R. O. (1998). *Multi-language glossary of permafrost and related ground-ice terms*. University of Calgary, Calgary, Alberta, Canada.

Fan, X., Lin, Z., Niu, F., Lan, A., Yao, M., & Li, W. (2022). Near-surface heat transfer at two gentle slope sites with differing aspects, Qinghai-Tibet Plateau. *Frontiers in Environmental Science*, *10*. https://doi.org/10.3389/fenvs.2022.1037331

Fan, X., Li, W., Wu, X., Yao, M., Niu, F., & Lin, Z. (2023). Heterogeneity of Surface Heat Exchange of Slopes and Potential Drivers of the Initiation of Thaw Slump, Qinghai-Tibet Plateau. *International Journal of Disaster Risk Science*, 14(4), 549-565.

Frappier, R., Lacelle, D., & Fraser, R. H. (2023). Landscape Changes in the Tombstone Territorial Park region (central Yukon, Canada) from Multi-Level Remote Sensing Analysis. *Arctic Science*, *9*(4). https://doi.org/10.1139/as-2022-0037

French, H. M. (2007). *The periglacial environment*. John Wiley & Sons.

French, H., & Shur, Y. (2010). The principles of cryostratigraphy. *Earth-Science Reviews*, 101(3-4), 190-206.

Frey, K. E., & McClelland, J. W. (2009). Impacts of permafrost degradation on arctic river biogeochemistry. *Hydrological Processes*, *23*(1), 169–182. https://doi.org/10.1002/hyp.7196

Fisher, J. P., Estop-Aragonés, C., Thierry, A., Charman, D. J., Wolfe, S. A., Hartley, I. P., Murton, J. B., Williams, M., & Phoenix, G. K. (2016). The influence of vegetation and soil characteristics on active-layer thickness of permafrost soils in boreal forest. *Global Change Biology*, *22*(9), 3127-3140. https://doi.org/10.1111/gcb.13248

Gabriel, A. K., Goldstein, R. M., & Zebker, H. A. (1989). Mapping small elevation changes over large areas: Differential radar interferometry. *Journal of Geophysical Research*, *94*(B7), 9183. https://doi.org/10.1029/jb094ib07p09183

Garibaldi, M. C., Bonnaventure, P. P., & Lamoureux, S. F. (2020). Utilizing the TTOP model to understand spatial permafrost temperature variability in a High Arctic landscape, Cape Bounty, Nunavut, Canada. *Permafrost and Periglacial Processes*, *32*(1), 19–34. https://doi.org/10.1002/ppp.2086

Garibaldi, M. C., Bonnaventure, P. P., Noad, N. C., & Kochtitzky, W. (2024a). Exploring the impact of surface lapse rate change scenarios on mountain permafrost distribution in four dissimilar valleys in Yukon, Canada. *Arctic Science*. https://doi.org/10.1139/as-2023-0066

Garibaldi, M. C., Bonnaventure, P. P., Noad, N. C., & Kochtitzky, W. (2024b). Modelling air, ground surface and permafrost temperature variability across four dissimilar valleys, Yukon, Canada. *Arctic Science*. https://doi.org/10.1139/as-2023-0067

GCOS. (2016). The global observing system for climate: Implementation needs. *Technical report GCOS-200, WMO, Geneva*.

Gibson, C., Cottenie, K., Gingras-Hill, T., Kokelj, S. V., Baltzer, J. L., Chasmer, L., & Turetsky, M. R. (2021). Mapping and understanding the vulnerability of northern peatlands to permafrost thaw at scales relevant to community adaptation planning. *Environmental Research Letters*, *16*(5), 055022. https://doi.org/10.1088/1748-9326/abe74b

Goodrich, L. E. (1982). The influence of snow cover on the ground thermal regime. *Canadian Geotechnical Journal*, *19*(4), 421-432.

Gornall, J. L., Jónsdóttir, I. S., Woodin, S. J., & Van der Wal, R. (2007). Arctic mosses govern below-ground environment and ecosystem processes. *Oecologia*, *153*(4), 931–941. https://doi.org/10.1007/s00442-007-0785-0

Gruber, S. (2012). Derivation and analysis of a high-resolution estimate of global permafrost zonation. *The Cryosphere*, *6*(1), 221–233. https://doi.org/10.5194/tc-6-221-2012

Gruber, S., Haeberli, W. (2007) Permafrost in steep bedrock slopes and its temperature-related destabilization following climate change. *Journal of Geophysical Research-Earth Surface* 112: F02S18.

Gruber, S., & Hoelzle, M. (2001). Statistical modelling of mountain permafrost distribution: local calibration and incorporation of remotely sensed data. *Permafrost and Periglacial Processes*, *12*(1), 69–77. https://doi.org/10.1002/ppp.374

Gubler, S., Fiddes, J., Keller, M., & Gruber, S. (2011). Scale-dependent measurement and analysis of ground surface temperature variability in alpine terrain. *The Cryosphere*, *5*(2), 431–443. https://doi.org/10.5194/tc-5-431-2011

Guglielmin, M. (2006). Ground surface temperature (GST), active layer and permafrost monitoring in continental Antarctica. *Permafrost and Periglacial Processes*, *17*(2), 133–143. https://doi.org/10.1002/ppp.553

Guo, D., & Wang, H. (2016). CMIP5 permafrost degradation projection: A comparison among different regions. *Journal of Geophysical Research: Atmospheres*, 121(9), 4499-4517.

Gusmeroli, A., Liu, L., Schaefer, K., Zhang, T., Schaefer, T., & Grosse, G. (2015). Active Layer Stratigraphy and Organic Layer Thickness at a Thermokarst Site in Arctic Alaska Identified Using Ground Penetrating Radar. *Arctic, Antarctic, and Alpine Research*, *47*(2), 195–202. https://doi.org/10.1657/aaar00c-13-301

Hachem, S., Duguay, C. R., & Allard, M. (2012). Comparison of MODIS-derived land surface temperatures with ground surface and air temperature measurements in continuous permafrost terrain. *The Cryosphere*, *6*(1), 51–69. https://doi.org/10.5194/tc-6-51-2012

Haeberli, W. (1973). Die Basistemperatur der winterlichen Schneedecke als möglicher Indikator für die Verbreitung von Permafrost in den Alpen. *Zeitschrift für Gletscherkunde und Glazialgeologie, 1–2*, 221–227.

Haeberli, W., Guodong, C., Gorbunov, A. P., & Harris, S. A. (1993). Mountain permafrost and climatic change. *Permafrost and Periglacial Processes*, *4*(2), 165–174. https://doi.org/10.1002/ppp.3430040208

Haeberli, W., Noetzli, J., Arenson, L., Delaloye, R., Gärtner-Roer, I., Gruber, S., Isaksen, K., Kneisel, C., Krautblatter, M., & Phillips, M. (2010). Mountain permafrost: development and challenges of a young research field. *Journal of Glaciology*, *56*(200), 1043–1058. https://doi.org/10.3189/002214311796406121

Haeberli, W., Schaub, Y., & Huggel, C. (2017). Increasing risks related to landslides from degrading permafrost into new lakes in de-glaciating mountain ranges. *Geomorphology*, *293*, 405–417. https://doi.org/10.1016/j.geomorph.2016.02.009

Hanson, S., & Hoelzle, M. (2004). The thermal regime of the active layer at the Murtèl rock glacier based on data from 2002. *Permafrost and Periglacial Processes, 15*(3), 273–282. https://doi.org/10.1002/ppp.499

Hargrave, M. L. (2006). Ground truthing the results of geophysical surveys. In *Remote sensing in archaeology: An explicitly North American perspective* (pp. 269-304).

Harris, C., & Mühll, V. D. (2001). Permafrost and climate in Europe. Climate change, mountain permafrost degradation and geotechnical hazard. *Global Change and Protected Areas*, 71-82.

Harris, C., & Murton, J. B. (2005). Interactions between glaciers and permafrost: an introduction. *Geological Society, London, Special Publications*, 242(1), 1-9.

Harris, S. A., & Pedersen, D. E. (1998). Thermal regimes beneath coarse blocky materials. *Permafrost and Periglacial Processes, 9*, 107–120.

Harris, S. A. (1981). Climatic Relationships of Permafrost Zones in Areas of Low Winter SnowCover. *Arctic*, *34*(1), 64–70. JSTOR. https://doi.org/10.2307/40509106

Harris, S. A., Anatoli Brouchkov, & Cheng Guodong. (2017). Geocryology. In *CRC Press eBooks*. Informa. https://doi.org/10.4324/9781315166988

Heginbottom, J. (1995). *Canada, permafrost:* Canada Map Office.

Heginbottom, J. (2002). Permafrost mapping: A review. *Progress in Physical Geography, 26*(4), 623-642.

Henry, K., & Smith, M. (2001). A model-based map of ground temperatures for the permafrost regions of Canada. *Permafrost and Periglacial Processes*, *12*(4), 389–398. https://doi.org/10.1002/ppp.399

Hinkel, K. M., Doolittle, J. A., Bockheim, J. G., Nelson, F. E., Paetzold, R., Kimble, J. M., & Travis, R. (2001). Detection of subsurface permafrost features with ground-penetrating radar, Barrow, Alaska. *Permafrost and Periglacial Processes*, *12*(2), 179–190. https://doi.org/10.1002/ppp.369

Hjort, J., Karjalainen, O., Aalto, J., Westermann, S., Romanovsky, V. E., Nelson, F. E., Etzelmüller, B., & Luoto, M. (2018). Degrading permafrost puts Arctic infrastructure at risk by mid-century. *Nature Communications*, *9*(1). https://doi.org/10.1038/s41467-018-07557-4

Hoelzle, M., Mittaz, C., Etzelmüller, B., & Haeberli, W. (2001). Surface energy fluxes and distribution models of permafrost in European mountain areas: an overview of current developments. *Permafrost and Periglacial Processes*, *12*(1), 53–68. https://doi.org/10.1002/ppp.385

Holloway, J. E., & Lewkowicz, A. G. (2019). Half a century of discontinuous permafrost persistence and degradation in western Canada. *Permafrost and Periglacial Processes*, *31*(1), 85–96. https://doi.org/10.1002/ppp.2017

Holloway, J. E., Lewkowicz, A. G., Douglas, T. A., Li, X., Turetsky, M. R., Baltzer, J. L., & Jin, H. (2020). Impact of wildfire on permafrost landscapes: A review of recent advances and prospects. *Permafrost and Periglacial Processes*, *31*(3), 371–382. https://doi.org/10.1002/ppp.2048

Hugelius, G., Strauss, J., Zubrzycki, S., Harden, J. W., Schuur, E. A. G., Ping, C.-L. ., Schirrmeister, L., Grosse, G., Michaelson, G. J., Koven, C. D., O'Donnell, J. A., Elberling, B., Mishra, U., Camill, P., Yu, Z., Palmtag, J., & Kuhry, P. (2014). Estimated stocks of circumpolar permafrost carbon with quantified uncertainty ranges and identified data gaps. *Biogeosciences*, *11*(23), 6573–6593. https://doi.org/10.5194/bg-11-6573-2014

Idrees, M., Burn, C. R., Moore, J., & Calmels, F. (2015). Monitoring permafrost conditions along the Dempster Highway. *In 7th Canadian Permafrost Conference: Proceedings of a conference held (pp. 20-23).*

Imhof, M., Pierrehumbert, G., Haeberli, W., & Kienholz, H. (2000). Permafrost investigation in the Schilthorn massif, Bernese Alps, Switzerland. *Permafrost and Periglacial Processes, 11*(3), 189-206.

Inkpen, R. (2005). *Science, philosophy, and physical geography.* Routledge.

Isaksen, K., Ødegård, R. S., Etzelmüller, B., Hilbich, C., Hauck, C., Farbrot, H., Eiken, T., Hygen, H. O., & Hipp, T. F. (2011). Degrading Mountain Permafrost in Southern Norway: Spatial and Temporal Variability of Mean Ground Temperatures, 1999-2009. *Permafrost and Periglacial Processes*, *22*(4), 361–377. https://doi.org/10.1002/ppp.728

Iwata, Y., Hirota, T., Suzuki, T., & Kazunobu Kuwao. (2012). Comparison of soil frost and thaw depths measured using frost tubes and other methods. *Cold Regions Science and Technology*, *71*, 111–117. https://doi.org/10.1016/j.coldregions.2011.10.010

Jafarov, E. E., Marchenko, S. S., & Romanovsky, V. E. (2012). Numerical modeling of permafrost dynamics in Alaska using a high spatial resolution dataset. *The Cryosphere*, *6*(3), 613–624. https://doi.org/10.5194/tc-6-613-2012

Jiang, H., Zhang, W., Yi, Y., Yang, K., Li, G., & Wang, G. (2018). The impacts of soil freeze/thaw dynamics on soil water transfer and spring phenology in the Tibetan Plateau. *Arctic, Antarctic, and Alpine Research*, *50*(1). https://doi.org/10.1080/15230430.2018.1439155

Jiang, H., Zheng, G., Yi, Y., Chen, D., Zhang, W., Yang, K., & Miller, C. E. (2020). Progress and Challenges in Studying Regional Permafrost in the Tibetan Plateau Using Satellite Remote Sensing and Models. *Frontiers in Earth Science*, *8*. https://doi.org/10.3389/feart.2020.560403

Johansson, M., Callaghan, T. V., Bosiö, J., H. Jonas Åkerman, Marcin Jackowicz-Korczynski, & Christensen, T. R. (2013). Rapid responses of permafrost and vegetation to experimentally increased snow cover in sub-arctic Sweden. *Environmental Research Letters*, *8*(3), 035025–035025. https://doi.org/10.1088/1748-9326/8/3/035025

Jones, D. B., Harrison, S., Anderson, K., & Whalley, W. B. (2019). Rock glaciers and mountain hydrology: A review. *Earth-Science Reviews*, *193*, 66–90. https://doi.org/10.1016/j.earscirev.2019.04.001

Juliussen, H., & Humlum, O. (2008). Thermal regime of openwork block fields on the mountains Elgåhogna and Sølen, central-eastern Norway. *Permafrost and Periglacial Processes*, *19*(1), 1–18. https://doi.org/10.1002/ppp.607

Juszak, I., Erb, A. M., Maximov, T. C., & Schaepman-Strub, G. (2014). Arctic shrub effects on NDVI, summer albedo and soil shading. *Remote Sensing of Environment*, *153*, 79–89. https://doi.org/10.1016/j.rse.2014.07.021

Kääb, A. (2008). Remote sensing of permafrost-related problems and hazards. *Permafrost and Periglacial Processes*, *19*(2), 107–136. https://doi.org/10.1002/ppp.619

Karunaratne, K. C., & Burn, C. R. (2003, July). Freezing n-factors in discontinuous permafrost terrain, Takhini River, Yukon Territory, Canada. In *Proceedings of the 8th International Conference on Permafrost* (Vol. 1, pp. 519-524). University of Alaska Fairbanks.

Kenner, R., Phillips, M., Hauck, C., Hilbich, C., Mulsow, C., Yves Bühler, Stoffel, A., & Manfred Buchroithner. (2017). *New insights on permafrost genesis and conservation in talus slopes based on observations at Flüelapass, Eastern Switzerland*. *290*, 101–113. https://doi.org/10.1016/j.geomorph.2017.04.011

Klene, A. E., Nelson, F. E., & Shiklomanov, N. I. (2001). The N-Factor as a Tool in Geocryological Mapping: Seasonal Thaw in the Kuparuk River Basin, Alaska. *Physical Geography*, *22*(6), 449–466. https://doi.org/10.1080/02723646.2001.10642754

Kneisel, C., Hauck, C., Fortier, R., & Moorman, B. (2008). Advances in geophysical methods for permafrost investigations. *Permafrost and Periglacial Processes*, *19*(2), 157–178. https://doi.org/10.1002/ppp.616

Kohler, T., Giger, M., Hurni, H., Ott, C., Wiesmann, U., Wymann von Dach, S., & Maselli, D. (2010). Mountains and Climate Change: A Global Concern. *Mountain Research and Development*, *30*(1), 53–55. https://doi.org/10.1659/mrd-journal-d-09-00086.1

Kremer, M., Lewkowicz, A. G., Bonnaventure, P. P., & Sawada, M. C. (2011). Utility of Classification and Regression Tree Analyses and Vegetation in Mountain Permafrost Models, Yukon, Canada. *Permafrost and Periglacial Processes*, *22*(2), 163–178. https://doi.org/10.1002/ppp.719

Krinsley, D. B. (1963). Influence of snow cover on frost penetration. *U.S. Geological Survey Professional Paper 475-B*, B144-B147.

Kuhn, M. (2008). Building predictive models in R using the caret package. *Journal of Statistical Software*, 28, 1-26.

Kwok, R. (2018). Arctic sea ice thickness, volume, and multiyear ice coverage: losses and coupled variability (1958–2018). *Environmental Research Letters*, 13(10), 105005.

Lacelle, D., St-Jean, M., Lauriol, B., Clark, I. D., Lewkowicz, A., Froese, D. G., ... & Zazula, G. (2009). Burial and preservation of a 30,000-year-old perennial snowbank in Red Creek valley, Ogilvie Mountains, central Yukon, Canada. *Quaternary Science Reviews*, 28(27-28), 3401-3413.

Lenaerts, J. T. M., van Angelen, J. H., van den Broeke, Michiel R., Gardner, A. S., Wouters, B., & van Meijgaard, E. (2013). Irreversible mass loss of canadian Arctic Archipelago glaciers. *Geophysical Research Letters*, 40(5), 870-874.

Langer, M., Westermann, S., Heikenfeld, M., Dorn, W., & Boike, J. (2013). Satellite-based modeling of permafrost temperatures in a tundra lowland landscape. *Remote Sensing of Environment*, *135*, 12–24. https://doi.org/10.1016/j.rse.2013.03.011

Lantz, T. C., & Kokelj, S. V. (2008). Increasing rates of retrogressive thaw slump activity in the Mackenzie Delta region, N.W.T., Canada. *Geophysical Research Letters*, *35*(6). https://doi.org/10.1029/2007gl032433

Léger, E., Dafflon, B., Robert, Y., Ulrich, C., Peterson, J. E., Biraud, S. C., Romanovsky, V. E., & Hubbard, S. S. (2019). A distributed temperature profiling method for assessing spatial variability in ground temperatures in a discontinuous permafrost region of Alaska. *The Cryosphere*, *13*(11), 2853–2867. https://doi.org/10.5194/tc-13-2853-2019

Lenton, T. M., Held, H., Kriegler, E., Hall, J. W., Lucht, W., Rahmstorf, S., & Schellnhuber, H. J. (2008). Tipping Elements in the Earth's Climate System. *Proceedings of the National Academy of Sciences*, *105*(6), 1786–1793. https://doi.org/10.1073/pnas.0705414105

Lewkowicz, A. G., & Duguay, C. R. (1999). Detection of Permafrost Features Using SPOT Panchromatic Imagery, Fosheim Peninsula, Ellesmere Island, N.W.T. *Canadian Journal of Remote Sensing*, *25*(1), 34–44. https://doi.org/10.1080/07038992.1999.10855261

Lewkowicz, A. G., & Ednie, M. (2004). Probability mapping of mountain permafrost using the BTS method, Wolf Creek, Yukon Territory, Canada. *Permafrost and Periglacial Processes*, *15*(1), 67–80. https://doi.org/10.1002/ppp.480

Lipovsky, P., Humphries, J., Stewart-Jones, E., & Cronmiller, D. (2022). Yukon permafrost database: A new baseline data resource. *Yukon Exploration and Geology 2021*, 37-49.

Liu, L., Schaefer, K., Chen, A. C., A. Gusmeroli, Zebker, H. A., & Zhang, T. (2015). Remote sensing measurements of thermokarst subsidence using InSAR. *Journal of Geophysical Research: Earth Surface*, *120*(9), 1935–1948. https://doi.org/10.1002/2015jf003599

Luo, D., Jin, H., Marchenko, S. S., & Romanovsky, V. E. (2018). Difference between near-surface air, land surface and ground surface temperatures and their influences on the frozen ground on the Qinghai-Tibet Plateau. *Geoderma*, *312*, 74–85. https://doi.org/10.1016/j.geoderma.2017.09.037

Lunardini, V. J. (1981). *Heat transfer in cold climates*. Van Nostrand Reinhold Company, Toronto.

Malingowski, J., Atkinson, D., Fochesatto, J., Cherry, J., & Stevens, E. (2014). An observational study of radiation temperature inversions in Fairbanks, Alaska. *Polar Science (Print)*, *8*(1), 24–39. https://doi.org/10.1016/j.polar.2014.01.002

Mauder, M., Foken, T., & Cuxart, J. (2020). Surface-Energy-Balance Closure over Land: A Review. *Boundary-Layer Meteorology*, *177*(2-3), 395–426. https://doi.org/10.1007/s10546-020-00529-6

Mackay, J. R. (1973). A frost tube for the determination of freezing in the active layer above permafrost. *Canadian Geotechnical Journal*, *10*(3), 392-396.

Marchenko, S., Romanovsky, V., & Tipenko, G. (2008). Numerical modeling of spatial permafrost dynamics in Alaska. In *Proceedings of the Ninth International Conference on Permafrost* (Vol. 29, pp. 1125-1130). Institute of Northern Engineering, University of Alaska Fairbanks.

Masson-Delmotte, V., Schulz, M., Abe-Ouchi, A., Beerling, D., Ganopolski, A., Jansen, E., & Lambeck, K. (2013). Information from paleoclimate archives. In T. F. Stocker, D. Qin, G.-K. Plattner, M. Tignor, S. K. Allen, J. Boschung, ... P. M. Midgley (Eds.), *Climate Change 2013: The Physical Science Basis. Contribution of Working Group I to the Fifth Assessment Report of the Intergovernmental Panel on Climate Change* (pp. 383-464). Cambridge University Press.

McCrystall, M. R., Stroeve, J., Serreze, M., Forbes, B. C., & Screen, J. A. (2021). New climate models reveal faster and larger increases in Arctic precipitation than previously projected. *Nature Communications, 12*(1), 6765. https://doi.org/10.1038/s41467-021-27031-y

Minder, J. R., Mote, P. W., & Lundquist, J. D. (2010). Surface temperature lapse rates over complex terrain: Lessons from the Cascade Mountains. *Journal of Geophysical Research, 115*(D14). https://doi.org/10.1029/2009jd013493

Miner, K. R., Turetsky, M. R., Malina, E., Bartsch, A., Tamminen, J., McGuire, A. D., ... & Miller, C. E. (2022). Permafrost carbon emissions in a changing Arctic. *Nature Reviews Earth & Environment, 3*(1), 55-67.

Mühll, V., Hauck, C., & Gubler, H. (2002). Mapping of mountain permafrost using geophysical methods. *Progress in Physical Geography, 26*(4), 643–660. https://doi.org/10.1191/0309133302pp356ra

Muller, S. W. (1947). *Permafrost: Or, permanently frozen ground and related engineering problems*. Ann Arbor, MI: J. W. Edwards.

Neal, A. (2004). Ground-penetrating radar and its use in sedimentology: principles, problems and progress. *Earth-Science Reviews, 66*(3-4), 261–330. https://doi.org/10.1016/j.earscirev.2004.01.004

Nitze, I., Grosse, G., Jones, B. M., Romanovsky, V. E., & Boike, J. (2018). Remote sensing quantifies widespread abundance of permafrost region disturbances across the Arctic and Subarctic. *Nature Communications, 9*(1). https://doi.org/10.1038/s41467-018-07663-3

Nixon, F. M., & Taylor, A. (1994). Active layer monitoring in natural environments, Mackenzie Valley, Northwest Territories. *Current Research, Geological Survey of Canada*, 27–34.

Nixon, F. M., Taylor, A. E., Allen, V. S., & Wright, F. (1995). Active layer monitoring in natural environments, lower Mackenzie Valley, Northwest Territories. *Interior Plains and Arctic Canada, 12*.

Noad, N. C., & Bonnaventure, P. P. (2022). Surface Temperature Inversion Characteristics in Dissimilar Valleys, Yukon Canada. *Arctic Science*. https://doi.org/10.1139/as-2021-0048

Noad, N. C., & Bonnaventure, P. P. (2023). Examining the influence of microclimate conditions on the breakup of surface-based temperature inversions in two proximal but dissimilar Yukon valleys. *Canadian Geographies / Géographies Canadiennes, 68*(3), 323–339. https://doi.org/10.1111/cag.12886

Noetzli, J., Arenson, L. U., Bast, A., Beutel, J., Delaloye, R., Farinotti, D., Gruber, S., Gubler, H., Haeberli, W., Hasler, A., Hauck, C., Hiller, M., Hoelzle, M., Lambiel, C., Pellet, C., Springman, S. M., Vonder Muehll, D., & Phillips, M. (2021). Best Practice for Measuring Permafrost Temperature in Boreholes Based on the Experience in the Swiss Alps. *Frontiers in Earth Science, 9*. https://doi.org/10.3389/feart.2021.607875

Noh, M. J., & Howat, I. M. (2017). The surface extraction from TIN-based search-space minimization (SETSM) algorithm. *ISPRS Journal of Photogrammetry and Remote Sensing, 129*, 55-76.

Nyland, K. E., Shiklomanov, N. I., Streletskiy, D. A., Nelson, F. E., Klene, A. E., & Kholodov, A. L. (2021). Long-term Circumpolar Active Layer Monitoring (CALM) program observations in Northern Alaskan tundra. *Polar Geography*, *44*(3), 167–185. https://doi.org/10.1080/1088937x.2021.1988000

O'Donnell, J. A., Romanovsky, V. E., Harden, J. W., & McGuire, A. D. (2009). The effect of moisture content on the thermal conductivity of moss and organic soil horizons from black spruce ecosystems in interior Alaska. *Soil Science, 174*, 646–651.

O'Neill, H. B., Burn, C. R., & Kokelj, S. V. (2015). Field measurements of permafrost conditions beside the Dempster Highway embankment, Peel Plateau, NWT. *In Proceedings from Conference: GEOQuébec.*

O'Neill, H. B., Smith, S. L., Burn, C. R., Duchesne, C., & Yu, Z. (2023). Widespread permafrost degradation and thaw subsidence in northwest Canada. *Journal of Geophysical Research: Earth Surface*. https://doi.org/10.1029/2023jf007262

O'Neill, H. B., Wolfe, S. A., & Duchesne, C. (2019). New ground ice maps for Canada using a paleogeographic modelling approach. *The Cryosphere,* 13(3), 753-773. https://doi.org/10.5194/tc-13-753-2019

Obu, J., Westermann, Obu, J., Westermann, S., Bartsch, A., Berdnikov, N., Christiansen, H., Dashtseren, A., Delaloye, R., Elberling, B., Etzelmüller, B., Kholodov, A., Khmutov, A., Kääb, A., Leibman, M. Lewkowicz, A., Panda, S., Romanovsky, V., Way, R., Westergaard-Nielsen, A., Wu, T., Defu Zou, J. Northern Hemisphere permafrost map based on TTOP modelling for 2000–2016 at 1 km² scale. *Earth-Science Reviews*.

Ødegård, R. S., Isaksen, K., Eiken, T., & Sollid, J. L. (2008). MAGST in mountain permafrost, Dovrefjell, southern Norway, 2001–2006. In *Ninth International Conference on Permafrost, University of Alaska Fairbanks* (Vol. 29, pp. 1311-1315).

Oke, T. R. (2002). *Boundary Layer Climates.* Routledge.

Onaca, A., Ardelean, A., Urdea, P., Ardelean, F., & Sîrbu, F. (2015). Detection of mountain permafrost by combining conventional geophysical methods and thermal monitoring in the Retezat Mountains, Romania. *Cold Regions Science and Technology*, *119*, 111–123. https://doi.org/10.1016/j.coldregions.2015.08.001

Onarheim, I. H., Smedsrud, L. H., Ingvaldsen, R. B., & Nilsen, F. (2014). Loss of sea ice during winter north of Svalbard. Tellus. *Series A, Dynamic Meteorology and Oceanography,* 66(1), 23933-9. https://doi.org/10.3402/tellusa.v66.23933

Outcalt, S. I., Nelson, F. E., & Hinkel, K. M. (1990). The zero-curtain effect: Heat and mass transfer across an isothermal region in freezing soil. *Water Resources Research*, *26*(7), 1509–1516. https://doi.org/10.1029/wr026i007p01509

Painter, S. L., Moulton, J. D., & Wilson, C. J. (2012). Modeling challenges for predicting hydrologic response to degrading permafrost. *Hydrogeology Journal*, *21*(1), 221–224. https://doi.org/10.1007/s10040-012-0917-4

Peel, M. C., Finlayson, B. L., & McMahon, T. A. (2007). Updated world map of the Köppen-Geiger climate classification. *Hydrology and Earth System Sciences*, *11*(5), 1633–1644. https://doi.org/10.5194/hess-11-1633-2007

Perryman, C. R., Wirsing, J., Bennett, K. A., Brennick, O., Perry, A. L., Williamson, N., & Ernakovich, J. G. (2020). Heavy metals in the Arctic: Distribution and enrichment of five metals in Alaskan soils. *PLOS ONE*, *15*(6), e0233297. https://doi.org/10.1371/journal.pone.0233297

Potapowicz, J., Szumińska, D., Szopińska, M., & Polkowska, Ż. (2019). The influence of global climate change on the environmental fate of anthropogenic pollution released from the permafrost: Part I. Case study of Antarctica. *Science of the Total Environment*, *651*, 1534-1548.

Rea, B. R., Whalley, W. Brian., Rainey, M. M., & Gordon, J. E. (1996). Blockfields, old or new? Evidence and implications from some plateaus in northern Norway. *Geomorphology*, *15*(2), 109–121. https://doi.org/10.1016/0169-555x(95)00118-o

Revich, B., Tokarevich, N., & Parkinson, A. J. (2012). Climate change and zoonotic infections in the Russian Arctic. *International Journal of Circumpolar Health*, *71*(1), 18792. https://doi.org/10.3402/ijch.v71i0.18792

Rey, D. M., Walvoord, M., Minsley, B., Rover, J., & Singha, K. (2019). Investigating lake-area dynamics across a permafrost-thaw spectrum using airborne electromagnetic surveys and remote sensing time-series data in Yukon Flats, Alaska. *Environmental Research Letters*, *14*(2), 025001. https://doi.org/10.1088/1748-9326/aaf06f

Riseborough, D. (2007). The effect of transient conditions on an equilibrium permafrost-climate model. *Permafrost and Periglacial Processes*, *18*(1), 21–32. https://doi.org/10.1002/ppp.579

Riseborough, D., Shiklomanov, N., Etzelmüller, B., Gruber, S., & Marchenko, S. (2008). Recent advances in permafrost modelling. *Permafrost and Periglacial Processes*, *19*(2), 137–156. https://doi.org/10.1002/ppp.615

Romanovsky, V. E., & Osterkamp, T. E. (1995). Interannual variations of the thermal regime of the active layer and near-surface permafrost in northern Alaska. *Permafrost and Periglacial Processes*, *6*(4), 313–335. https://doi.org/10.1002/ppp.3430060404

Romanovsky, E., Smith, S. L., Isaksen, K., Shiklomanov, N. I., Streletskiy, D. A., Kholodov, A. L., ... & Marchenko, S. S. (2016). Terrestrial permafrost. *Bulletin of the American Meteorological Society*.

Rouyet, L., Lauknes, T. R., Christiansen, H. H., Strand, S. M., & Larsen, Y. (2019). Seasonal dynamics of a permafrost landscape, Adventdalen, Svalbard, investigated by InSAR. *Remote Sensing of Environment, 231*, 111236. https://doi.org/10.1016/j.rse.2019.111236

Saito, K., Machiya, H., Iwahana, G., Ohno, H., & Yokohata, T. (2020). Mapping simulated circum-Arctic organic carbon, ground ice, and vulnerability of ice-rich permafrost to degradation. *Progress in Earth and Planetary Science*, 7, 1-15.

Sadurtdinov, M., Sudakova, M., Tsarev, A., Skvortsov, A., & Malkova, G. (2019). GPR Active Layer Monitoring at CALM Sites (European North) in 2015–2018. *25th European Meeting of Environmental and Engineering Geophysics*, 1–5. https://doi.org/10.3997/2214-4609.201903468

Sawada, Y., Ishikawa, M., & Ono, Y. (2003). Thermal regime of sporadic permafrost in a block slope on Mt. Nishi-Nupukaushinupuri, Hokkaido Island, Northern Japan. *Geomorphology*, *52*(1-2), 121–130. https://doi.org/10.1016/s0169-555x(02)00252-0

Scapozza, C. (2015). Investigation on protalus ramparts in the Swiss Alps. *Geographica Helvetica*, *70*(2), 135–139. https://doi.org/10.5194/gh-70-135-2015

Schaefer, K., Elshorbany, Y., Jafarov, E., Schuster, P. F., Striegl, R. G., Wickland, K. P., & Sunderland, E. M. (2020). Potential impacts of mercury released from thawing permafrost. *Nature Communications*, *11*(1). https://doi.org/10.1038/s41467-020-18398-5

Schetselaar, A. B., & Burn, C. R. (2024). Increases in Highway Maintenance Costs in a Permafrost Environment Undergoing Climate Change, Yukon, Canada. In *Proceedings of the 12th International Conference on Permafrost* (pp. 373-381). Ottawa, ON: International Permafrost Association.

Schneider von Deimling, T., Lee, H., Ingeman-Nielsen, T., Westermann, S., Romanovsky, V., Lamoureux, S., Walker, D. A., Chadburn, S., Trochim, E., Cai, L., Nitzbon, J., Jacobi, S., & Langer, M. (2021). Consequences of permafrost degradation for Arctic infrastructure – bridging the model gap between regional and engineering scales. *The Cryosphere*, *15*(5), 2451–2471. https://doi.org/10.5194/tc-15-2451-2021

Schuur, E. A. G., Abbott, B. W., Bowden, W. B., Brovkin, V., Camill, P., Canadell, J. G., Chanton, J. P., Chapin, F. S., Christensen, T. R., Ciais, P., Crosby, B. T., Czimczik, C. I., Grosse, G., Harden, J., Hayes, D. J., Hugelius, G., Jastrow, J. D., Jones, J. B., Kleinen, T., & Koven, C. D. (2013). Expert assessment of vulnerability of permafrost carbon to climate change. *Climatic Change*, *119*(2), 359–374. https://doi.org/10.1007/s10584-013-0730-7

Schuur, E. A. G., Bockheim, J., Canadell, J. G., Euskirchen, E., Field, C. B., Goryachkin, S. V., Hagemann, S., Kuhry, P., Lafleur, P. M., Lee, H., Mazhitova, G., Nelson, F. E., Rinke, A., Romanovsky, V. E., Shiklomanov, N., Tarnocai, C., Venevsky, S., Vogel, J. G., & Zimov, S. A. (2008). Vulnerability of Permafrost Carbon to Climate Change: Implications for the Global Carbon Cycle. *BioScience*, *58*(8), 701–714. https://doi.org/10.1641/b580807

Schuur, E. A. G., McGuire, A. D., Schädel, C., Grosse, G., Harden, J. W., Hayes, D. J., Hugelius, G., Koven, C. D., Kuhry, P., Lawrence, D. M., Natali, S. M., Olefeldt, D., Romanovsky, V. E., Schaefer, K., Turetsky, M. R., Treat, C. C., & Vonk, J. E. (2015). Climate change and the permafrost carbon feedback. *Nature*, *520*(7546), 171–179. https://doi.org/10.1038/nature14338

Shahgedanova, M. (2021). Climate change and melting glaciers. *Elsevier EBooks*, 53–84. https://doi.org/10.1016/b978-0-12-822373-4.00007-0

Shiklomanov, N. I. (2005). From Exploration to Systematic Investigation: Development of Geocryology in 19th- and Early—20th-Century Russia. *Physical Geography*, *26*(4), 249–263.

Shirley, I., Mekonnen, Z. A., Wainwright, H. M., Romanovsky, V. E., Grant, R. F., Hubbard, S. S., Riley, W. J., & Baptiste Dafflon. (2022). Near-Surface Hydrology and Soil Properties Drive Heterogeneity in Permafrost Distribution, Vegetation Dynamics, and Carbon Cycling in a Sub-Arctic Watershed. *Journal of Geophysical Research: Biogeosciences*, *127*(9).

Sommer, C., Seehaus, T., Glazovsky, A., & Braun, M. H. (2022). Brief communication: Increased glacier mass loss in the Russian High Arctic (2010–2017). *The Cryosphere*, 16(1), 35-42.

Shur, Y. L., & Jorgenson, M. T. (2007). Patterns of permafrost formation and degradation in relation to climate and ecosystems. *Permafrost and Periglacial Processes*, *18*(1), 7–19.

Smith, M. W., & Riseborough, D. W. (1996). Permafrost monitoring and detection of climate change. *Permafrost and Periglacial Processes, 7*(4), 301-309.

Smith, M. W., & Riseborough, D. W. (2002). Climate and the limits of permafrost: a zonal analysis. *Permafrost and Periglacial Processes*, *13*(1), 1–15. https://doi.org/10.1002/ppp.410

Smith, S. L., Wolfe, S. A., Riseborough, D. W., & Nixon, F. M. (2009). Active-layer characteristics and summer climatic indices, Mackenzie Valley, Northwest Territories, Canada. *Permafrost and Periglacial Processes*, *20*(2), 201–220. https://doi.org/10.1002/ppp.651

Stammerjohn, S., Massom, R., Rind, D., & Martinson, D. (2012). Regions of rapid sea ice change: An inter-hemispheric seasonal comparison. *Geophysical Research Letters*, *39*(6), n/a-n/a. https://doi.org/10.1029/2012gl050874

Stockton, E. J., Burn, C. R., Idrees, M., Calmels, F., & Elmer, K. (2019). Monitoring ground temperatures in permafrost along the Dempster Highway, Yukon and NWT. In *18th International Conference on Cold Regions Engineering and 8th Canadian Permafrost Conference* (pp. 92-101). Reston, VA: American Society of Civil Engineers.

Strand, S. M., Christiansen, H. H., Johansson, M., Åkerman, J., & Humlum, O. (2020). Active layer thickening and controls on interannual variability in the Nordic Arctic compared to the circum-Arctic. *Permafrost and Periglacial Processes*, *32*(1), 47–58. https://doi.org/10.1002/ppp.2088

Strandberg, G., & Lind, P. (2021). The importance of horizontal model resolution on simulated precipitation in Europe – from global to regional models. *Weather and Climate Dynamics*, *2*(1), 181–204. https://doi.org/10.5194/wcd-2-181-2021

Streletskiy, D., Anisimov, O., & Vasiliev, A. (2015). Permafrost Degradation. *Snow and Ice-Related Hazards, Risks and Disasters*, 303–344. https://doi.org/10.1016/b978-0-12-394849-6.00010-x

Streletskiy, D., Biskaborn, B. K., Smith, S., Noetzli, J., Viera, G., & Schoeneich, P. (2017). Strategy and Implementation Plan 2016-2020 for the Global Terrestrial Network for Permafrost (GTN-P). *Strategy and Implementation Plan 2016-2020 for the Global Terrestrial Network for Permafrost (GTN-P).*

Strozzi, T., Antonova, S., Günther, F., Mätzler, E., Vieira, G., Wegmüller, U., Westermann, S., & Bartsch, A. (2018). Sentinel-1 SAR Interferometry for Surface Deformation Monitoring in Low-Land Permafrost Areas. *Remote Sensing*, *10*(9), 1360. https://doi.org/10.3390/rs10091360

Sudakova, M., Sadurtdinov, M., Skvortsov, A., Tsarev, A., Malkova, G., Molokitina, N., & Romanovsky, V. (2021). Using Ground Penetrating Radar for Permafrost Monitoring from 2015–2017 at CALM Sites in the Pechora River Delta. *Remote Sensing*, *13*(16), 3271. https://doi.org/10.3390/rs13163271

Sun, Z., Zhao, L., Hu, G., Qiao, Y., Du, E., Zou, D., & Xie, C. (2019). Modeling permafrost changes on the Qinghai–Tibetan plateau from 1966 to 2100: A case study from two boreholes along the Qinghai–Tibet engineering corridor. *Permafrost and Periglacial Processes*, *31*(1), 156–171. https://doi.org/10.1002/ppp.2022

Tarnocai, C., Mark Nixon, F., & Kutny, L. (2004) Circumpolar Active Layer Monitoring (CALM) sites in the Mackenzie Valley, northwestern Canada. *Permafrost and Periglacial Processes*, *15*(2), 141–153. https://doi.org/10.1002/ppp.490

Throop, J., Lewkowicz, A. G., & Smith, S. L. (2012). Climate and ground temperature relations at sites across the continuous and discontinuous permafrost zones, northern Canada. Canadian Journal of Earth Sciences, 49(8), 865-876.

van Vliet-Lanoë, B. (1985). Frost effects in soils. In *Soils and Quaternary Landscape Evolution* (pp. 117-158).

van Huissteden, J., & Dolman, A. (2012). Soil carbon in the Arctic and the permafrost carbon feedback. *Current Opinion in Environmental Sustainability*, *4*(5), 545-551. https://doi.org/10.1016/j.cosust.2012.09.008

Walker, J., Arnborg, L., & Peippo, J. (1987). Riverbank erosion in the Colville delta, Alaska. *Geografiska Annaler: Series A, Physical Geography*, *69*(1), 61-70.

Wakonigg, H. (1996). Unterkühlte schutthalden. *Arbeiten aus dem Geographischen Institut der Universität, Graz (AGIUG, 33): S209–S223*.

Wang, K., Jafarov, E., & Overeem, I. (2020). Sensitivity evaluation of the Kudryavtsev permafrost model. *Science of the Total Environment*, *720*, 137538. https://doi.org/10.1016/j.scitotenv.2020.137538

Way, R. G., & Lewkowicz, A. G. (2018). Environmental controls on ground temperature and permafrost in Labrador, northeast Canada. *Permafrost and Periglacial Processes*, *29*(2), 73–85.

Westermann, S., Langer, M., & Boike, J. (2011). Spatial and temporal variations of summer surface temperatures of high-Arctic tundra on Svalbard—Implications for MODIS LST-based permafrost monitoring. *Remote Sensing of Environment*, *115*(3), 908-922.

Westermann, S., Duguay, C. R., Grosse, G., & Kääb, A. (2014). Remote sensing of permafrost and frozen ground. *Remote Sensing of the Cryosphere*, 307–344. https://doi.org/10.1002/9781118368909.ch13

Westermann, S., Østby, T., Gisnås, K., Schuler, T. V., & Etzelmüller, B. (2015). A ground temperature map of the North Atlantic permafrost region based on remote sensing and reanalysis data. *The Cryosphere*, *9*(3), 1303–1319. https://doi.org/10.5194/tc-9-1303-2015

Whalen, D., Forbes, D. l., Kostylev, V., Lim, M., Fraser, P., Nedimović, M. r., & Stuckey, S. (2022). Mechanisms, volumetric assessment, and prognosis for rapid coastal erosion of Tuktoyaktuk Island, an important natural barrier for the harbour and community. *Canadian Journal of Earth Sciences*, *59*(11), 945–960. https://doi.org/10.1139/cjes-2021-0101

Wild, G. O. (1882). Air temperature in the Russian Empire. St. Petersburg, Russia: Izdatel'stvo Russkogo Geograficheskogo Obshestva.

Woo, M. K., & Young, K. L. (1997). Hydrology of a small drainage basin with polar oasis environment, Fosheim Peninsula, Ellesmere Island, Canada. *Permafrost and Periglacial Processes*, *8*(3), 257-277.

Woo, M. (1986). Permafrost hydrology in North America. *Atmosphere-Ocean*, *24*(3), 201–234. https://doi.org/10.1080/07055900.1986.9649248

Wright, J. F., Duchesne, C., & Côté, M. M. (2003, July). Regional-scale permafrost mapping using the TTOP ground temperature model. In *Proceedings of the 8th International Conference on Permafrost*. Swets and Zeitlinger, Lisse (pp. 1241-1246).

Yang, Z., Fang, W., Xia, L., Sheng, G., Graham, D. E., Liang, L., Wullschleger, S. D., & Gu, B. (2016). Warming increases methylmercury production in an Arctic soil. *Environmental Pollution*, *214*, 504–509. https://doi.org/10.1016/j.envpol.2016.04.069

Yi, Y., Kimball, J. S., Chen, R. H., Moghaddam, M., Reichle, R. H., Mishra, U., Zona, D., & Oechel, W. C. (2018). Characterizing permafrost active layer dynamics and sensitivity to landscape spatial heterogeneity in alaska. *The Cryosphere*, 12(1), 145-161. https://doi.org/10.5194/tc-12-145-2018

Zhang, T., Barry, R. G., Knowles, K., Heginbottom, J. A., & Brown, J. (2008). Statistics and characteristics of permafrost and ground-ice distribution in the Northern Hemisphere. *Polar Geography*, *31*(1-2), 47–68. https://doi.org/10.1080/10889370802175895

Zhang, T., Heginbottom, J. A., Barry, R. G., & Brown, J. (2000). Further statistics on the distribution of permafrost and ground ice in the Northern Hemisphere1. *Polar Geography*, *24*(2), 126–131. https://doi.org/10.1080/10889370009377692

Zhang, Y., Ohata, T., & Kadota, T. (2003). Land-surface hydrological processes in the permafrost region of the eastern Tibetan Plateau. *Journal of Hydrology*, *283*(1-4), 41–56. https://doi.org/10.1016/s0022-1694(03)00240-3

Zhang, Y., Olthof, I., Fraser, R., and Wolfe, S. A.: A new approach to mapping permafrost and change incorporating uncertainties in ground conditions and climate projections, *The Cryosphere*, 8, 2177–2194, https://doi.org/10.5194/tc-8-2177-2014, 2014.

Zhang, T., Osterkamp, T. E., & Stamnes, K. (1997). Effects of climate on the active layer and permafrost on the North Slope of Alaska, USA. *Permafrost and Periglacial Processes*, *8*(1), 45-67.

Zhang, Y., Wang, X., Fraser, R., Olthof, I., Chen, W., Mclennan, D., Ponomarenko, S., & Wu, W. (2013). Modelling and mapping climate change impacts on permafrost at high spatial resolution for an Arctic region with complex terrain. *The Cryosphere*, *7*(4), 1121–1137. https://doi.org/10.5194/tc-7-1121-2013

Zwieback, S., Liu, L., Rouyet, L., Short, N., & Strozzi, T. (2024). Advances in InSAR Analysis of Permafrost Terrain. *Permafrost and Periglacial Processes*, *35*(4), 544–556. https://doi.org/10.1002/ppp.2248